CHAPTER 1

Electromagnetic Wave Propagation

1.1 PROPERTIES OF PLANE ELECTROMAGNETIC WAVE

1.1.1 Equation of Wave or Propagation

Electromagnetic waves are propagated in a vacuum, in dielectrics and conductors; here we will be interested in the propagation of radiated waves of periodic type that are characterized by a wavelength defined by a wave velocity which depends on the permittivity and permeability of the crossed medium.

Thus we consider a plane wave, as represented in Figure 1.1, propagating in direction x of an orthogonal reference system (x, y, z) while transporting the electric field **E** polarized in the direction y and the magnetic induction **B** in the direction z. The properties of such a wave can be deduced from Maxwell's equations, which link together the electric field **E**, the magnetic induction **B**, and the current density **J**:

$$\text{Curl } E = -\frac{\partial B}{\partial t} \quad \text{(Faraday's law)} \tag{1.1}$$

$$\text{Curl } B = \mu J + \varepsilon\mu \frac{\partial E}{\partial t} \quad \text{(Ampere's generalized theorem)} \tag{1.2}$$

where μ = absolute permeability of medium of propagation (H m^{-1})
ε = its absolute permittivity (F m^{-1})

These equations can also be written in differential form by considering, for example, a nonconducting medium ($J = 0$):

$$\frac{\partial E}{\partial x} = -\frac{\partial B}{\partial t} \tag{1.3}$$

$$\frac{\partial B}{\partial x} = -\varepsilon\mu \frac{\partial E}{\partial t} \tag{1.4}$$

Microwave Engineering: Land & Space Radiocommunications, by Gérard Barué

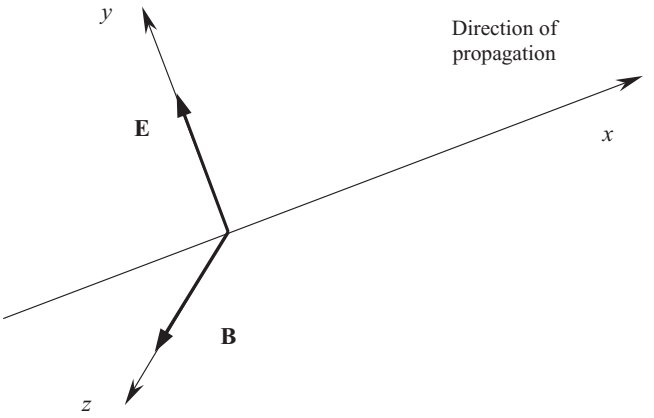

Figure 1.1 Plane electromagnetic wave.

After a second derivation according to x and t, these equations become

$$\frac{\partial^2 E}{\partial x^2} = -\frac{\partial}{\partial x}\left(\frac{\partial B}{\partial t}\right) = -\frac{\partial}{\partial t}\left(\frac{\partial B}{\partial x}\right) = \varepsilon\mu\frac{\partial^2 E}{\partial t^2}$$

$$\frac{\partial^2 B}{\partial x^2} = \varepsilon\mu\frac{\partial^2 B}{\partial t^2}$$

A simple solution is a wave varying sinusoidally over time whose electric field and magnetic induction amplitudes are given by the relations

$$E = E_{\max}\cos(\beta x - \omega t) \tag{1.5}$$

$$B = B_{\max}\cos(\beta x - \omega t) \tag{1.6}$$

where

$$\beta = \frac{2\pi}{\lambda}$$

$$\omega = 2\pi f = \frac{2\pi}{T} \quad \text{angular velocity (rad s}^{-1}\text{)}$$

$$\lambda = \frac{v}{f} = vT \quad \text{wavelength (m)}$$

where v = wave velocity (m s^{-1})
f = frequency (Hz)
T = period (s)

By deriving these two last expressions, we obtain

$$\frac{\partial E}{\partial x} = -\beta E_{\max} \sin(\beta x - \omega t)$$

$$\frac{\partial B}{\partial t} = \omega B_{\max} \sin(\beta x - \omega t)$$

Then, starting from expression (1.3), we can write

$$\beta E_{\max} = \omega B_{\max}$$

$$\frac{E_{\max}}{B_{\max}} = \frac{\omega}{\beta} = \lambda f = \frac{\lambda}{T} = v \tag{1.7}$$

The general expression of a sinusoidal periodic electromagnetic plane wave propagating in the direction x can thus be written in its complex form:

$$E = E_{\max} e^{-\alpha x} e^{j(\omega t - \beta x)} \tag{1.8}$$

where α is the attenuation constant of the medium ($\alpha = 0$ in a vacuum).

1.1.2 Wave Velocity

The velocity of an electromagnetic wave in a vacuum is a universal constant (speed of light) used to define the meter in the International System of Units (SI) and has as a value

$$c = \frac{1}{\sqrt{\varepsilon_0 \mu_0}} = 299{,}792{,}458 \,\mathrm{m\,s^{-1}} \tag{1.9}$$

where

$$\mu_0 = 4\pi \times 10^{-7} \,\mathrm{H\,m^{-1}} \quad \text{absolute magnetic permeability of vacuum}$$

$$\varepsilon_0 = \frac{1}{\mu_0 c^2} = 8.8542 \times 10^{-12} \,\mathrm{F\,m^{-1}} \quad \text{absolute permittivity of vacuum}$$

The wave velocity in a medium of absolute permittivity ε and permeability μ corresponding to a relative permittivity ε_r and a relative permeability μ_r compared to those of the vacuum is given by the relation

$$v = \frac{1}{\sqrt{\varepsilon \mu}} = \frac{c}{\sqrt{\varepsilon_r \mu_r}}$$

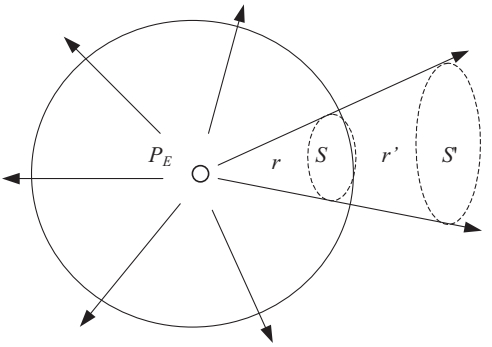

Figure 1.2 Radiation of isotropic source.

As the magnetic permeability of the medium can be regarded as equal to that of the vacuum, the wave velocity becomes

$$v \approx \frac{c}{\sqrt{\varepsilon_r}} \tag{1.10}$$

1.1.3 Power Flux Density

A very small surface that emits a uniform radiation in all directions of space inside a transparent medium is shown in Figure 1.2. The quantity of energy E radiated by such a fictitious element, called a point source or an isotropic antenna,[1] that crosses per second a certain surface S located on a sphere at a distance r is called the flux, and the ratio of this quantity to this surface is the power flux density. If we consider a second surface S' at a distance r' based on the contour of S, we see that the power flux density which crosses S' varies by a factor S/S' compared to that which crosses S, that is, by the inverse ratio of the square of the distance. Consequently, a transmitter of power P_E supplying an isotropic antenna generates a power flux density P_D on the surface of the sphere of radius r equal to

$$P_D = \frac{P_E}{4\pi r^2} \tag{1.11}$$

[1]An isotropic antenna radiating in an identical way in all directions of space could not have physical existence because of the transverse character of the electromagnetic wave propagation, but this concept has been proven to be very useful and it is common practice to define the characteristics of an antenna compared to an isotropic source, whose theoretical diagram of radiation is a sphere, rather than to the elementary doublet of Hertz or the half-wave doublet.

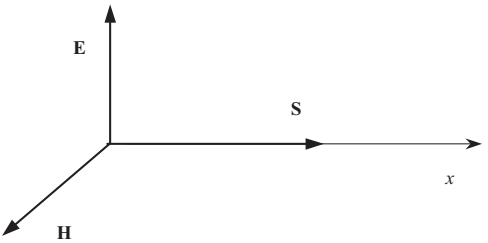

Figure 1.3 Poynting's vector.

1.1.4 Field Created in Free Space by Isotropic Radiator

The power flux density, created at a sufficiently large distance d so that the spherical wave can be regarded as a plane wave,[2] can also be expressed by using Poynting's vector, illustrated in Figure 1.3, which is defined by the relation

$$\mathbf{S} = \mathbf{E} \wedge \mathbf{H} \qquad (\mathrm{W\,m^{-2}}) \tag{1.12}$$

where $\mathbf{H} = \mathbf{B}/\mu_0$ in a vacuum and the electric field **E** in volts per meter, magnetic field **H** amperes per meter, and Poynting vector **S** watts per square meter orientated in the direction of propagation form a direct trirectangular trihedron.

The electric field and magnetic field are connected in the vacuum by the scalar relation

$$\frac{E}{H} = \sqrt{\frac{\mu_0}{\varepsilon_0}} = Z_0 = 120\pi \approx 377\,\Omega \tag{1.13}$$

where Z_0 is the impedance of the vacuum and the modulus of Poynting's vector—or power flux density—is completely defined by the electric field in the relation

$$S = \frac{E^2}{Z_0} \tag{1.14}$$

1.1.5 Wave Polarization

An important property of an electromagnetic wave is its polarization, which describes the orientation of the electric field E. In general, the electric field of

[2]A plane wave is a mathematical and nonphysical solution of Maxwell's equations because it supposes an infinite energy, but a spherical wave all the more approaches the structure of the plane wave since it is distant from its point of emission.

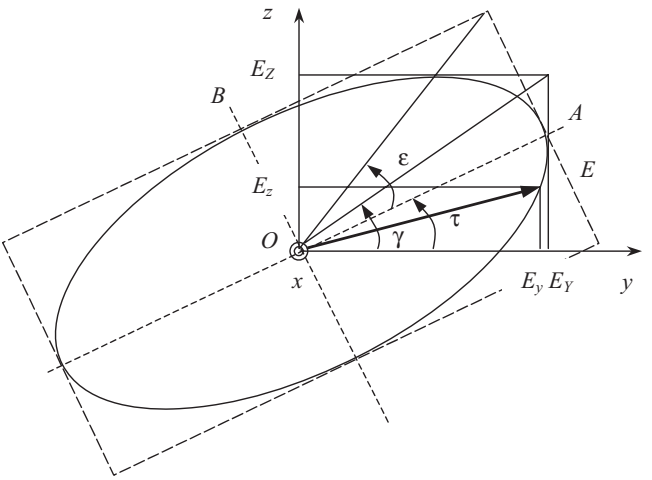

Figure 1.4 Electric field resultant vector.

a wave traveling in one direction may have components in both other orthogonal directions and the wave is said to be elliptically polarized.

Consider a plane wave traveling out through the page in the positive x direction, as shown in Figure 1.4, with electric field components in the y and z directions as given by

$$E_y = E_Y \sin(\omega t - \beta x) \tag{1.15}$$

$$E_z = E_Z \sin(\omega t - \beta x + \delta) \tag{1.16}$$

where E_Y = modulus of component according to y (constant)
E_Z = modulus of component according to z (constant)
δ = phase difference between E_y and E_z

Equations (1.15) and (1.16) describe two linearly polarized waves which combine vectorially to give the resultant field:

$$\mathbf{E} = \mathbf{E}_y + \mathbf{E}_z$$

It follows that

$$\mathbf{E} = \mathbf{E}_Y \sin(\omega t - \beta x) + \mathbf{E}_Z \sin(\omega t - \beta x + \delta)$$

At the origin ($x = 0$),

$$E_y = E_Y \sin \omega t$$

$$E_z = E_Z \sin(\omega t + \delta)$$

$$E_z = E_Z(\sin \omega t \cos \delta + \cos \omega t \sin \delta)$$

and thus

$$\sin \omega t = \frac{E_y}{E_Y}$$

$$\cos \omega t = \sqrt{1 - \left(\frac{E_y}{E_Y}\right)^2}$$

Rearranging these equations in order to eliminate time yields

$$\frac{E_y^2}{E_Y^2} - \frac{2E_y E_z \cos \delta}{E_Y E_Z} + \frac{E_z^2}{E_Z^2} \tag{1.17}$$

or $aE_y^2 - bE_y E_z + cE_z^2$ where

$$a = \frac{1}{E_Y^2 \sin^2 \delta} \qquad b = \frac{2 \cos \delta}{E_Y E_Z \sin^2 \delta} \qquad c = \frac{1}{E_Z^2 \sin^2 \delta}$$

Equation (1.17) describes the polarization ellipse with tilt angle τ and whose semimajor axis OA and semiminor axis OB determine the axial ratio AR $\ni (1, \infty)$:

$$\text{AR} = \frac{OA}{OB} \tag{1.18}$$

If $E_Y = 0$, the wave is linearly polarized in the z direction.
If $E_Z = 0$, the wave is linearly polarized in the y direction.
If $E_Y = E_Z$, the wave is linearly polarized in a plane at angle of 45°.
If $E_Y = E_Z$ with $\delta = \pm 90°$, the wave is circularly polarized (left circularly polarized for $\delta = +90°$ and right circularly polarized for $\delta = -90°$).

The polarization is right circular if the rotation of the electric field is clockwise with the wave receding and left circular if it is counterclockwise. It is also possible to describe the polarization of a wave in terms of two circularly polarized waves of unequal amplitude, one right (E_r) and the other left (E_l). Thus, at $x = 0$

$$E_r = E_R e^{j\omega t} \qquad E_l = E_L e^{-j(\omega t + \delta')}$$

where δ' is the phase difference. Then,

$$E_y = E_R \cos\omega t + E_L \cos(\omega t + \delta') \qquad E_z = E_R \sin\omega t + E_L \sin(\omega t + \delta') \tag{1.19}$$

The other parameters can be determined from the properties of Poincaré's sphere:

$$\cos 2\gamma = \cos 2\varepsilon \cos 2\tau \qquad \tan\delta = \frac{\tan 2\varepsilon}{\sin 2\tau}$$

$$\tan 2\tau = \tan 2\gamma \cos\delta \qquad \sin 2\varepsilon = \sin 2\gamma \sin\delta$$

As a function of time and position, the electric field of a plane wave traveling in the positive x direction is given by

$$E_y = E_Y e^{j(\omega t - \beta x)} \qquad E_z = E_Z e^{-j(\omega t - \beta x + \delta)}$$

$$\mathbf{E} = \mathbf{E}_Y e^{j(\omega t - \beta x)} + \mathbf{E}_Z e^{-j(\omega t - \beta x + \delta)}$$

The magnetic field components H associated respectively to E_y and E_z are

$$H_z = H_Y e^{j(\omega t - \beta x - \theta)} \qquad H_y = -H_Z e^{j(\omega t - \beta x + \delta - \theta)}$$

where θ is the phase lag of H in the absorbing medium ($\theta = 0$ in a lossless medium).

The total H field vector is thus

$$\mathbf{H} = \mathbf{H}_Y e^{j(\omega t - \beta x + \theta)} - \mathbf{H}_Z e^{j(\omega t - \beta x + \delta - \theta)}$$

The average power of the wave per unit area, or power flux density, is given by the Poynting's vector formula:

$$S = \frac{1}{2}[E_Y H_Y + E_Z H_Z]\cos\theta$$

which in a lossless medium becomes[3]

$$S = \frac{1}{2}\frac{E_Y^2 + E_Z^2}{Z_0} \tag{1.20}$$

as

$$E = \sqrt{E_Y^2 + E_Z^2} \qquad H = \sqrt{H_Y^2 + H_Z^2}$$

[3]This equation takes into account the absolute values of the electric field instead of the root-mean-square (rms) values for relation (1.14).

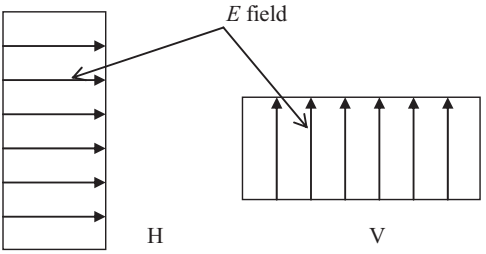

Figure 1.5 Representation of linear polarization H and V.

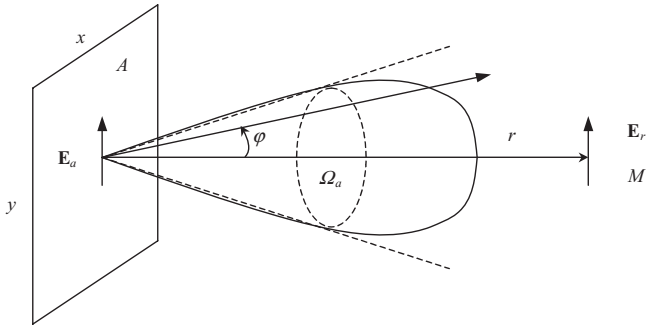

Figure 1.6 Radiation pattern of planar rectangular aperture.

As linear polarization is mostly used, Figure 1.5 shows the direction of the electric field relative to the position of a waveguide for horizontal (H) and vertical (V) polarizations.

1.2 RADIANT CONTINUOUS APERTURE

1.2.1 Expression of Directivity and Gain

Consider planar rectangular aperture of surface A uniformly illuminated by an electromagnetic wave whose field conserves an intensity E_a and a direction constant, as illustrated in Figure 1.6, and a point M located in the normal direction and at a sufficiently large distance r so that the wave reradiated by the aperture and received at this point can be regarded as a plane wave. Moreover, the dimensions of the aperture are large in front of the wavelength λ, we suppose that is, $x, y > 10\lambda$. By summing the contributions at distance r of all the elements of current uniformly distributed in the aperture of dimensions (x, y), we obtain the relation

$$E_r(\varphi) = -\frac{j\omega\mu y e^{-j\beta r}}{4\pi r Z} \int E(x) e^{j\beta x \sin\varphi} dx \tag{1.21}$$

where $E(x) = E_a$
- x = transverse dimension of aperture
- y = vertical dimension of aperture
- φ = angle compared to perpendicular to aperture
- A = area of aperture, = $x\ y$
- Z = intrinsic wave impedance of propagation medium

The field E_r has as a modulus

$$|E_r| = \frac{|E_a|}{r\lambda} A \tag{1.22}$$

We can associate a radiation pattern to the radiant aperture characterized by the following:

- A gain G compared to isotropic radiation:

$$G = \frac{P}{P'} \tag{1.23}$$

  where P, P' are the powers of the transmitter which would generate the same field at a given distance by means respectively of an isotropic antenna and the radiant aperture.
- A beam solid angle Ω_a, in which would be concentrated all the energy if the power flux density remained constant and equal to the maximum value inside this angle, represented by φ and ϕ in two orthogonal planes:

$$\Omega_a = \iint_{4\pi} g(\varphi, \phi) d\Omega$$

  where

$$g(\varphi, \phi) = \frac{G(\varphi, \phi)}{G}$$

Under these conditions, the power radiated by the aperture can be written as

$$P = \frac{|E_a|^2}{Z} A = \frac{|E_r|^2}{Z} r^2 \Omega_a$$

which yields

$$\Omega_a = \frac{|E_a|^2}{|E_r|^2}\frac{A}{r^2}$$
$$= \frac{\lambda^2}{A}$$

Since $G = 4\pi/\Omega_a$, we find the general expression of the directivity of an antenna,

$$G = \frac{4\pi A}{\lambda^2} \tag{1.24}$$

and, taking account of the efficiency, its gain,

$$G = \frac{\eta 4\pi A}{\lambda^2} = \frac{4\pi A_e}{\lambda^2} \tag{1.25}$$

where η = efficiency of antenna
A_e = its effective area

or, according to the diameter of the antenna when it is about a circular aperture,

$$G = \eta\left[\frac{\pi D}{\lambda}\right]^2 \tag{1.26}$$

with $A = \pi D^2/4$. An isotropic antenna having a theoretical gain equal to unity we can deduce its equivalent area, which still does not have physical significance, while posing from the relation (1.24):

$$\frac{4\pi A_{\text{eq}}}{\lambda^2} = 1$$

that is,

$$A_{\text{eq}} = \frac{\lambda^2}{4\pi} \tag{1.27}$$

According to the principle of reciprocity, the characteristics of an antenna are the same at the emission as at the reception.

Using the power received by an isotropic antenna, which is equal to

$$P = A_{\text{eq}} S$$

we can deduce the power flux density:

$$S = \frac{4\pi P}{\lambda^2} \tag{1.28}$$

1.2.2 Radiation Pattern

Here we will consider aperture-type antennas whose dimensions are at least 10 times higher than the wavelength used. When a conducting element of infinite size is placed in an electromagnetic field, it undergoes a certain induction; a current of induction then circulates on its surface and this element in turn radiates energy. The spatial distribution of this radiation can be defined by integration of the distribution of these elements of surface current by using the principle of superposition of energy. As the dimensions of the antennas are necessarily finished, we observe additional radiation located in angular zones not envisaged by calculations relating to the radiation and which are due to diffraction on the edges of the aperture.

The distribution of the field $E(\sin\varphi)$ at long distances corresponds to Fourier's transform of the distribution of the field $E(X)$ in the aperture, which can be written as

$$E(\sin\varphi) = \int_{-\infty}^{+\infty} E(X) e^{j2\pi X \sin\varphi} dX$$

where $X = x/\lambda$ and reciprocally as

$$E(X) = \int_{-\infty}^{+\infty} E(\sin\varphi) e^{-j2\pi X \sin\varphi} d(\sin\varphi)$$

When the aperture has a finished dimension L, these expressions become

$$E(\sin\varphi) = \int_{-L/2}^{+L/2} E(X) e^{j2\pi X \sin\varphi} dX \tag{1.29}$$

$$E(X) = \int_{-L/2}^{+L/2} E(\sin\varphi) e^{-j2\pi X \sin\varphi} d(\sin\varphi)$$

where $L = l/\lambda$. The radiation pattern thus depends on both the distribution of the field in the aperture, or the law of illumination, and its dimensions. Expression (1.29) is similar to expression (1.21), previously obtained by integration of the distribution of surface current, the first giving the relative value of the remote field and the second its absolute value.

For example, we will consider a rectangular aperture of sides a and b subjected to a uniform primary illumination, as shown in Figure 1.7. The radiation pattern can be expressed by the relation

$$\frac{E}{E_0} = \frac{\sin u}{u} \tag{1.30}$$

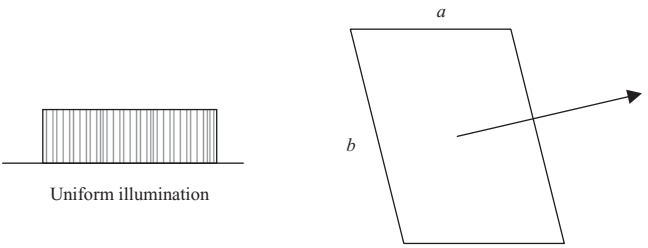

Figure 1.7 Rectangular aperture subjected to uniform illumination.

where

$$u = \begin{cases} \dfrac{\pi a}{\lambda}\sin\varphi \quad \text{(rad)} & \text{according to dimension } a \\ \dfrac{\pi b}{\lambda}\sin\varphi \quad \text{(rad)} & \text{according to dimension } b \end{cases}$$

from which

$$\frac{P}{P_0} = \left(\frac{\sin u}{u}\right)^2$$

The radiation pattern is presented versus u in Figure 1.8. As shown in the figure, this radiation pattern has a main beam, or main lobe, associated with minor lobes, called side lobes, whose relative levels are –13.3 dB for the first side lobe, –17.9 dB for the second, –20.8 dB for the third, and so on.

There are a number of factors that affect the side-lobe performance of an antenna, such as the aperture illumination function, the edge diffraction, and the feed spillover. By using a decreasing primary illumination toward the edges of the aperture (e.g., parabolic law, triangular, Gaussian, cosine squared), it is possible to reduce and even remove the minor lobes but at the cost of a widening of the main lobe and a reduction of the nominal gain.

The total beamwidth at half power for each dimension of the aperture corresponds to the values

$$\theta_{T3\text{dB}} = \begin{cases} 0.886\dfrac{\lambda}{a} & \text{according to dimension } a \\ 0.886\dfrac{\lambda}{b} & \text{according to dimension } b \end{cases}$$

In the case of a circular aperture of diameter D subjected to a uniform illumination, the diagram of radiation is given by the relation

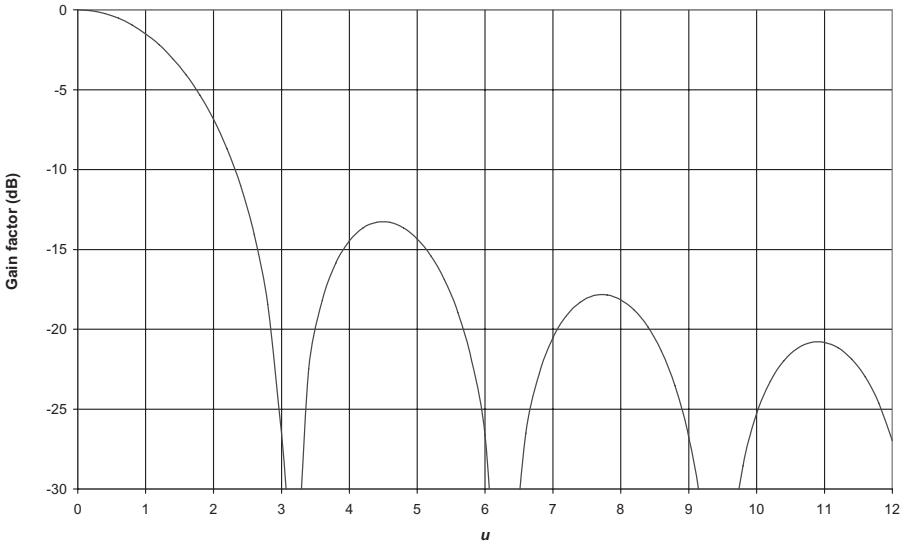

Figure 1.8 Radiation pattern of rectangular aperture subjected to uniform illumination.

$$\frac{E}{E_0} = C\frac{J_1(u)}{u} \tag{1.31}$$

where $J_1(u)$ is Bessel's function of order 1 and

$$u = \frac{\pi D}{\lambda}\sin\varphi \qquad \text{(rad)}$$

that is,

$$\frac{P}{P_0} = \left(C\frac{J_1(u)}{u}\right)^2$$

The levels of the minor lobes relative to the main lobes, as illustrated by Figure 1.9, are located respectively at –17.6 dB, –22.7 dB, –25.3 dB, and so on.

In the same way, it is possible to reduce the side-lobe level with decreasing illumination toward the edges. Using, for example, a tapered parabolic distribution of the form $(1 - r^2)^p$ with

$$r = \frac{\rho}{R}$$

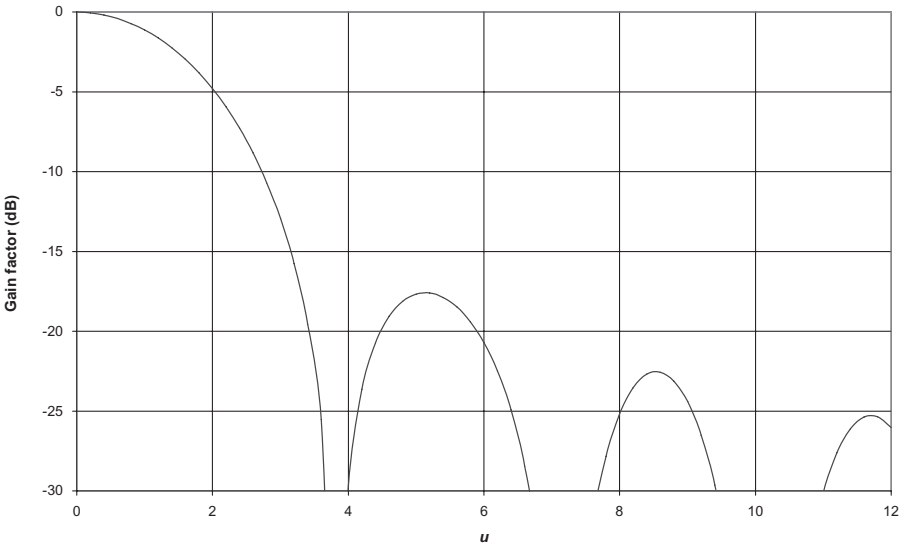

Figure 1.9 Radiation pattern of circular aperture subjected to uniform illumination.

where R is the radius of the aperture ($0 < \rho < R$), we obtain for various decreasing scale parameter p the characteristics of the radiation pattern presented in the table below (Silver, 1986):

p	Gain Reduction	Total Half-Power Beamwidth (rad)	First Zero	First Lobe (dB)
0 (uniform)	1	$1.02\frac{\lambda}{D}$	$\arcsin\left(\frac{1.22\lambda}{D}\right)$	17.6
1	0.75	$1.27\frac{\lambda}{D}$	$\arcsin\left(\frac{1.63\lambda}{D}\right)$	24.6
2	0.56	$1.47\frac{\lambda}{D}$	$\arcsin\left(\frac{2.03\lambda}{D}\right)$	30.6

1.2.3 Near Field and Far Field

Three zones in a field diffracted by a radiating aperture versus distance are illustrated in Figure 1.10, with each features well defined:

1. *Rayleigh's Zone* This is the near-field zone, which extends at the distance

$$Z_{\text{Rayleigh}} = \frac{D^2}{2\lambda} \tag{1.32}$$

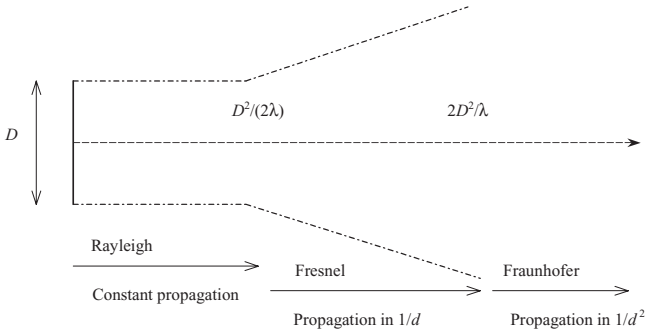

Figure 1.10 Zones of radiation of an aperture.

in a square projected aperture of size D (in meters) uniformly illuminated at a wavelength λ (in meters). Inside this zone, the energy is propagated in a tube delimited by the aperture D by presenting an equal-phase wave front and some oscillations of the amplitude versus the longitudinal axis. The extent of Rayleigh's zone depends on the form of the aperture and the distribution of the field inside the zone; for instance:

(a) For a circular projected aperture of diameter D and uniform illumination

$$Z_{\text{Rayleigh}} = 0.82\frac{D^2}{2\lambda}$$

(b) For a circular aperture and illumination of parabolic type

$$Z_{\text{Rayleigh}} = 0.61\frac{D^2}{2\lambda}$$

2. *Fresnel's Zone* This is the intermediate zone, where the diffracted field starts and the wave front tends to become spherical, which extends with a law for attenuation in $1/d$ at the distance

$$Z_{\text{Fresnel}} = 2\frac{D^2}{\lambda} \tag{1.33}$$

3. *Fraunhofer's Zone* Beyond Fresnel's zone, the energy is propagated in an inverse ratio to the square of the distance (law in $1/d^2$) and the radiant characteristics of the aperture are well defined (radiation pattern, positions and levels of the minor lobes, gain in the axis, spherical wave front).

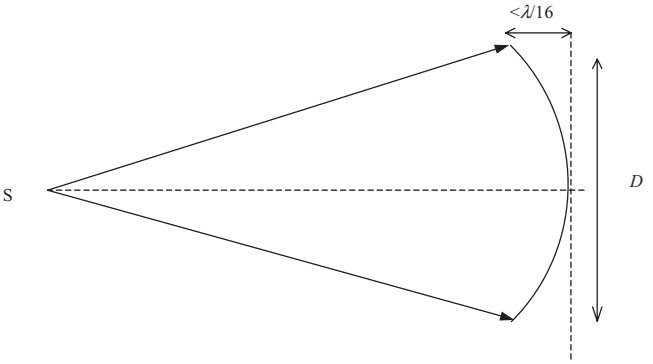

Figure 1.11 Plane wave in far field.

The far-field zone also corresponds to the distance beyond which the difference between the spherical wave and the plane wave becomes lower than $\lambda/16$, as shown in the Figure 1.11.

1.2.4 Effective Aperture

The effective aperture of an antenna for an electromagnetic plane wave linearly polarized at the emission as at the reception is defined by the relation

$$A_e = \frac{P_R}{P_D} \tag{1.34}$$

where P_R = power available at antenna port
P_D = power flux density given by relation (1.11)

1.2.5 Skin Effect

This effect appears when a conductor is traversed by a sinusoidal current and results in an increase of high-frequency resistance; in particular, the efficiency of the feeders as well as the reflectors of the antennas is thus affected.

By considering a conductor of conductivity σ and permeability μ limited by an insulator by which arrives the plane wave at frequency f whose direction of propagation is perpendicular to the surface of the conductor, we show that the current density amplitude decreases exponentially inside the conductor starting from the surface of separation according to the relation

$$i = i_0 \exp\left(-\frac{x}{\delta}\right) \tag{1.35}$$

where x is the penetration depth in meters and the critical depth δ (in meters) is given by the relation

$$\delta = \frac{1}{\sqrt{\pi\mu\sigma f}} = \frac{503.3}{\sqrt{\mu_r \sigma f}}$$

where μ = absolute permeability ($\mathrm{H\,m^{-1}}$)
μ_r = relative permeability, = μ/μ_0
σ = conductivity (S)
f = frequency (Hz)

For example, for steel and copper, we obtain the following δ values by frequency f:

	50 Hz	10 kHz	1 MHz	100 MHz	10 GHz
Steel	0.33 mm	0.024 mm	2.4 μm	0.24 μm	0.024 μm
Copper	8.5 mm	0.6 mm	60 μm	6 μm	0.6 μm

In the case of propagation in a round conductor, the current density decreases in the same way starting from its periphery.

1.3 GENERAL CHARACTERISTICS OF ANTENNAS

1.3.1 Expression of Gain and Beamwidth

The nominal or maximum isotropic gain in the far field of circular aperture-type antennas, expressed in dBi, can be calculated by using the relation in Section 1.2.1:

$$G_{\max} = \eta\left[\frac{\pi D}{\lambda}\right]^2 \tag{1.36}$$

where η = total efficiency[4] of antenna, in general between 0.5 and 0.7
D = diameter (m)
λ = wavelength (m)

The total half-power beamwidth (3 dB) of the antenna, expressed in degrees, is given by the approximate formula

$$\alpha_T \approx 69.3\frac{\lambda}{D} \tag{1.37}$$

[4]The total efficiency of the antenna depends on numerous factors, such as the tapering illumination function, the spillover loss, the phase error, and the surface accuracy.

or $\pm 34.65(\lambda/D)$. The gain $G(\varphi)$ relative to the isotropic antenna, expressed in dBi, in the direction φ relative to the axis is given by the following approximate relation which is valid for the main lobe of radiation:

$$G(\varphi) = G_{\max} - 12\left(\frac{\varphi}{\alpha_T}\right)^2 \tag{1.38}$$

where φ and α_T are in degrees. These formulas are also used to determine the following:

- Antennas gain loss due to their possible misalignment (e.g., action of the wind) or variation of the launch and arrival angles of the rays according to the conditions of refractivity of the atmosphere
- Discrimination of reflected ray compared to direct ray
- Level of signals coming from other transmitters of a network that interfere with the useful signal during setup of the frequency and polarization plan

Figure 1.12 illustrates the nominal isotropic gain and total half-power beamwidth versus frequency, calculated using relations (1.36) and (1.37), for various sizes of antennas usually employed in terrestrial microwave links and satellite communications.

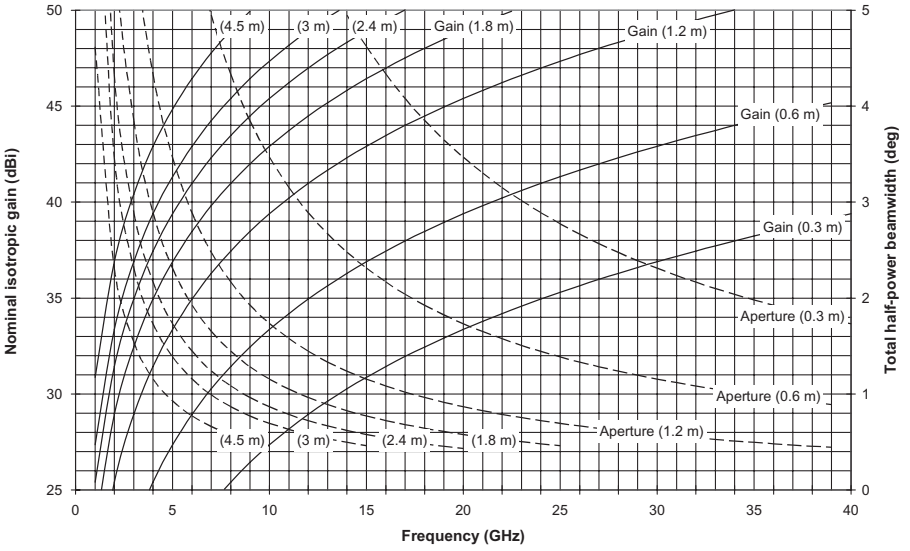

Figure 1.12 Nominal isotropic gain and total half-power beamwidth versus frequency.

When the apertures are not of revolution type, we can employ the general relation

$$G_{\max} = \eta \frac{4\pi(\text{sr})}{\alpha_T \beta_T} = \eta \frac{4\pi(57.3^\circ)^2}{\alpha_T \beta_T} = \eta \frac{41{,}253}{\alpha_T \beta_T} \tag{1.39}$$

or

$$G_{\max} = \eta \frac{4\pi D_\alpha D_\beta}{\lambda^2} = \frac{4\pi A_{\text{eff}}}{\lambda^2}$$

where α_T = total half-power beamwidth corresponding to D_α dimension
β_T = total half-power beamwidth corresponding to D_β dimension
A_{eff} = effective aperture area

By taking account of the efficiency, we can employ the approximate formulas

$$G_{\max} \approx \begin{cases} \dfrac{25{,}000}{\alpha_T \beta_T} & \text{at } 1\text{–}6\,\text{GHz} \\ \dfrac{30{,}000}{\alpha_T \beta_T} & \text{at } 6\text{–}18\,\text{GHz} \end{cases}$$

Generally, the size of the antennas is determined by the microwave radio link budget, which is necessary to achieve the performances goals of the connection.

1.3.2 Reference Radiation Patterns

Radiation patterns must comply with rules of coordination defined by the International Telecommunication Union (ITU)[5] in order to reduce mutual interference as much as possible not only between microwave line-of-sight radio relay systems but also between radio relay systems and services of satellite communications. In the absence of particular features concerning the radiation pattern of antennas used in line-of-sight radio relay systems, ITU-R F.699 recommends for coordination aspects adopting the reference radiation pattern given in dBi by the following formulas, which are valid between 1 and 40 GHz in the far field:

[5]The complete texts of the ITU recommendations cited can be obtained from Union Internationale des Télécommunications, Secrétariat Général—Service des Ventes et Marketing, Place des Nations CH-1211, Genera 20, Switzerland.

- If $D/\lambda \le 100$:

$$G(\varphi) = \begin{cases} G_{MAX} - 2.5 \times 10^{-3} \left[\dfrac{D}{\lambda} \varphi \right]^2 & \text{FOR } 0 < \varphi < \varphi_m \\ G_1 & \text{FOR } \varphi_m \le \varphi < \dfrac{100\lambda}{D} \\ 52 - 10 \log \left[\dfrac{D}{\lambda} \right] - 25 \log \varphi & \text{FOR } \dfrac{100\lambda}{D} \le \varphi < 48^\circ \\ 10 - 10 \log \left[\dfrac{D}{\lambda} \right] & \text{FOR } 48^\circ \le \varphi \le 180^\circ \end{cases} \tag{1.40}$$

- If $D/\lambda > 100$:

$$G(\varphi) = \begin{cases} G_{\max} - 2.5 \times 10^{-3} \left[\dfrac{D}{\lambda} \varphi \right]^2 & \text{for } 0 < \varphi < \varphi_m \\ G_1 & \text{for } \varphi_m \le \varphi < \varphi_r \\ 32 - 25 \log \varphi & \text{for } \varphi_r \le \varphi < 48^\circ \\ -10 & \text{for } 48^\circ \le \varphi \le 180^\circ \end{cases} \tag{1.41}$$

where $G(\varphi)$ = gain referred to isotropic antenna (dBi)
G_{Max} = maximum isotropic gain of main lobe (dBi)
φ = angle off the axis (deg)
D = diameter of antenna (m)
λ = wavelength (m)
G_1 = gain of first minor lobe (dBi), $= 2 + 15 \log(D/\lambda)$
φ_m $= (20\lambda/D)\sqrt{G_{\max} - G_1}$
ϕ_r $= 15.85[D/\lambda]^{-0.6}$

Figure 1.13 presents reference antenna radiation patterns related to $G_{\max}$ for the main-lobe and side-lobe envelopes which correspond to standard antennas. Antennas with high-performance radiation have a notably weaker side-lobe level as well as a higher front-to-back ratio. If only the maximum gain of the antenna is known, the ratio D/λ can be evaluated by using

$$20 \log \left[\frac{D}{\lambda} \right] \approx G_{MAX} - 7.7$$

When the total half-power beamwidth is known, $G_{\max}$ can be obtained by the relation

$$G_{\max} = 44.5 - 20 \log \alpha_T$$

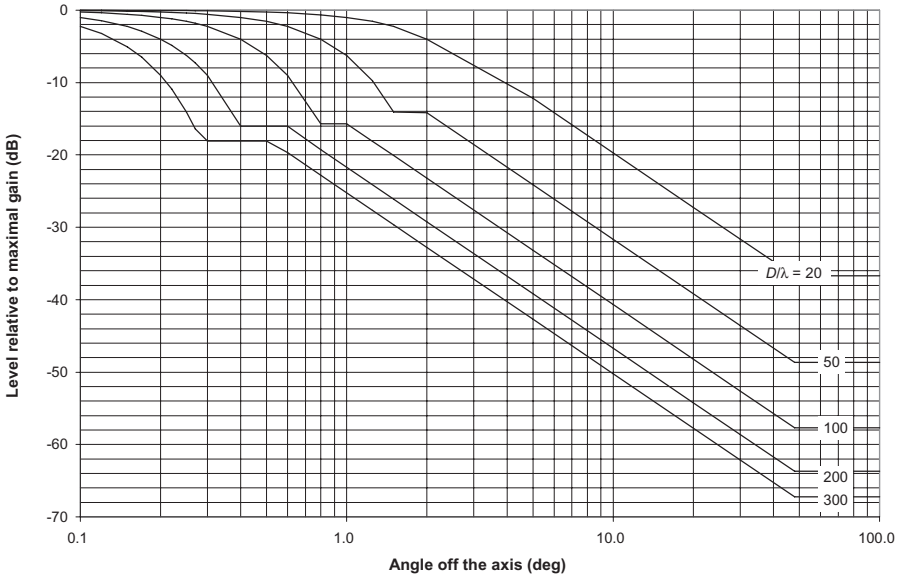

Figure 1.13 Reference antenna radiation patterns compared to G_{max}.

In horn-type and "offset" antennas, we can employ the following relation, which is valid apart from the main lobe and for $\varphi < 90°$:

$$G = 88 - 30\log\frac{D}{\lambda} - 40\log\varphi \tag{1.42}$$

It is of course preferable to take into account the real or guaranteed radiation patterns of the antennas in the budget links and calculations related to jamming in order to avoid problems when using frequency sharing and frequency reuse techniques.

More specifically, concerning the coordination between fixed services by satellite, recommendation ITU-R S.465 gives the following values for antenna radiation patterns, expressed in dBi, in the frequency bands ranging between 2 and 30 GHz:

$$G = \begin{cases} 32 - 25\log\varphi & \text{for } \varphi_{min} \le \varphi \le 48° \\ -10 & \text{for } 48° \le \varphi \le 180° \end{cases} \tag{1.43}$$

where φ_{min} equals 1° or $100\lambda/D$ by taking the highest value. In systems used before 1993 and for $D/\lambda \le 100$

$$G = \begin{cases} 52 - 10\log\left(\dfrac{D}{\lambda}\right) - 25\log\varphi & \text{for } \left(\dfrac{100\lambda}{D}\right) \le \varphi \le 48^\circ \\ 10 - 10\log\left(\dfrac{D}{\lambda}\right) & \text{for } 48^\circ \le \varphi \le 180^\circ \end{cases}$$

The gain variation due to reflector surface errors can be obtained by the following approximate formula, by considering the effective value of the irregularities ε:

$$\Delta G = 10\log\left[\exp\left(-\frac{4\pi\varepsilon}{\lambda}\right)^2\right] \approx -686\left(\frac{\varepsilon}{\lambda}\right)^2 \tag{1.44}$$

It is advisable to make sure that the radiation pattern of the selected antenna makes it possible to respect the maximum levels of equivalent isotropic radiated power [EIRP, in decibels related to 1 W (dBW)] or maximum equivalent isotropic radiated spectral densities (dBW per hertz) which are authorized by the ITU rules of radiocommunications concerning both useful signal and nonessential radiations.

The values to be taken into account depend on the frequency band as well as the type of service to protect (fixed or mobile service using, e.g., radio relay systems or satellites); for example:

- The direction of the maximum radiation of an antenna delivering higher EIRP than +35 dBW must deviate by at least 2° the orbit of the geostationary satellites in the frequency bands ranging between 10 and 15 GHz.
- If it is not possible to conform to this recommendation, the EIRP should not exceed +47 dBW in any direction deviating by less 0.5° the geostationary orbit or from +47 to +55 dBW (8 dB per degree) in any direction ranging between 0.5° and 1.5°.
- The power provided to the antenna should not exceed +13 dBW in the frequency bands ranging between 1 and 10 GHz and +10 dBW in the higher-frequency bands.

These arrangements must be taken at both emission and reception sites in order to ensure the highest possible protection against jamming.

1.3.3 Characteristics of Polarization

In practice, the majority of antennas radiate in linear or circular polarization, which are particular cases of elliptic polarization as described in Section 1.1.5.

For any elliptic polarization, we can define an orthogonal polarization whose direction of rotation is opposite; two waves with orthogonal polarization in theory being insulated, the same antenna can simultaneously receive and/or emit two carriers at the same frequency with polarizations horizontal and vertical or circularly right and left. We can also show that any radio wave with elliptic polarization can be regarded as the sum of two orthogonal components, for example, of two waves with perpendicular linear polarization or two waves circularly right and left polarized.

In ordinary radio communication systems, waves are usually completely polarized and the electric field corresponding to the useful signal is great compared to the cross-polarized unwanted signal; under such conditions, the moduli of the orthogonal components are close to the semimajor and semiminor axes of the polarization ellipse presented in Figure 1.4.

Elliptic polarization may thus be characterized by the maximum and minimum levels according to the nominal polarization and its opposite in the following parameters:

- Axial ratio:

$$\mathrm{AR} = \frac{E_{\max}}{E_{\min}} \tag{1.45}$$

- Ellipticity ratio:

$$\mathrm{ER} = \frac{\mathrm{AR}+1}{\mathrm{AR}-1} = \frac{E_{\max}+E_{\min}}{E_{\max}-E_{\min}} \tag{1.46}$$

or, in decibels,

$$\mathrm{ER} = 20\log\left[\frac{E_{\max}+E_{\min}}{E_{\max}-E_{\min}}\right]$$

An important feature of the radio wave consists in its purity of polarization, that is, the relationship between the copolarized component, which represents the useful signal, and the cross-polarized component, which constitutes the unwanted signal. The relationship between the useful signal and the unwanted one is called cross-polarization discrimination[6] XPD, expressed in decibels and given by the relation

[6]Between orthogonally polarized signals, a cross-polarization discrimination on the order of 30–40 dB can be expected.

$$\mathrm{XPD} = 20\log[\mathrm{AR}] = 20\log\left(\frac{\mathrm{ER}+1}{\mathrm{ER}-1}\right) \tag{1.47}$$

For an ellipticity ratio lower or equal to 3 dB, we can also employ the following approximate formulas with XPD and ER expressed in decibels:

$$\mathrm{XPD} = 24.8 - 20\log[\mathrm{ER}] \qquad \mathrm{ER} = 17.37\ 10^{-\mathrm{XPD}/20}$$

Due to its imperfections, an antenna will thus generate some useful signal on the regular polarization at the same time as an unwanted signal on the orthogonal polarization, which may parasitize another carrier; this feature is related to the purity of polarization at the transmission side. In the same way, an antenna may receive some useful signal on one polarization at the same time as some part of another signal transmitted on the opposite polarization; this feature concerns the cross-polarization isolation at the reception side.

1.4 FREE-SPACE LOSS AND ELECTROMAGNETIC FIELD STRENGTH

1.4.1 Attenuation of Propagation

Consider an isotropic source supplied with a transmitter of power P_E and an isotropic reception antenna located at a distance d. The received power P_R is the product of the power flux density created at the distance d by the effective aperture area A_e of the reception antenna. Starting from relations (1.11) and (1.34), we can write

$$P_R = \frac{P_E A_e}{4\pi d^2} \tag{1.48}$$

where A_e = effective area of isotropic radiator (m^2) = $\lambda^2/(4\pi)$
d = distance (m)
λ = wavelength (m)

The free-space attenuation A_{FS} between two isotropic antennas is thus equal to

$$\frac{P_R}{P_E} = \frac{1}{4\pi d^2}\frac{\lambda^2}{4\pi}$$

that is,

$$\frac{P_R}{P_E} = \left[\frac{\lambda}{4\pi d}\right]^2 = \frac{1}{A_{\mathrm{FS}}} \tag{1.49}$$

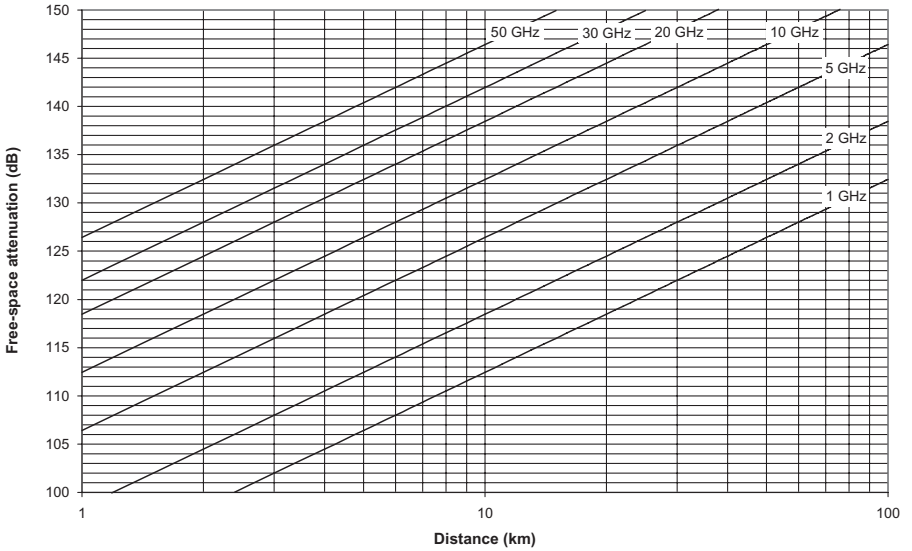

Figure 1.14 Free-space attenuation versus distance.

from which, expressed in decibels,

$$A_{\text{FS}} = 20\log\left(\frac{4\pi d}{\lambda}\right)$$

Supposing, now, that the transmitting antenna has a gain G_E compared to an isotropic[7] radiator and the reception antenna a gain G_R, we obtain the general relation of free-space loss according to the wavelength and the distance expressed in meters:

$$\frac{P_R}{P_E} = G_E G_R\left[\frac{\lambda}{4\pi d}\right]^2 \tag{1.50}$$

Figure 1.14 shows the free-space attenuation versus distance at various frequencies.

1.4.2 Electromagnetic Field Strength

The product of the emitted power and the gain of the transmitting antenna corresponds to the EIRP, expressed in Watts, and the received power can still be expressed by the relation

[7]It is shown that in free space the absolute gain of a Hertz doublet is 1.75 dB and that of a half-wave doublet is 2.15 dB.

$$P_R = \text{EIRP} G_R \left[\frac{\lambda}{4\pi d}\right]^2 \tag{1.51}$$

where

$$\text{EIRP} = P_E G_E \tag{1.52}$$

In the transmission omnidirectional-type a system or one that is common to several receivers, such as broadcasting or telecommunications by satellite, it may be preferable to express the field strength in terms of power flux density or of electric field or even of magnetic field by using the following relations for free space:

$$\text{Power flux density:} \quad S(\text{W m}^{-2}) = \frac{\text{EIRP}}{4\pi d^2} = \frac{E^2(\text{V m}^{-1})}{120\pi} = \frac{4\pi p_{\text{riso}}}{\lambda^2}$$

$$\text{Electric field:} \quad E(\text{V m}^{-1}) = \frac{\sqrt{30\text{EIRP}}}{d}$$

$$\text{Magnetic field:} \quad H(\text{A m}^{-1}) = \frac{E(\text{V m}^{-1})}{120\pi} = \sqrt{\frac{\text{EIRP}}{480\pi^2 d^2}}$$

where P_{riso} is the power, expressed in watts, collected by an isotropic radiator. Certain authors also use the unit dBμV, which is equivalent to the power received by comparison to that which would be developed by a field of $1\,\mu\text{V m}^{-1}$ expressed in decibels. Then

$$1\,\mu\text{V m}^{-1} = 10^{-6}\,\text{V m}^{-1}$$

from which

$$P(\mu\text{V m}^{-1}) = 10^{-12} P(\text{V m}^{-1})$$

or

$$0\,\text{dB}(\mu\text{V m}^{-1}) \Leftrightarrow -120\,\text{dB}(\text{V m}^{-1})$$

$$0\,\text{dB}(\mu\text{V m}^{-1}) \Leftrightarrow -145.8\,\text{dB}(\text{W m}^{-2})$$

$$0\,\text{dB}(\text{W m}^{-2}) \Leftrightarrow 0\,\text{dBW} + 10\log\left(\frac{\lambda^2}{4\pi}\right)$$

Figure 1.15 shows, for example, the relationship between the electric field expressed in Volts per meter and the power flux density in decibels (watts per square meter). In addition, the unit used to characterize transmitter–antenna

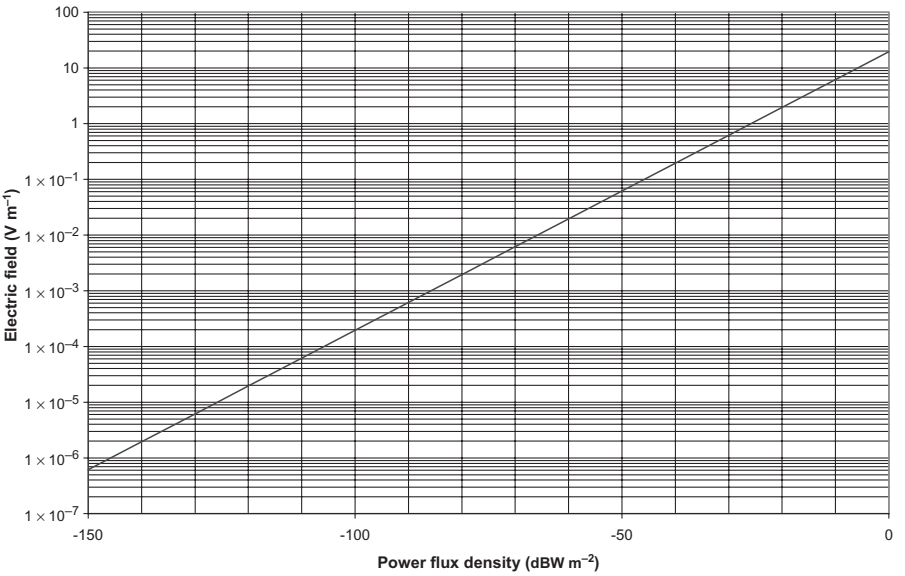

Figure 1.15 Relationship between electric field and power flux density.

systems for broadcasting purposes, called cymomotive force, is the product of the electric field and the distance and is usually expressed in volts and, according to the type of reference antenna, has the expression

$$E(\text{mV m}^{-1})d(\text{km}) = k\sqrt{P(\text{kW})}$$

where

$$K = \begin{cases} 173 & \text{for isotropic radiator} \\ 212 & \text{for Hertz doublet} \\ 222 & \text{for half-wave doublet} \end{cases}$$

Finally, a unit of power often employed, dBm, refers to decibels relative to 1 mW of power, that is,

$$0\,\text{dBm} \leftrightarrow -30\,\text{dBW} \qquad 0\,\text{dBW} \leftrightarrow 30\,\text{dBm}$$

1.5 REFLECTOR AND PASSIVE REPEATER

1.5.1 Reflector in Far Field

A reflector of surface S, as illustrated in Figure 1.16, reflects, under an angle of incidence α referred to the normal to the reflector, an electromagnetic wave

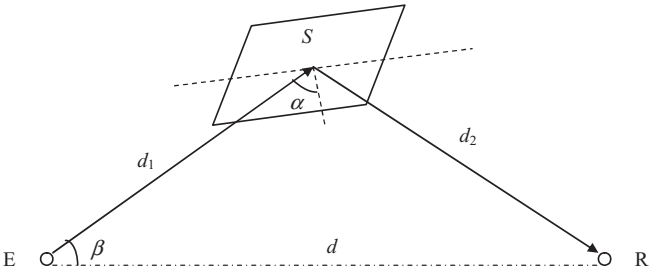

Figure 1.16 Reflector in far field.

issued from a transmitter located at a distance d_1 toward a receiver located at a distance d_2 with an efficiency of reflection η. In the case of a plane reflector, the reflected wave presents the same coherence of phase as the incidental wave and, because of the symmetry inherent in the reflection, the apparent area S_a (projected surface) seen by the transmitter is identical to that which is seen by the receiver and can be written as

$$S_a = S\cos\alpha \tag{1.53}$$

Indicating by G_{rp} the directivity of the reflector in the direction of the receiver, we can write, according to relation (1.25), that

$$G_{rp} = \frac{\eta 4\pi S_a}{\lambda^2} \tag{1.54}$$

Assuming that the antennas used at the emission and at the reception are isotropic and that the reflector is placed in the far field of both antennas, we can write that the ratio of the received power to the emitted power is equal to

$$\left(\frac{P_R}{P_E}\right)_{\text{iso}} = \frac{\eta S_a}{4\pi d_1^2} G_{rp}\left[\frac{\lambda}{4\pi d_2}\right]^2$$

that is, the product of flux density per unit power created at the level of the reflector at distance d_1 according to relation (1.11) by

- the effective area of the reflector $\eta\, Sa$,
- the gain G_{rp} of the reflector toward the receiver compared to an isotropic antenna according to relation (1.54), and
- the attenuation between isotropic antennas at distance d_2 according to relation (1.49), from which we get the general relation for isotropic radiating–receiving antennas which is independent of wavelength:

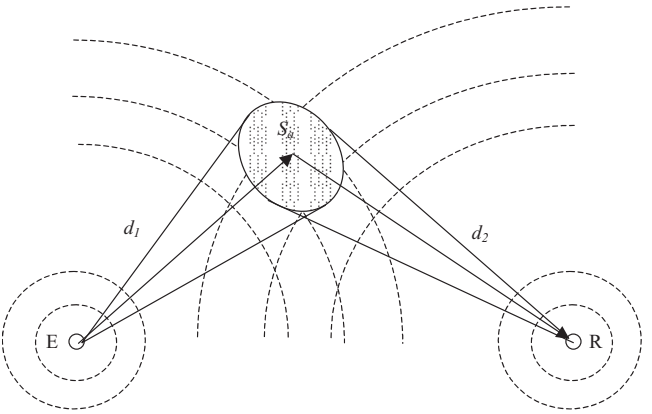

Figure 1.17 Transmitter and receiver solid angles.

$$\left(\frac{P_R}{P_E}\right)_{\text{iso}} = \left[\frac{\eta S_a}{4\pi d_1 d_2}\right]^2 \tag{1.55}$$

We easily find the same result when considering, as illustrated in Figure 1.17, solid angles seen by the transmitter and the receiver of the same effective surface ηS_a; the relationship between the received power and the emitted power is then equal to the product of the ratios:

- $\eta S_a/(4\pi d_1^2)$ (effective surface of reflector/surface of sphere of radius d_1)
- $\eta S_a/(4\pi d_2^2)$ (effective surface of reflector/surface of sphere of radius d_2)

The total reflection efficiency η^2 is a function of the dimensions of the reflector, its surface condition, and the incidence angle. By supposing that the radiating and receiving antennas are not isotropic but have respectively gains G_E and G_R, we obtain the general relation

$$\frac{P_R}{P_E} = G_E G_R \left[\frac{\eta S_a}{4\pi d_1 d_2}\right]^2 \tag{1.56}$$

or

$$\frac{P_R}{P_E} = G_E G_R \left[\frac{\eta S \cos\alpha}{4\pi d_1 d_2}\right]^2$$

The reflector gain is defined from

$$\left(\frac{P_R}{P_E}\right)_{\text{iso}} = G_P \left[\frac{\lambda}{4\pi d_1}\right]^2 \left[\frac{\lambda}{4\pi d_2}\right]^2 = \left[\frac{\eta S \cos\alpha}{4\pi d_1 d_2}\right]^2$$

from which

$$G_P = \left[\frac{4\pi\eta S\cos\alpha}{\lambda^2}\right]^2 \tag{1.57}$$

We can also deduce the total equivalent gain G_{Pe} of the link comprising a far-field reflector compared to the direct link which would be carried out in free space between the transmitter and the receiver using isotropic antennas:

$$\left(\frac{P_R}{P_E}\right)_{\text{iso}} = \left[\frac{\eta S_a}{4\pi d_1 d_2}\right]^2 \approx G_{Pe}\left[\frac{\lambda}{4\pi d}\right]^2$$

that is,

$$G_{Pe} \approx \left[\frac{\eta S_a}{4\pi d_1 d_2}\right]^2\left[\frac{4\pi d}{\lambda}\right]^2$$

where the first term represents the total attenuation of propagation in two hops by reflection on the reflector according to relation (1.55) and the second term corresponds to the attenuation of propagation between isotropic antennas over the overall length of the link in free space according to the relation (1.49) while supposing $d \approx d_1 + d_2$, resulting in

$$G_{Pe} \approx \left[\frac{\eta S_a d}{\lambda d_1 d_2}\right]^2 \tag{1.58}$$

Alternatively, if

$$d = (d_1 + d_2)\frac{\sin\alpha}{\sin(\alpha+\beta)}$$

then

$$G_{Pe} \approx \left[\frac{\eta S\cos\alpha(d_1+d_2)\sin\alpha}{\lambda d_1 d_2\sin(\alpha+\beta)}\right]^2 \tag{1.59}$$

using the meter as the unit.

Apart from the zones close to the source of emission or the receiving antenna, the gain of the system with the reflector compared to the direct link is lower than unity and is a minimum value when $d_1 = d_2$, that is, when the reflector is in the middle of the connection, which is the case for the target radar.

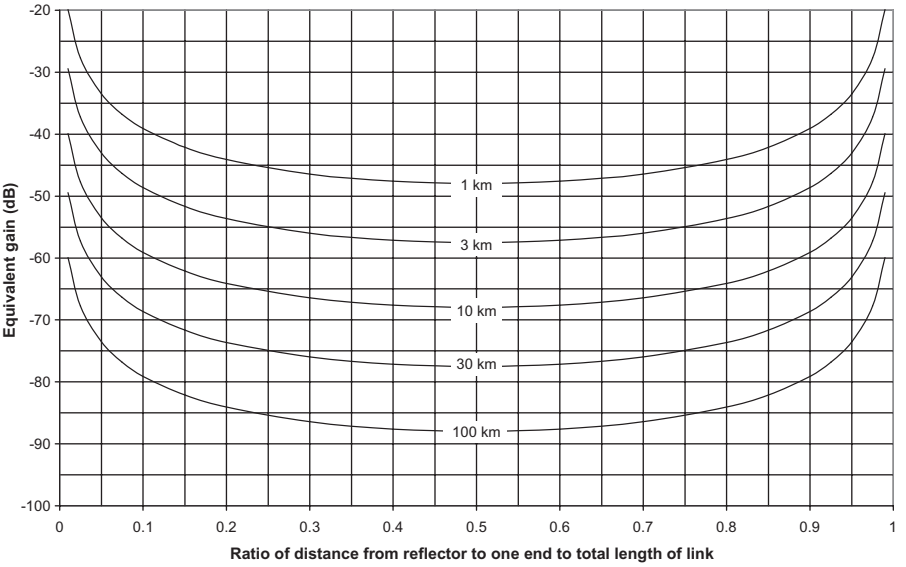

Figure 1.18 Equivalent gain of reflector of reduced surface $S_a/\lambda = 1$ in far field versus length of connection and relative position to one of the ends.

Figure 1.18 illustrates the equivalent gain G_{Pe} of a system using a reflector of reduced surface $S_a/\lambda = 1$ versus the relationship between the distance from the reflector to one of the ends and the overall length of the link, d_1/d or d_2/d, assuming $d \approx d_1 + d_2$. To determine the equivalent gain of a given system using a reflector, of which the dimensions and the relative position to the ends are known, it is enough to add to the results obtained on the graph 1.18 the quantity $[\eta S_a/\lambda]^2$ expressed in decibels with S_a in square meters and λ in meters.

The use of a far-field reflector is thus of interest only if it is set up close to one end of the link and its performance has to be compared with the attenuation resulting from diffraction on the obstacle to ensure there is no risk of self-interference. We will avoid, consequently, placing the reflector in the same plane as the two stations in order to benefit from the discrimination brought on by the antennas. Moreover, since the reflection polarizes the electromagnetic waves, the plane of reflection will have to coincide as much as possible with the plane of polarization for, by supposing that they differ by an angle θ, it would result in a significant reduction in gain, which can be evaluated using the general relation for antennas:

$$G(\theta) = G_0 \cos^2 \theta \tag{1.60}$$

For a radar-type reflector at a distance d which returns the wave toward the source, we indicate the product $G_{rp}\eta S_a$ by the equivalent target cross section S_{eq} and obtain the equation of the radar for an isotropic source:

$$\frac{P_R}{P_E} = S_{\text{eq}} \frac{\lambda^2}{(4\pi)^3 d^4}$$

where $S_{\text{eq}} = G_{rp}\eta S_a$. If the radar antenna has a gain G, we then obtain the general equation for a radar system:

$$\frac{P_R}{P_E} = G^2 S_{\text{eq}} \frac{\lambda^2}{(4\pi)^3 d^4} \tag{1.61}$$

1.5.2 Passive Repeater in Far Field

A passive repeater consists of two antennas placed at a distance d_1 from the transmitter and d_2 from the receiver and connected back to back as presented in Figure 1.19. By supposing that the transmitting antenna has a gain G_E compared to an isotropic radiator and the receiving antenna a gain G_R, just as the antennas constituting the passive repeater have a gain G'_E and G'_R, and by considering a loss in the connecting feeder P_f, we can write the general relation of global loss, which includes two sections of length d_1 and d_2 in cascade, according to relation (1.50):

$$\frac{P_R}{P_E} = \frac{G_E G'_R}{P_f}\left[\frac{\lambda}{4\pi d_1}\right]^2 G'_E G_R \left[\frac{\lambda}{4\pi d_2}\right]^2$$

That is,

$$\frac{P_R}{P_E} = \frac{G_E G_R G'_E G'_R}{P_f}\left[\frac{\lambda^2}{(4\pi)^2 d_1 d_2}\right]^2 \tag{1.62}$$

This expression can also be written if both repeater antennas are identical:

$$\frac{P_R}{P_E} = \frac{G_E G_R}{P_f}\left[\frac{\eta A}{4\pi d_1 d_2}\right]^2 \qquad G'_E = G'_R = \frac{\eta 4\pi A}{\lambda^2}$$

where A is the area of the antennas back to back. We find the same formula, independent of the wavelength, than that one for the far-field reflector, (1.56),

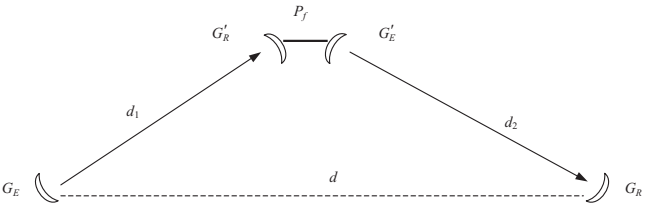

Figure 1.19 Passive far-field repeater composed of back-to-back antennas.

by replacing the apparent surface of the reflector by the effective area of the antennas connected back to back.

The gain of the passive repeater, G_P, is then equal to

$$G_P = \frac{G'_E G'_R}{P_f} \tag{1.63}$$

or

$$G_P = \left[\frac{4\pi}{\lambda^2}\right]^2 \frac{\eta_E A_E \eta_R A_R}{P_f}$$

and can also be expressed according to the antenna diameters D'_E and D'_R:

$$G_P = \frac{\eta_E D'^2_E \eta_R D'^2_R}{P_f}\left(\frac{\pi}{\lambda}\right)^4$$

with

$$A_E = \frac{1}{4}\pi D'^2_E \qquad A_R = \frac{1}{4}\pi D'^2_R$$

that is, by using identical antennas of diameter D' and efficiency η':

$$G_P = \frac{1}{P_f}\left[\frac{\eta' D'^2 \pi^2}{\lambda^2}\right]^2$$

As in the case of the far-field reflector, we can determine the total equivalent gain G_{Pe} of the link comprising a passive far-field repeater compared to the direct link which would be carried out in free space between the transmitter and the receiver using isotropic antennas while supposing $d \approx d_1 + d_2$:

$$\frac{P_R}{P_E} = G_P\left[\frac{\lambda^2}{(4\pi)^2 d_1 d_2}\right]^2 \approx G_{Pe}\left[\frac{\lambda}{4\pi d}\right]^2$$

from which

$$G_{Pe} \approx G_P\left[\frac{\lambda d}{4\pi d_1 d_2}\right]^2 \tag{1.64}$$

or

$$G_{Pe} \approx \frac{1}{P_f}\left[\frac{\eta' D'^2 \pi d}{4\lambda d_1 d_2}\right]^2$$

It appears that the only advantage of the passive repeater on the reflector lies in the fact that the back-to-back antennas are pointed respectively toward the transmitter and the receiver, which makes the device independent of the angle of deflection and makes it possible to reduce its size for an equivalent gain; however, the efficiency of a reflector can be higher than that of an antenna, which results in a higher side-lobe level.

As above, the equivalent gain G_{Pe} of the passive repeater can easily be deduced from Figure 1.18 by replacing the apparent surface of the reflector by that of the repeater antennas, that is, the quantity $\eta S_a/\lambda$ by $\eta' \pi D'^2/4\lambda$.

1.5.3 Reflector in Near Field (Periscope)

The gain of the far-field reflector, as defined previously, tends toward infinity when we bring it closer to one of the two ends of the link; this is of course not the case in reality. When the reflector, also called a "mirror," is placed in the near field of an antenna, the device constitutes a periscope, as illustrated in Figure 1.20.

The equivalent gain is defined as

$$G_{Per} = \left(\frac{G_{\text{passive}}}{G_{\text{antenna}}} \right) \left(\frac{\eta_{\text{illumination}}}{P_{\text{spillover}}} \right)$$

where the gain of the passive repeater corresponds to that of the projected aperture of area S_a given by the relation (1.25) and that of the antenna by relation (1.26):

$$G_{\text{passive}} = \frac{4\pi S_a}{\lambda^2} \qquad G_{\text{antenna}} = \eta \left[\frac{\pi D}{\lambda} \right]^2$$

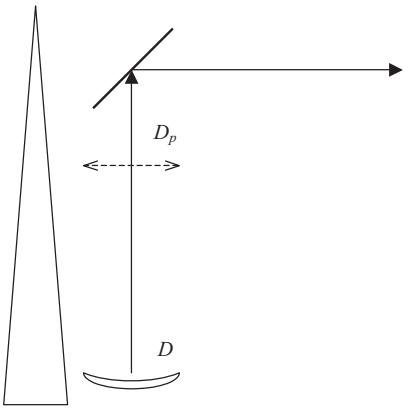

Figure 1.20 Periscope.

and the efficiency of illumination ($\eta_{\text{Illumination}}$) and the loss by spillover ($p_{\text{Spill-over}}$) depend on the height of the reflector, the relative dimensions of the antenna and reflector, and the form of the latter. Generally, the gain of this device is close to unity, which makes it possible for the unit to be freed from the usual branching losses by coaxial cables or waveguides on the height of the tower, or even greater than unity. Preferably the periscope must be placed in the meridian plane containing the antennas of both stations in order to not modify the plane of polarization. The reflector can be rectangular, octogonal, elliptic, plane, or curved, according to whether we want to improve the gain or the radiation pattern or both at the same time, the worse results being obtained with the rectangular form. For example, Figure 1.21 presents relative gain compared to the nominal gain of the antenna calculated for an elliptic plane reflector for various ratios D/D_p of respective size according to the parameter P defined by

$$P = \frac{\lambda H}{D_p^2}$$

where λ = wavelength (m)
D = antenna diameter (m)
D_p = projected diameter of reflector (m)
H = relative height of reflector (m)

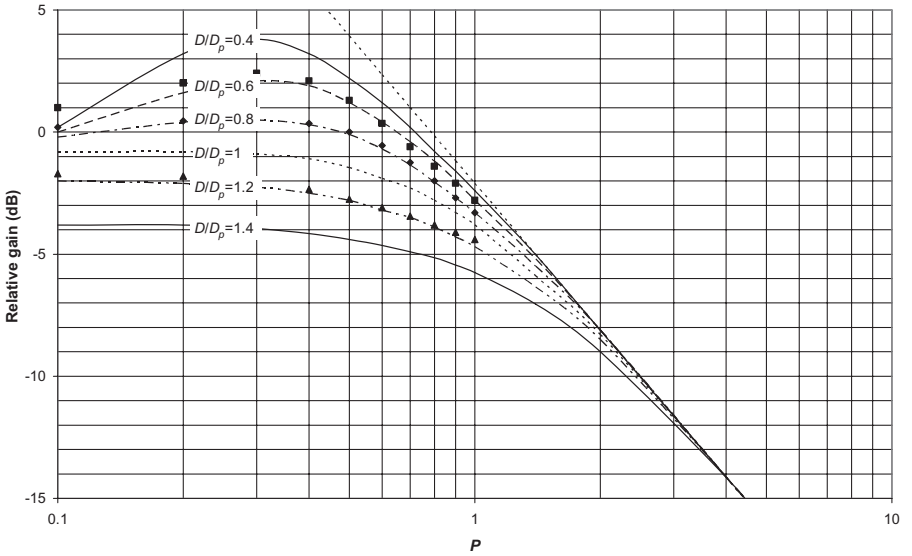

Figure 1.21 Gain of periscope comprising elliptic plane reflector versus parameter P.

These curves converge toward the asymptote, defined by the relation[8]:

$$20\log\left(\frac{\pi D_P^2}{4\lambda H}\right)$$

Also reproduced in the figure are experimental values obtained using a 46-cm antenna operating at the frequency of 8.4 GHz in combination with three elliptic plane reflectors of different sizes with the following projected diameters and relevant size ratios:

77 cm (D/Dp = 0.6)
57 cm (D/Dp = 0.8)
38 cm (D/Dp = 1.2)

For $0.6 \le D/D_p \le 1.2$ we can use the empirical formula

$$G_{Per} = \begin{cases} [0.3125\times 10^{0.9(Dp/D)} + 0.8](1+\log P) - 0.75\left(\dfrac{D}{D_p}\right)^{5.5} & P < 2 \\ \quad - 2.703\times 10^{0.41(Dp/D)}(1+\log P)^2 & \\ 20\log\left(\dfrac{\pi}{4P}\right) - \dfrac{D}{D_p(2+\log P)} & P \ge 2 \end{cases}$$

In addition to the significant gain corresponding to the suppression of the usual branching losses on the tower height, the disadvantages of this system are as follows:

- The dimensions of the reflector are in general higher than the diameter of the antenna, which can result in an increased catch of wind.
- The loss of gain due to the misalignment of the reflector varies by twice that of a parabolic antenna placed under the same conditions, since it is about a reflection, requiring a more rigid tower.
- The characteristics of radiation with reference to the side-lobe level and especially the front-to-back ratio are in general worse than those of a parabolic antenna and the presence of the tower can cause parasitic reradiations.

1.6 MODEL OF PROPAGATION

1.6.1 Spherical Diffraction

Previously a radiated wave was shown to propagate in all directions of space and that, to connect two points in space called transmitter and receiver, we

[8]This relation can be related to the relation (1.58), which corresponds to the equivalent gain of the device comprising a far-field reflector.

introduced the concept of a radioelectric ray that is characterized by an electromagnetic field and a wavelength.

According to wave motion theory, electromagnetic waves are propagated gradually due to the phenomenon of spherical diffraction, which consists in considering that each point of a wave front reemits in its turn in all directions; Augustin Fresnel showed that backward reradiation of all these point sources was destroyed and that their forward contribution depended on their respective position on the wave front.

1.6.2 Fresnel's Ellipsoid

Consider a source of emission E, a receiver R, and any plane (P) perpendicular to the line joining E and R, as shown in Figure 1.22, and determine the properties of the field received in R. James Clerck Maxwell's theory makes it possible to calculate the field received in R starting from the field created by a source E in all the points of the space that separates E and R. We can see that all points of the same circle centerd on the axis *ER* contribute by the same share since they are at the same distance from E and R and the waves they produce are consequently in phase. By neglecting the aspects related to polarization, the point at R thus receives energy coming from all the points of the plane (P) which one can break up into concentric rings by taking account of the phase which rises from the difference in pathlength, ΔL, between the axis *ER*, which constitutes the shortest path, and any path *EPR* given by the relation

$$\Delta L = EP + PR - ER$$

The contribution is positive if ΔL is smaller than a half wavelength or an add number of it and negative if not; the space between the source E and the receiver R can thus be divided into concentric ellipsoids of focus at E and R, called Fresnel's ellipsoids, such as

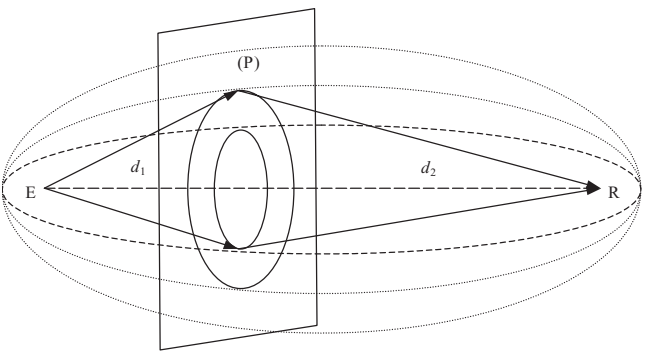

Figure 1.22 Fresnel's ellipsoid.

$$\Delta L = n\frac{\lambda}{2}$$

The first ellipsoid, obtained for $n = 1$, contains most of energy and delimits the free space. To determine the radius of each ellipsoid, we can write

$$n\frac{\lambda}{2} = \sqrt{d_1^2 + R_F^2} + \sqrt{d_2^2 + R_F^2} - d \qquad d \approx d_1 + d_2$$

from which, by limited development,

$$n\frac{\lambda}{2} \approx \frac{R_F^2}{2}\left(\frac{1}{d_1} + \frac{1}{d_2}\right) \qquad R_F \approx \sqrt{\frac{d_1 d_2 n\lambda}{d_1 + d_2}} \tag{1.65}$$

where d_1, d_2, and λ are in meters. The equatorial radius, obtained for $d_1 = d_2$, has as a value

$$R_{FM} \approx \frac{1}{2}\sqrt{dn\lambda}$$

1.7 REFLECTION AND REFRACTION

1.7.1 General Laws

An electromagnetic wave undergoes the laws of reflection and refraction at the passage of a surface separating two different media; it will be assumed that this surface is large with respect to the wavelength, just as its radius of curvature.

Figure 1.23 illustrates an electromagnetic wave reaching the surface of separation between two media of respective refractive indexes n_1 and n_2.

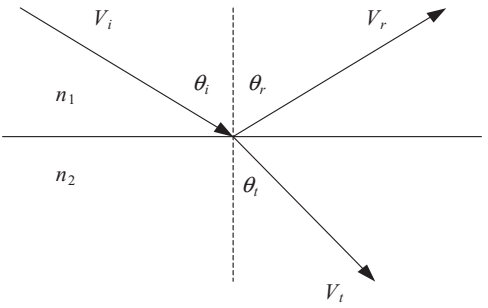

Figure 1.23 Reflection and refraction of plane electromagnetic wave.

Calling V_i, V_r, and V_t the respective velocities of propagation of the rays incident, reflected, and refracted, we can write

$$\frac{V_i}{\sin\theta_i} = \frac{V_r}{\sin\theta_r} = \frac{V_t}{\sin\theta_t} \tag{1.66}$$

where

$$V_i = \frac{c}{n_1} \qquad V_r = \frac{c}{n_1} \qquad V_t = \frac{c}{n_2}$$

from which $V_i = V_r$ and $\theta_i = \theta_r$ and

$$n_1 \sin\theta_i = n_2 \sin\theta_t \qquad \text{(Descartes' law of refraction)}$$

From relation (1.13), for each medium, we can also write

$$\frac{E}{H} = \sqrt{\frac{\mu}{\varepsilon}} = Z_0\sqrt{\frac{\mu_r}{\varepsilon_r}}$$

where Z_0 is the impedance of the vacuum and

$$c = \frac{1}{\sqrt{\varepsilon_0\mu_0}} \qquad v = \frac{c}{\sqrt{\varepsilon_r\mu_r}}$$

As μ is in general close to unity, one has $\sqrt{\varepsilon_r} \approx n$.

The coefficients of reflection E_r/E_i for horizontal polarization R_H and vertical polarization R_V are given by the fundamental relations of Fresnel:

$$R_H = \frac{\sin(\theta_i - \theta_t)}{\sin(\theta_i + \theta_t)} \qquad R_V = \frac{\tan(\theta_i - \theta_t)}{\tan(\theta_i + \theta_t)}$$

It appears that the coefficient of reflection in vertical polarization is canceled for

$$\theta_i + \theta_t = \frac{1}{2}\pi \quad \text{to which corresponds Brewster's angle}$$

$$\tan\theta_i = \frac{n_2}{n_1} \quad \text{for which the wave is completely refracted}$$

Using the angle of inclination φ, complementary to the angle of incidence θ_i, we obtains

$$R_H = \frac{\sin\varphi - \sqrt{(n_2/n_1)^2 - \cos^2\varphi}}{\sin\varphi + \sqrt{(n_2/n_1)^2 - \cos^2\varphi}}$$
$$R_V = \frac{(n_2/n_1)^2 \sin\varphi - \sqrt{[(n_2/n_1)^2 - \cos^2\varphi]/\eta^2}}{(n_2/n_1)^2 \sin\varphi + \sqrt{[(n_2/n_1)^2 - \cos^2\varphi]/\eta^2}} \tag{1.67}$$

For two media with similar indexes of refraction, for example two layers of the atmosphere separated by a plane surface through which the refractive index undergoes a small discontinuity *dn* positive or negative, the preceding relations become, with $(n_2/n_2)^2 \approx 1 + 2\ dn$,

$$R_H = \frac{\sin\varphi - \sqrt{\sin^2\varphi + 2dn}}{\sin\varphi + \sqrt{\sin^2\varphi + 2dn}}$$
$$R_V = \frac{(1+2dn)\sin\varphi - \sqrt{\sin^2\varphi + 2dn}}{(1+2dn)\sin\varphi + \sqrt{\sin^2\varphi + 2dn}} \tag{1.68}$$

Figure 1.24 presents the magnitude of the reflection coefficient according to the inclination angle and the discontinuity *dn* positive and negative for horizontal polarization. The reflection coefficient has practically the same value for both polarizations and reflection is total when the discontinuity is negative for all angles lower than the limit angle given by

$$\varphi_{\text{lim}} = \sqrt{2|dn|} \tag{1.69}$$

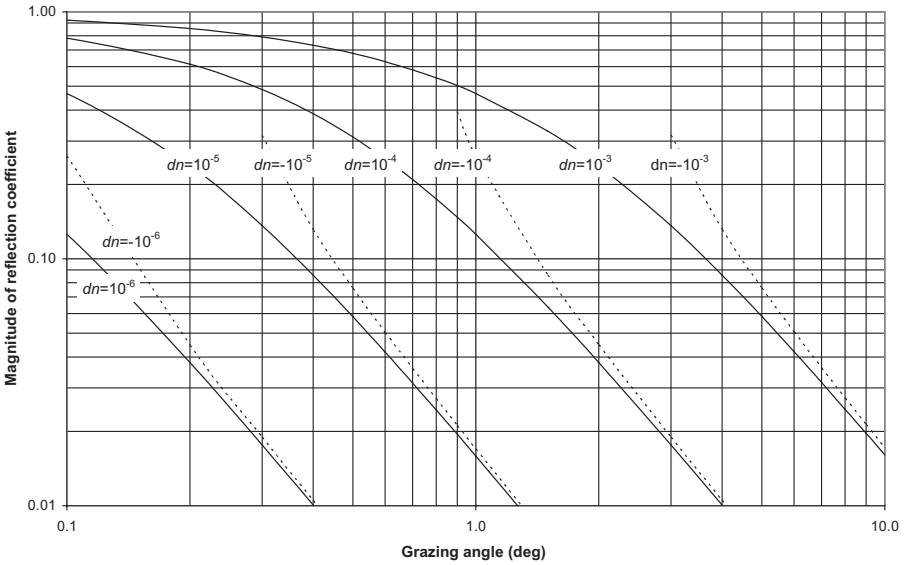

Figure 1.24 Reflection due to discontinuity of refractive index between two dielectric media.

When the surface of separation is between a dielectric medium and a conducting medium of conductivity σ, the reflection coefficient is given by the following formulas (ITU-R Rep.1008):

$$R_H = \frac{\sin\varphi - \sqrt{\eta - \cos^2\varphi}}{\sin\varphi + \sqrt{\eta - \cos^2\varphi}}$$
$$R_V = \frac{\sin\varphi - \sqrt{(\eta - \cos^2\varphi)/\eta^2}}{\sin\varphi + \sqrt{(\eta - \cos^2\varphi)/\eta^2}} \tag{1.70}$$

with the complex permittivity $\eta = \varepsilon - j60\sigma\lambda$.

The amplitude and phase difference of the reflected wave vary according to the nature of the terrain, the frequency, the grazing angle, and the polarization, as shown in Figures 1.25*a* and 1.25*b*, which illustrate reflections on the sea and on average ground. We can see that the magnitude of the reflection coefficient is close to unity for radio waves that are horizontally polarized either on the sea or on the ground.

For the majority of microwave links where the angles of reflection on the ground or in the low layers of the atmosphere are small, the magnitude of the reflection coefficient and the phase difference of the reflected wave are respectively equal to unity and 180° for horizontal polarization and close to these values for vertical polarization at frequencies greater than gigahertz and angles of reflection less than a few degrees. The reflection coefficient also depends on other factors such as divergence, related to the terrestrial curvature, roughness of the ground, and size of the reflection zone.

We have seen that most of the energy of an electromagnetic wave was contained in the first Fresnel's ellipsoid; it is necessary thus to take account of the Fresnel's ellipsoid of the reflected wave, which corresponds to that generated by a fictitious transmitter E′ symmetrical to transmitter E relative to the surface of reflection, as shown in Figure 1.26.

1.7.2 Divergence Factor

The divergence factor is given by the relation

$$D = \frac{1}{\sqrt{1 + 2d_1d_2/(Rd\sin\varphi)}} \tag{1.71}$$

where R = radius of curvature of reflective surface (km)

$$\varphi \approx \frac{H_1 + H_2}{d} - \frac{d}{4R}\left[1 + \left(\frac{d_1 - d_2}{d_1 + d_2}\right)^2\right] \quad \text{(mrad)}$$

H_1, H_2 = heights of antennas above reflection plane (m)

d, d_1, d_2 = distances (km)

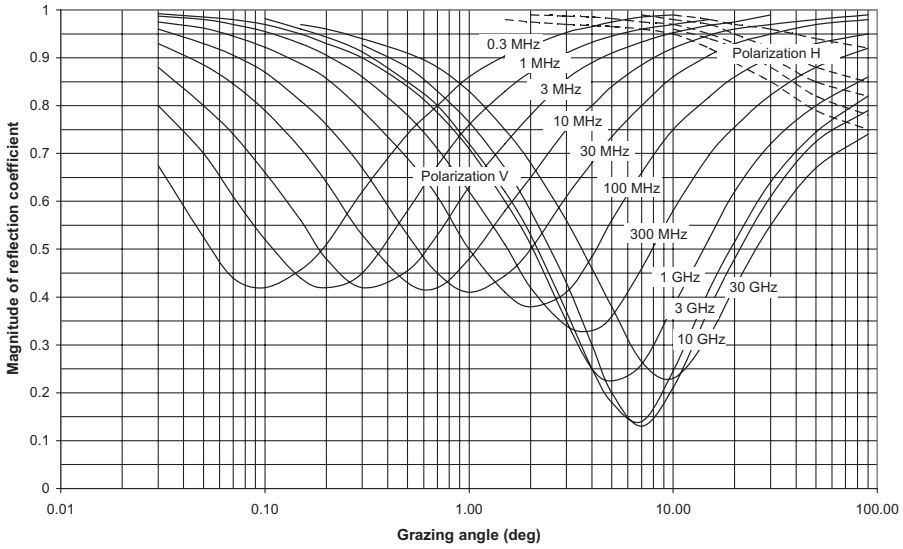

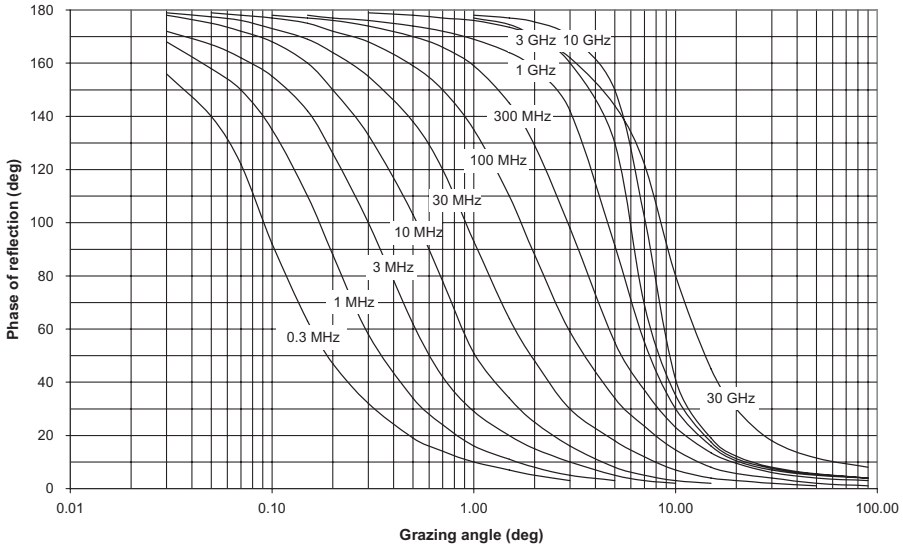

(*a*)

Figure 1.25 (*a*) Reflection on sea: magnitude and phase of coefficient of reflection of plane surface versus grazing angle in vertical (V) and horizontal (H) polarization. (*b*) Reflection on ground (average ground): Magnitude and phase coefficient of reflection of plane surface versus grazing angle in vertical (V) and horizontal (H) polarization.

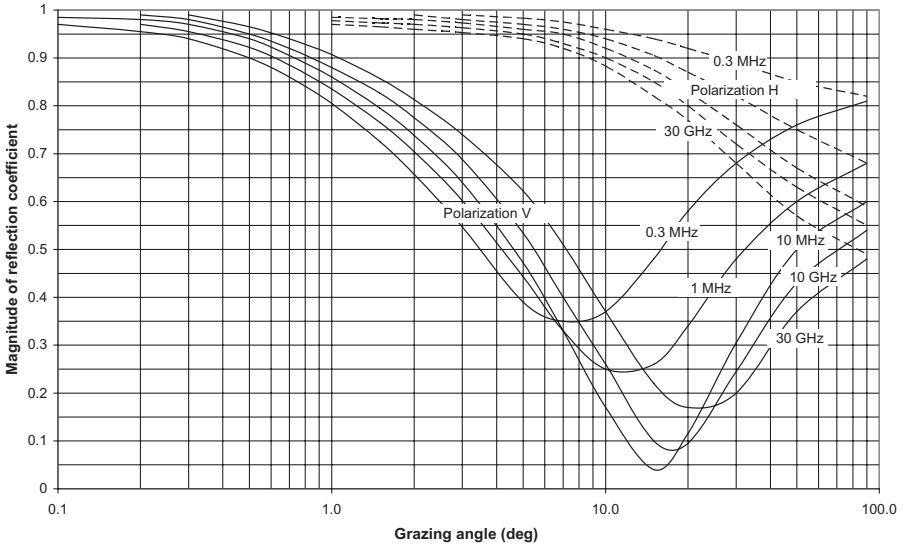

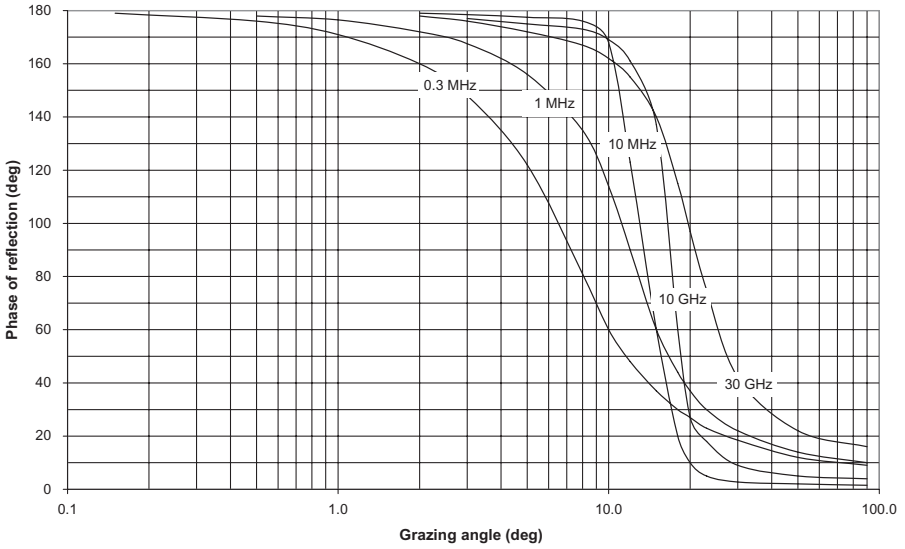

(*b*)

Figure 1.25 *Continued*

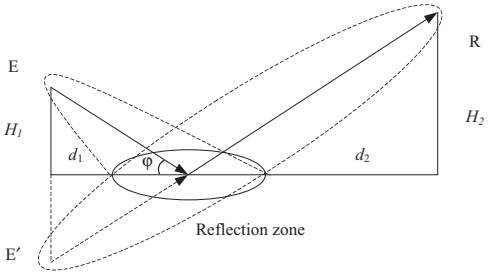

Figure 1.26 Fresnel's zone of reflected wave.

for a reflection angle higher than the limit angle:

$$\varphi_{\text{lim}} = \sqrt[3]{10\lambda} \qquad \text{(mrad)}$$

In the case of Earth–space paths, this formula becomes

$$D = \frac{1}{\sqrt{1 + 2H\tan\theta/(Rd\sin\varphi)}}$$

where $\varphi \approx E + \dfrac{H\,\text{cotan}\,\theta}{R+H}$

θ = elevation angle toward satellite

H = height of Earth station

1.7.3 Roughness Factor

The roughness factor of the reflection zone is given by a relation in ITU-R Rep.1008:

$$\rho = \exp\left[-0.5\left(\frac{4\pi\, dh\sin\varphi}{\lambda}\right)^2\right] \tag{1.72}$$

where dh is the rms height of the irregularities and $4\pi\, dh\, \sin\varphi/\lambda$ constitutes the Rayleigh criterion, illustrated in Figure 1.27. Figure 1.28 presents the magnitude of the roughness factor according to the ratio dh/λ for various values of the reflection angle.

1.7.4 Factor of Limitation of Reflection Zone

It is shown (Boithias 1983) that the limitation factor of the zone of reflection, if its edges are not too far from the reflection point, is given by the approximate relation

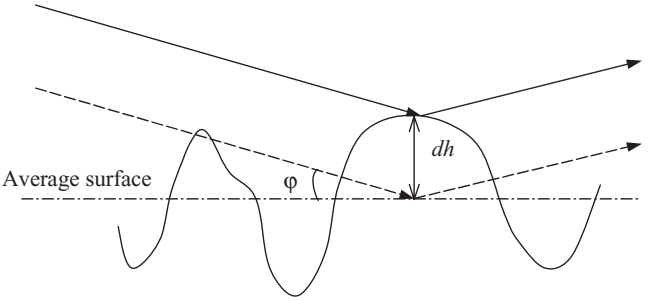

Figure 1.27 Rayleigh criterion.

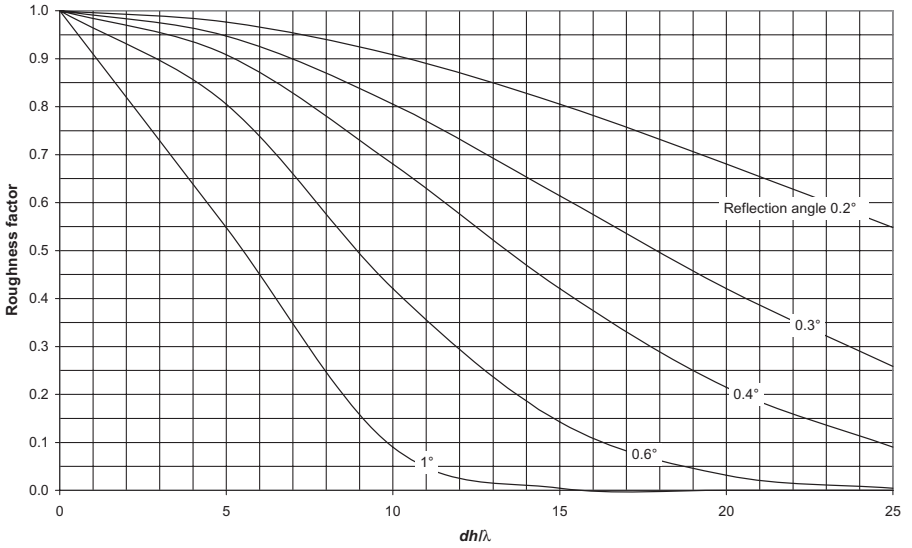

Figure 1.28 Roughness factor due to irregularities of reflective surface.

$$\frac{P}{P_0} \approx \frac{(H_1 + H_2)^4 \Delta x^2}{H_1 H_2 \lambda d^3} \tag{1.73}$$

where P = power received by reflection (W)
P_0 = power received in free space (W)
H_1, H_2 = heights of antennas above reflective surface (m)
λ = wavelength (m)
d = hop length (m)
Δx = size (m) of reflection zone extending on both sides of reflection point, represented in Figure 1.29

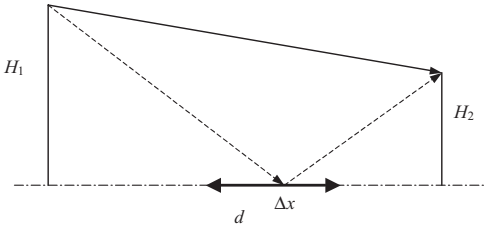

Figure 1.29 Limitation of the reflection zone.

1.8 INFLUENCE OF ATMOSPHERE

1.8.1 Refractivity

We saw that the influence of the propagation medium is entirely determined by its refractive index; the refractive index n of the air being very close to unity, we substitute the value N to it, called refractivity and expressed in N-units, such as

$$N = (n-1)\times 10^6 \tag{1.74}$$

The atmospheric pressure, temperature, and water vapor concentration influence the refractivity according to the following relation, which is valid for all frequencies up to 100 GHz:

$$N = N_{\text{dry}} + N_{\text{wet}} = 77.6\frac{P}{T} + (3.732\times 10^5)\frac{p_v}{T^2} \tag{1.75}$$

where T = temperature (K)
P = atmospheric pressure (hPa)
p_v = water vapor pressure (hPa)

The surface refractivity N_S varies with altitude according to the relation

$$N_S = N_0 \exp(-0.136h) \tag{1.76}$$

where N_0 = mean value of atmospheric refractivity reduced to sea level (N-units)
h = altitude (km)

1.8.2 Vertical Gradient of Refractive Index

World charts of monthly averages of N_0 reduced to sea level are presented in Figures 1.30 and 1.31 for the months of February and August, respectively. Failing these data, one can consider the average exponential atmosphere:

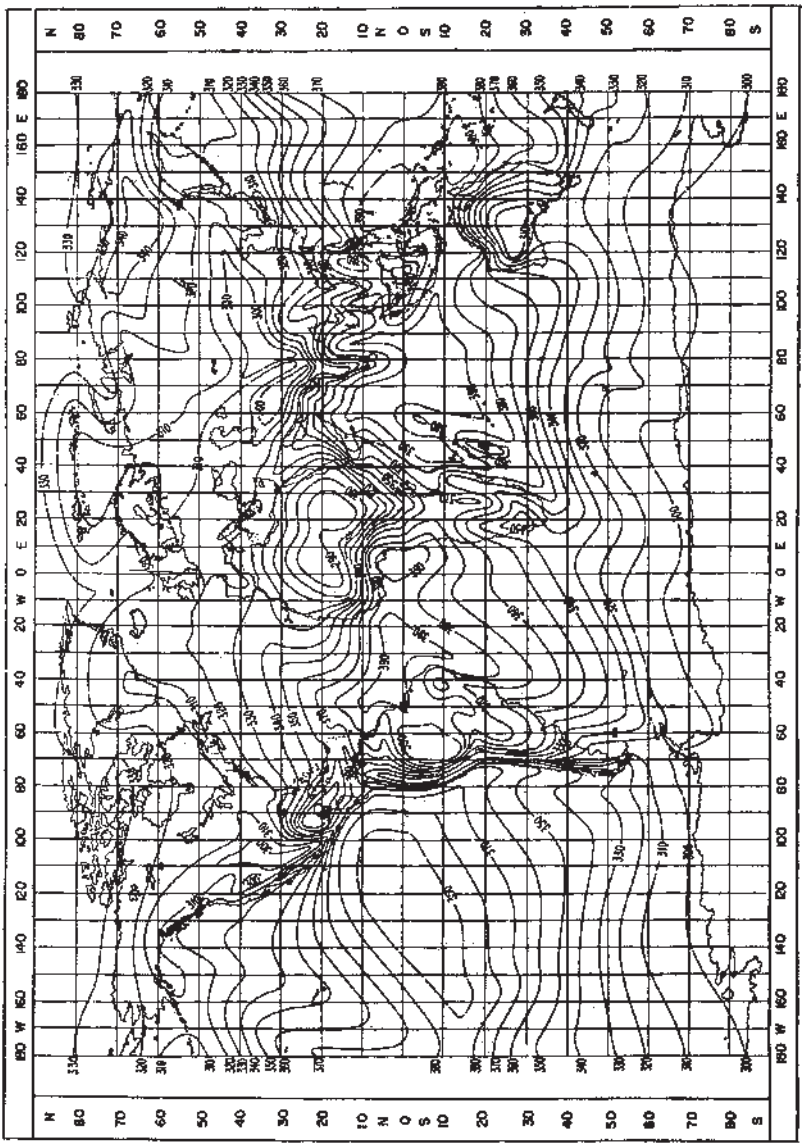

Figure 1.30 Monthly mean value of atmospheric refractivity N_0 in February (ITU-R P.453).

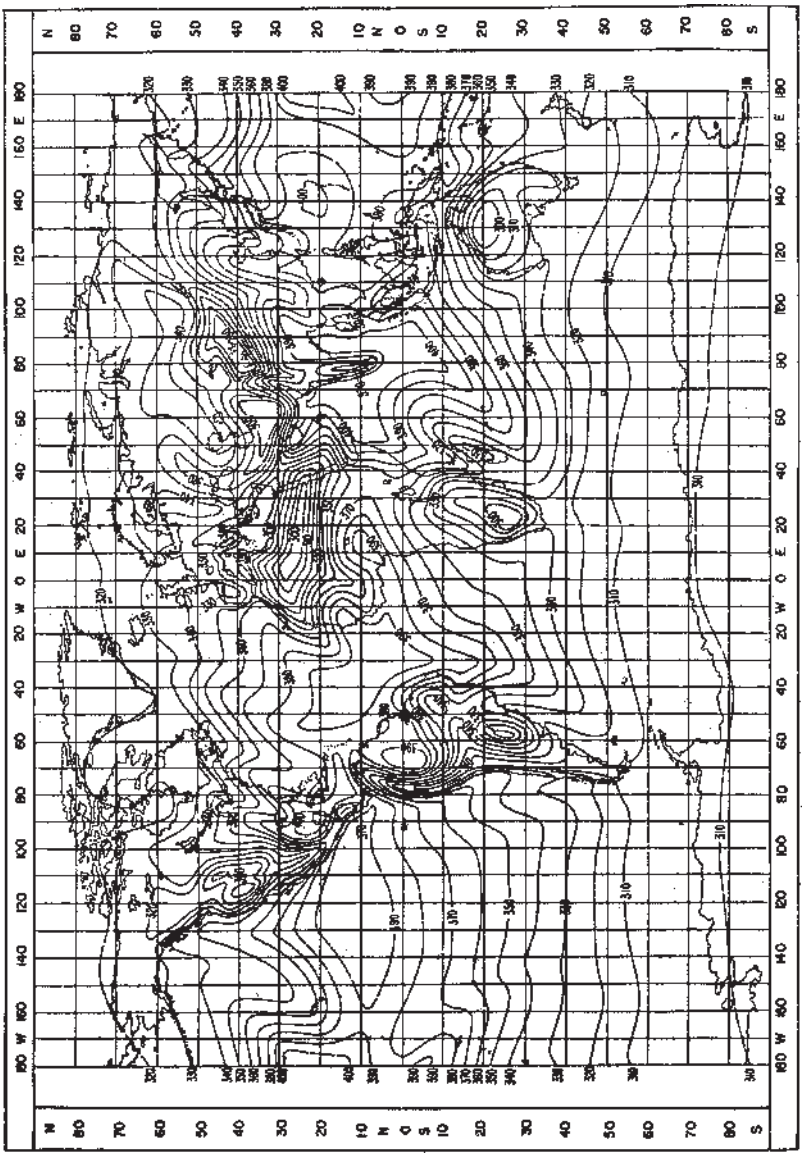

Figure 1.31 Monthly mean value of atmospheric refractivity N_0 in August (ITU-R P.453).

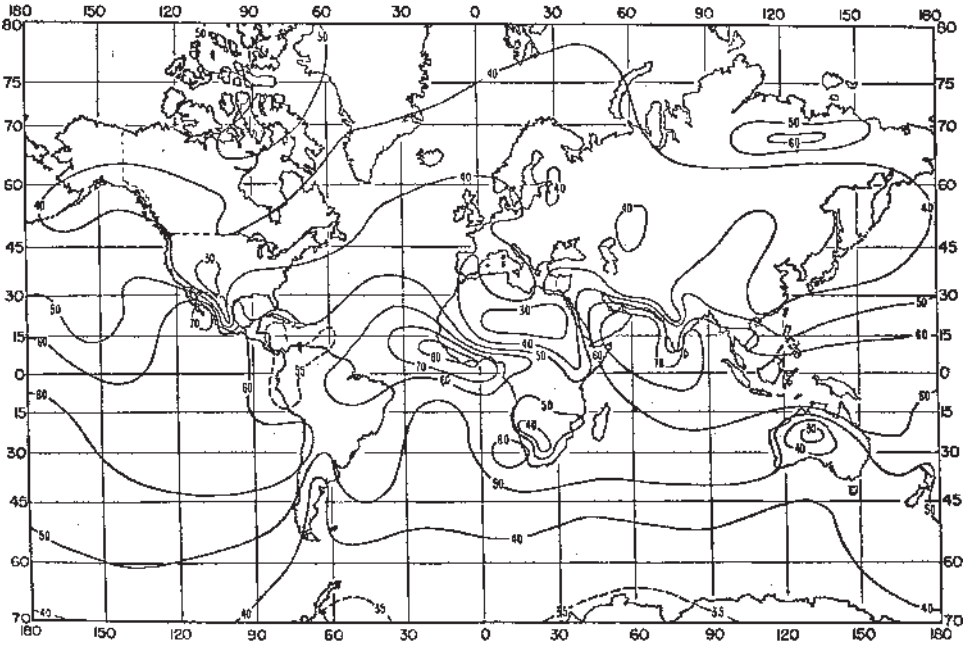

Figure 1.32 Monthly average of ΔN in February (ITU-R P.453).

$$N_S = N_A \exp(-0.136h) \tag{1.77}$$

where N_A = 315 N-units is the average value on the surface of Earth that corresponds to the standard refractivity gradient of $-40\,\mathrm{N\,km^{-1}}$ on the first kilometer. The vertical refractivity gradient *dN/dh* in the low layer of the atmosphere is an important parameter for the estimate of the effects of refraction on the electromagnetic wave propagation (ray curvature, multipath, atmospheric ducts).

Figures 1.32–1.35 show the monthly average decreases of the refractivity ΔN in a layer 1 km above the Earth surface for February, May, August, and November, respectively: that is,

$$\Delta N = N_S - N_1$$

where N_1 is the value of the refractivity at a height of 1 km above the surface, ΔN not being reduced to the reference surface. The vertical refractivity gradient varies not only according to the geographical localization but also statistically in the course of time; we thus found that, in Florida, in the first 100 m, the refractivity gradient was between 230 and $-370\,\mathrm{N\,km^{-1}}$ in values exceeded for percentages of time corresponding to 0.05 and 99.9%, respectively.

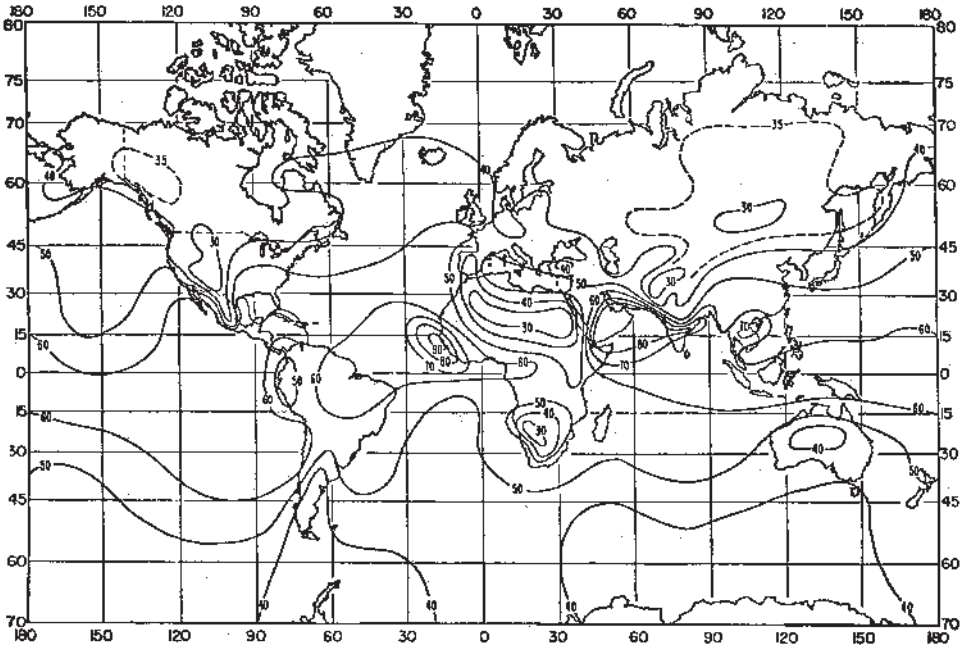

Figure 1.33 Monthly average of ΔN in May (ITU-R P.453).

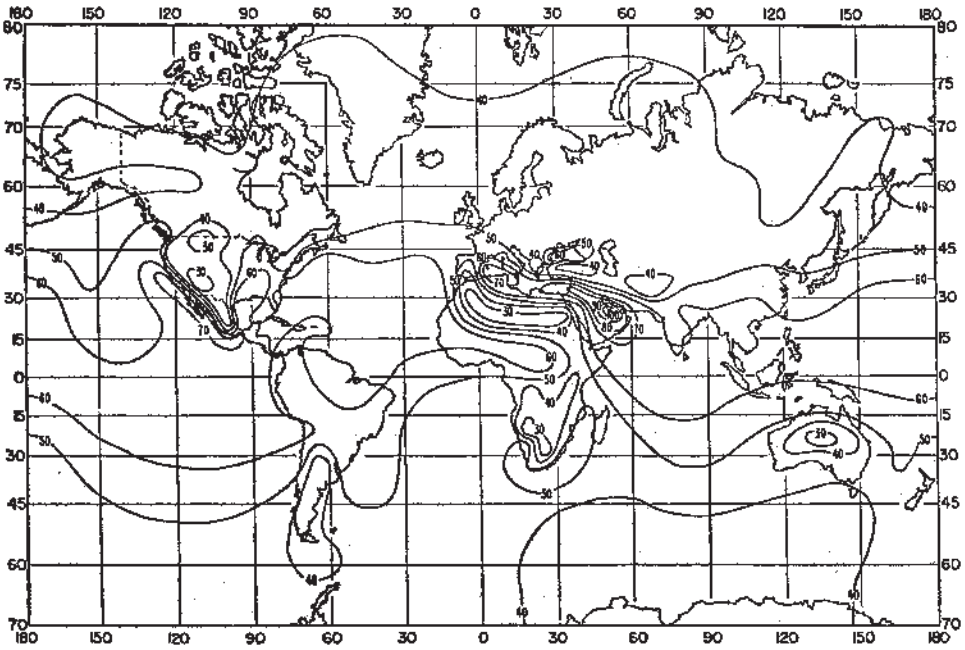

Figure 1.34 Monthly average of ΔN in August (ITU-R P.453).

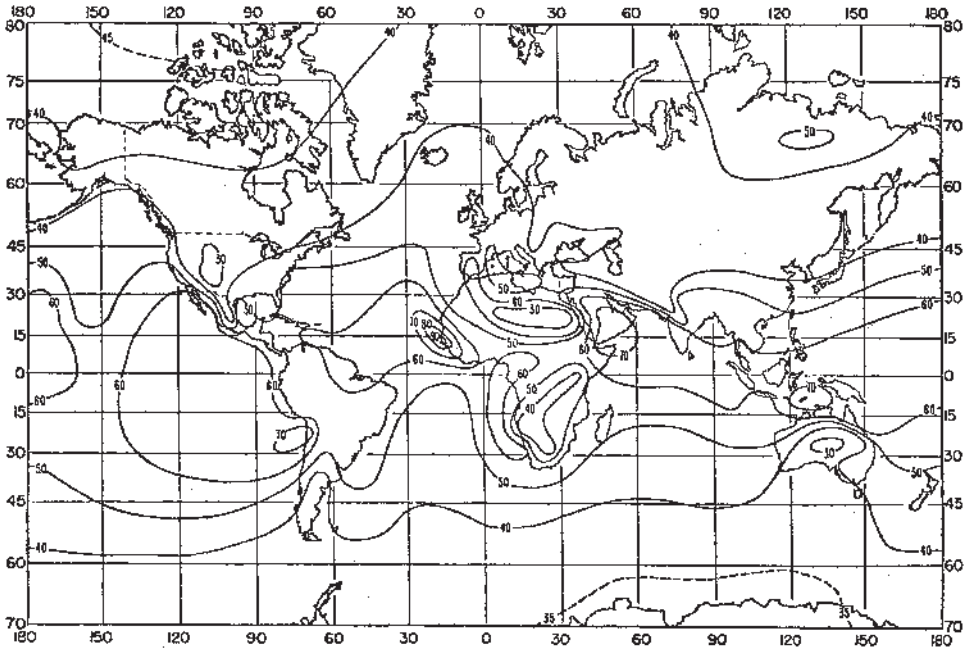

Figure 1.35 Monthly average of ΔN in November (ITU-R P.453).

Figures 1.36–1.39 indicate the percentage of time during which the vertical refractivity gradient is lower or equal to $-100\,\mathrm{N\,km^{-1}}$ in the first 100 m during February, May, August, and November, respectively; this value, called climatic variable P_L, corresponds to the particular conditions of trapping or ducting of the electromagnetic waves which are at the origin of severe fading with deep depressions of the transmitted signal (radioelectric holes).

To use the weather data given in relation (1.75), the following relations exist between water vapor concentration ($\mathrm{g\,m^{-3}}$), water vapor pressure (hPa), and humidity ratio (%) which are valid between –20 and +50 °C:

- Water vapor concentration ($\mathrm{g\,m^{-3}}$):

$$v = 216.7\,\frac{p_v}{T} \tag{1.78}$$

- Humidity ratio (%):

$$\mathrm{HR} = 100\,\frac{p_v}{p_s}$$

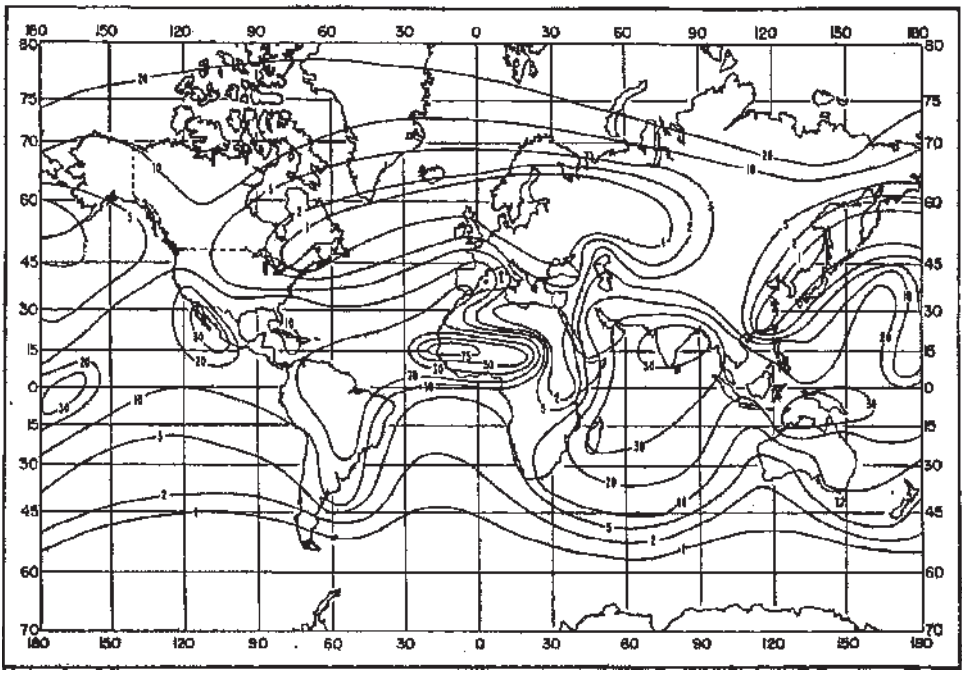

Figure 1.36 Percentage of time $dN/dh < -100\,\mathrm{N\,km^{-1}}$ in February (ITU-R P.453).

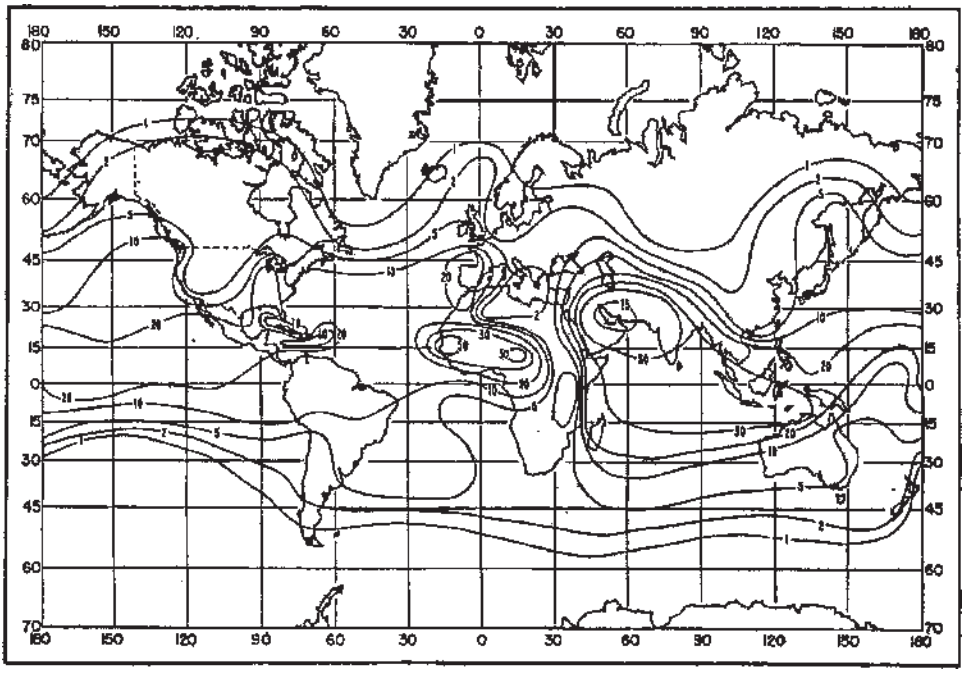

Figure 1.37 Percentage of time $dN/dh < -100\,\mathrm{N\,km^{-1}}$ in May (ITU-R P.453).

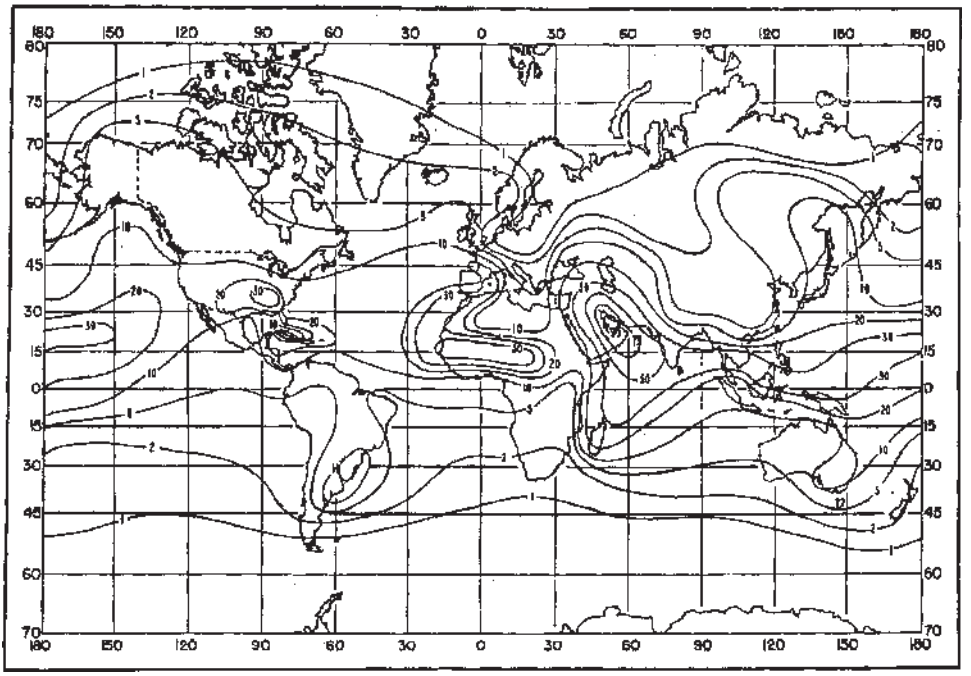

Figure 1.38 Percentage of time $dN/dh < -100\,\mathrm{N\,km^{-1}}$ in August (ITU-R P.453).

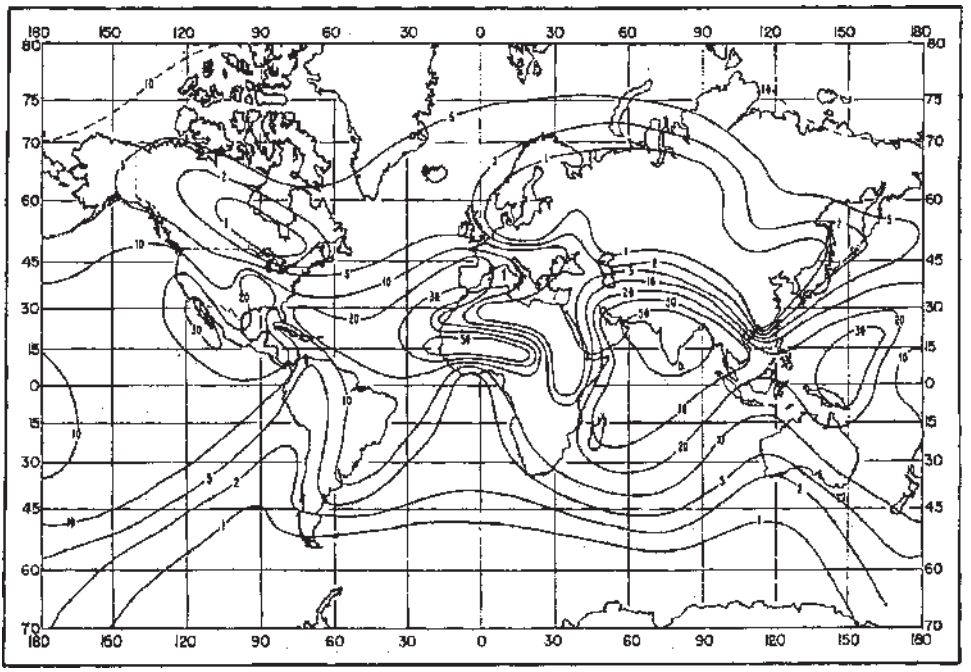

Figure 1.39 Percentage of time $dN/dh < -100\,\mathrm{N\,km^{-1}}$ in November (ITU-R P.453).

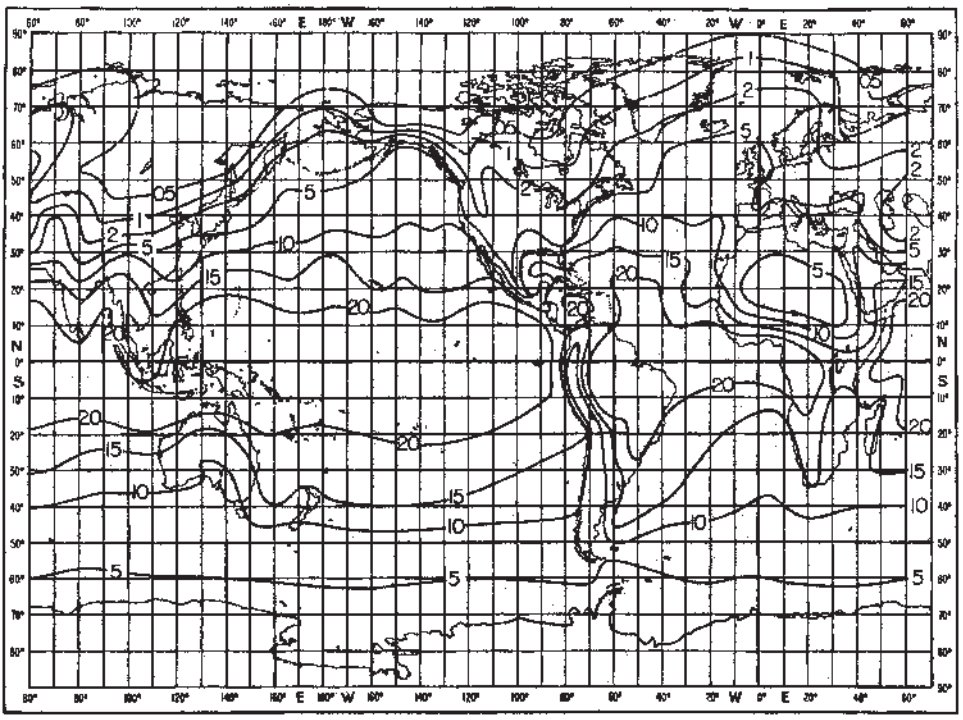

Figure 1.40 Water vapor concentration ($g\,m^{-3}$) in February (ITU-R Rep.563).

- Water vapor pressure at saturation (hPa):

$$p_s = 6.1121 \exp\left[17.502 \frac{t}{t + 240.97}\right]$$

where p_v = water vapor pressure (hPa)
T = absolute temperature (K)
t = température (°C) (0 °C = 273.16 K)

Figure 1.40 presents the distribution of water vapor concentration for February. Figure 1.41 presents the distribution of water vapour concentration for August. Figure 1.42 presents the psychrometric chart[9] which links water vapor concentration and humidity ratio (HR) to temperature. Figure 1.43 illustrates the distribution versus percentage of time of vertical refractivity gradient for various standard climates.

[9]The psychrometric chart can be used to solve numerous process problems with moist air; the concepts of internal energy, enthalpy, and entropy are linked to it.

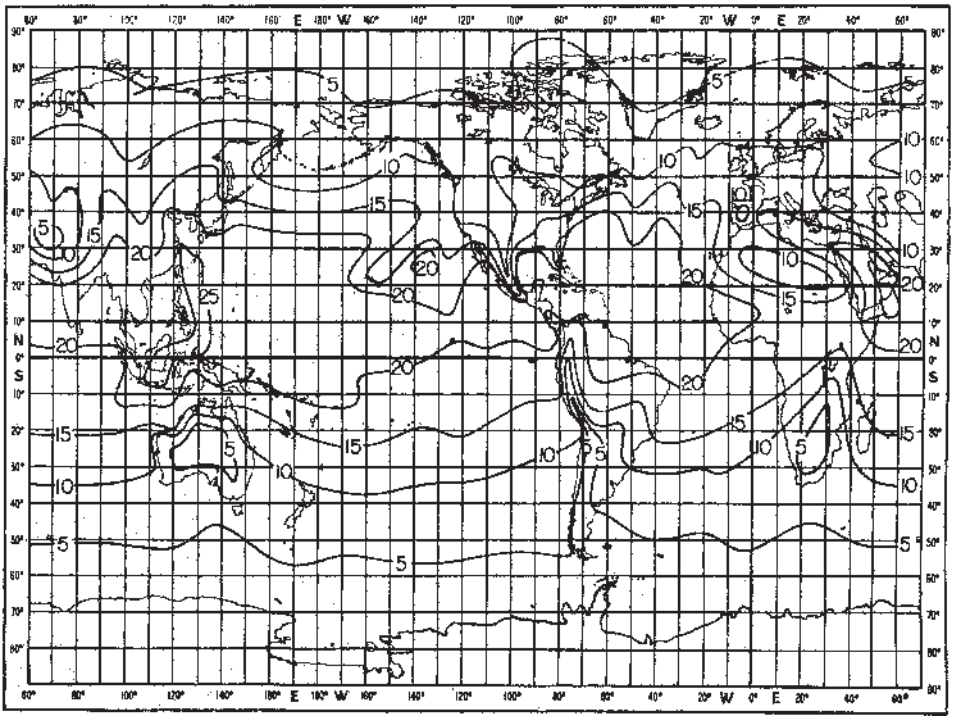

Figure 1.41 Water vapor concentration ($g\,m^{-3}$) in August (ITU-R Rep. 563).

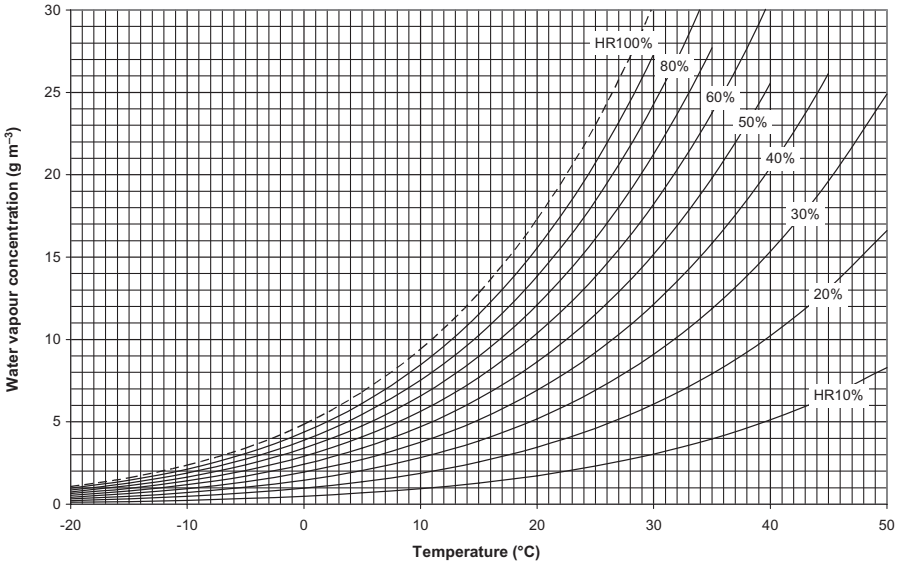

Figure 1.42 Psychrometric chart.

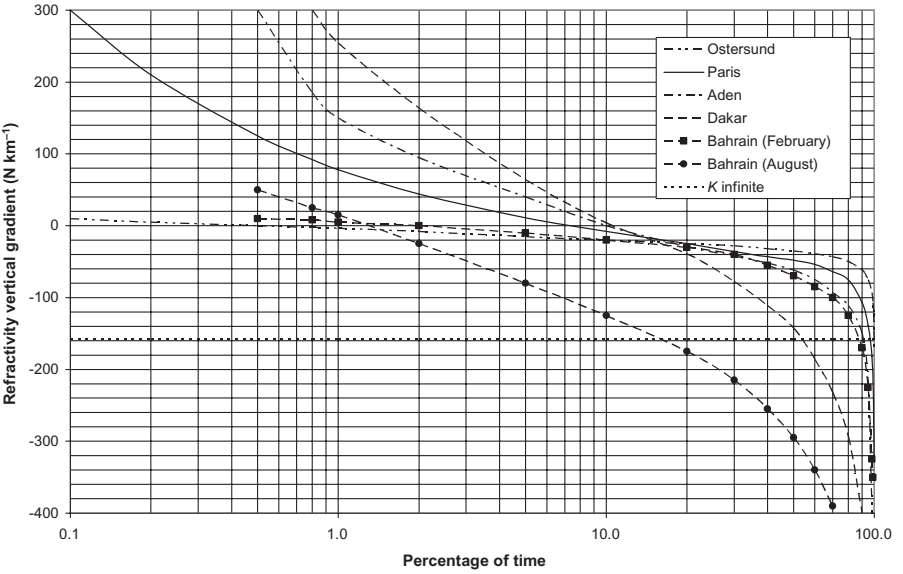

Figure 1.43 Typical distributions of vertical refractivity gradient.

The pressure, temperature, and humidity ratio vary with altitude. It is the same for the vertical refractivity gradient; one can apply, as a first approximation, the following differential equation:

$$\frac{dN}{dh} = 0.35\frac{dP}{dh} - 1.3\frac{dt}{dh} + 7\frac{dv}{dh} \tag{1.79}$$

where P = atmospheric pressure (hPa)
t = temperature (°C)
v = water vapor concentration ($g\,kg^{-1}$ dry air) for an air density

$$\rho \approx (1.2\,kg\,m^{-3})\frac{293}{t+273}$$

Figure 1.44 shows the evolution of the vertical refractivity gradient in a layer 100 m thick, expressed in N-units × km^{-1} or $N\,km^{-1}$, according to the relevant gradients of temperature and water vapor concentration assuming the pressure remains constant.

Generally, the atmosphere above the ground is made homogeneous by the wind or during the day by the convection caused by the heating action of the sun. However, in certain circumstances, a stratification of the atmosphere can occur in the shape of layers at different temperature, pressure, and hygrometry which present very different refractive indexes as well as different vertical

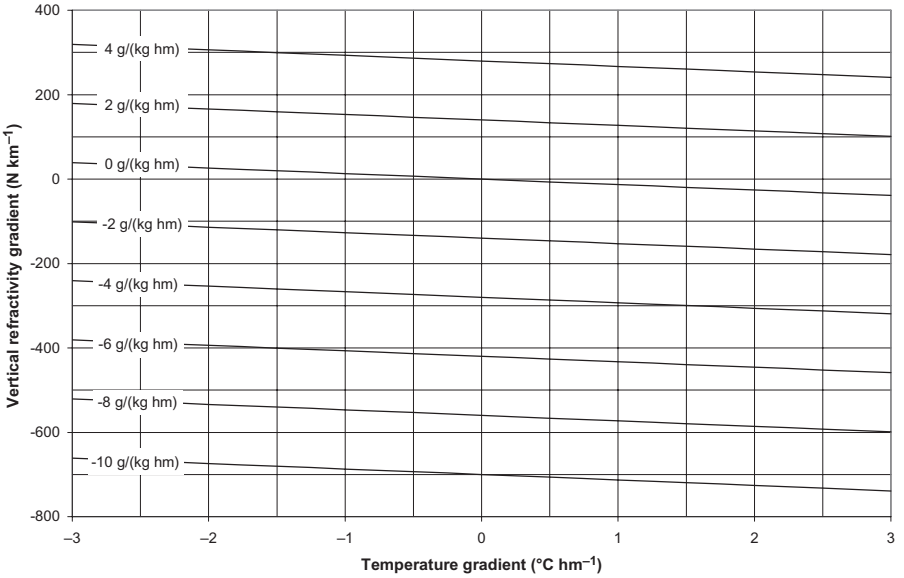

Figure 1.44 Evolution of vertical refractivity gradient (*dN/dh*) at constant pressure versus gradients of temperature and water vapor concentration in layer 100 m high.

refractive gradients. Then tropospheric radio ducts from that extend a few tens to a few hundred meters vertically and several tens to several hundred kilometers horizontally inside which the radio waves are guided. For example, the psychrometric chart for moist air shows that, for high temperatures and a humidity ratio of about 40%, the water vapor concentration can exceed $30\,\mathrm{g\,m^{-3}}$, which corresponds to current weather conditions in the area of the Persian Gulf in summer when the phenomena of ducting propagation dominate. Then we can calculate the air density variation according to temperature and water vapor concentration as follows:

- Temperature

$$\rho = \rho_0 \frac{273 + t_0}{273 + t} \approx (1.2\,\mathrm{kg\,m^{-3}}) \frac{293}{273 + t} \tag{1.80}$$

  from which $d\rho/dt \approx -4.1 \times 10^{-3}\,\mathrm{kg\,m^{-3}\,K^{-1}}$
- Water vapor concentration:

$$\rho \approx \rho_0(\mathrm{kg\,m^{-3}}) + v(\mathrm{g\,m^{-3}}) \times 10^{-3}$$

  from which $d\rho/dv \approx 10^{-3}\,\mathrm{kg/m^{-3}}\ (\mathrm{g/m^{-3}})^{-1}$

It is seen that an increase in water vapor concentration of some $4\,\mathrm{g\,m^{-3}}$ compensates for the reduction in air density due to an increase in temperature of 1 °C, which explains why a layer of hot and wet air can be formed under a layer of cold and dry air (phenomenon of inversion of temperature) with a very negative refractivity gradient, as shown in Figure 1.44. A positive vertical temperature gradient and/or a negative water vapor concentration gradient thus result in a negative refractivity gradient, whereas a negative temperature gradient and/or a positive water vapor concentration gradient result in a positive refractivity gradient.

1.8.3 Curvature of Radioelectric Rays

The propagation of radio waves is rectilinear in a dielectric medium whose index remains constant at any point of crossed space. On the other hand, it is not the same when this index varies and it is shown, using a spherical model of atmosphere, that the trajectory of the rays undergoes a continuous deflection when the index varies continuously in the vertical direction.

The phenomenon of ray curvature may be understood by dividing the atmosphere into layers with discrete values for the refractive index in each layer, as shown in Figure 1.45. Since each successive value of n_n is smaller than the preceding value n_{n-1}, as shown in the figure, the angle φ_n must increase and the ray curves in the downward direction as

$$n_1 \sin \varphi_1 = n_2 \sin \varphi_2 = n_3 \sin \varphi_3 = \cdots = n_n \sin \varphi_n$$

This results in a curvature radius r of the trajectory of the radioelectric rays expressed in the form

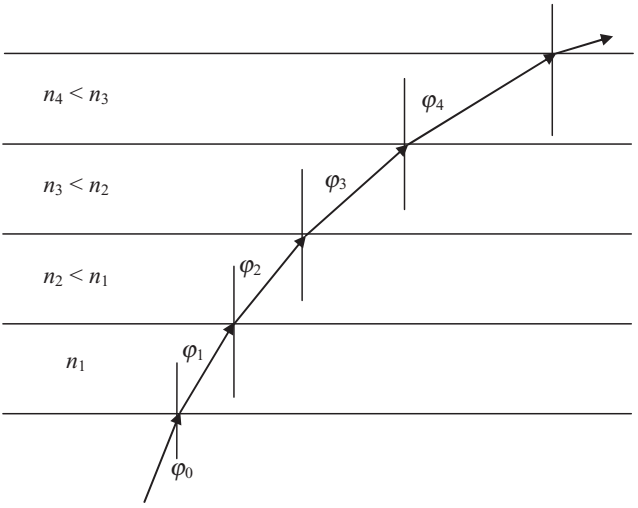

Figure 1.45 Ray curvature.

$$\frac{1}{r} = -\frac{dn}{dh}$$

1.8.4 Effective Earth Radius

To obtain a rectilinear representation of the rays trajectory of the rays in the vicinity of Earth, the actual terrestrial radius R is modified by a factor K, called the effective Earth radius factor:

$$\frac{dn}{dh} + \frac{1}{R} = \frac{1}{KR}$$

that is,

$$K = \frac{1}{1 + R(dn/dh)}$$

where $R = 6.38 \times 10^3$ km and

$$\frac{dn}{dh} = \frac{dN}{dh} \times 10^{-6}$$

We obtain

$$K = \frac{1}{1 + (6.38 \times 10^3)(dN/dh) \times 10^{-6}}$$

Then

$$K = \frac{157}{157 + dN/dh} \tag{1.81}$$

The factor K can also be obtained using the following empirical formula from technical note NBS-101 [National Bureau of Standards (NBS), 1966] which connects dN/dh to the surface refractivity N_S for a layer 1 km high:

$$\frac{dN}{dh} = -7.32 \exp(0.005577 N_S)$$

Thus

$$K = \frac{1}{1 - 0.04665 \exp(0.005577 N_S)} \tag{1.82}$$

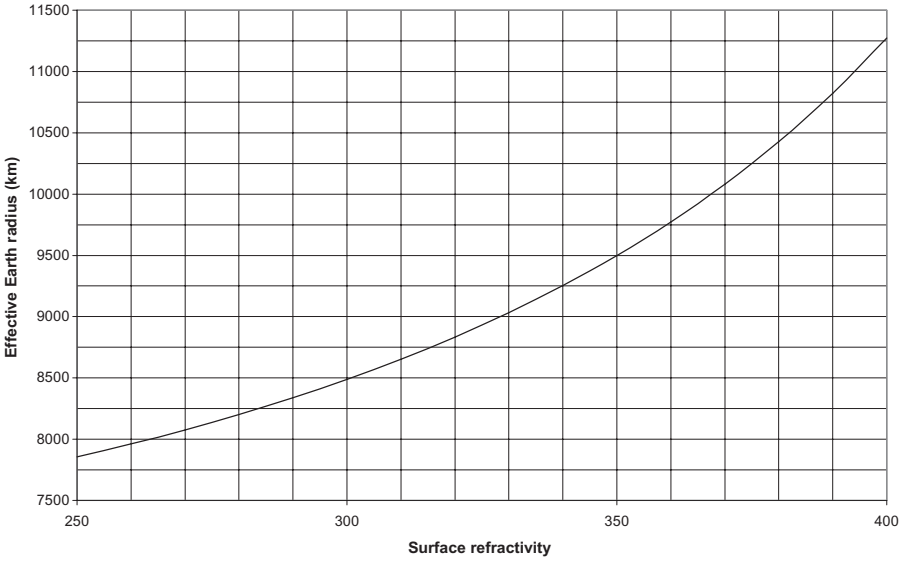

Figure 1.46 Effective terrestrial radius versus surface refractivity N_S.

The effective Earth radius a is then

$$a = KR = \frac{157R}{157 + dN/dh} \tag{1.83}$$

Figure 1.46 presents the effective Earth radius versus surface refractivity N_S. The effective Earth radius becomes

- infinite when $dN/dh = -157\,\mathrm{N\,km^{-1}}$ ($K \pm \infty$), in which case the trajectory of the rays follows the actual curvature of Earth;
- equal to the actual Earth radius for $dN/dh = 0\,\mathrm{N\,km^{-1}}$ ($K = 1$);
- negative for $dN/dh < -157\,\mathrm{N\,km^{-1}}$ (concave Earth for $K < 0$); or
- lower than the real Earth-radius for $dN/dh > 0\,\mathrm{N\,km^{-1}}$ ($K < 1$).

Figure 1.47 illustrates the trajectory of the rays compared to the actual Earth radius and to a model utilizing an effective Earth radius versus factor K.

The standard radio atmosphere corresponds to a spherical atmosphere whose vertical refractivity gradient would be constant and equal to the median value (50% of time) in a moderate climate:

$$\frac{dN}{dh} = -40\,\mathrm{N\,km^{-1}}$$

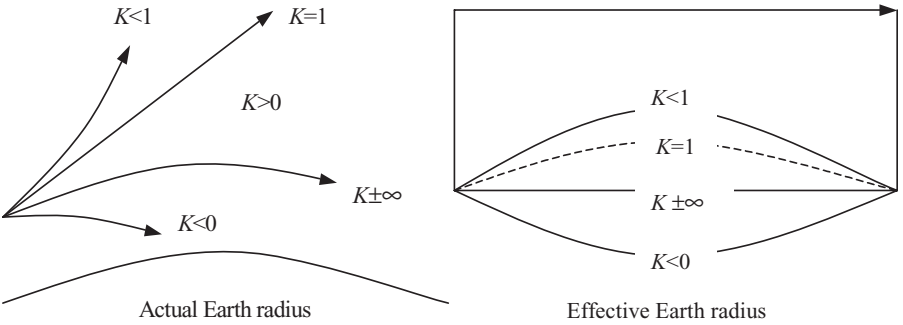

Figure 1.47 Trajectory of rays and effective Earth radius versus *K*.

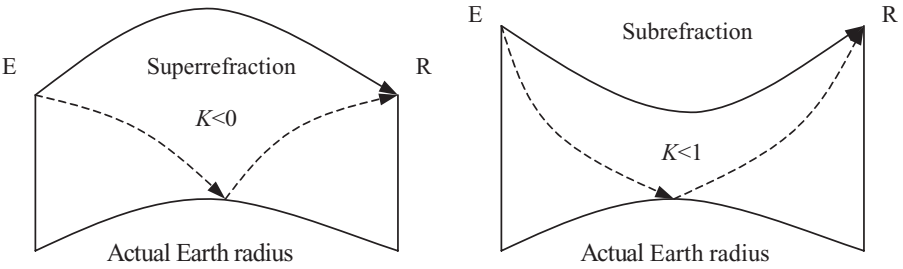

Figure 1.48 Relative position of rays compared to ground.

that is, $K \approx \frac{4}{3} \rightarrow a \approx 8470\,\text{km}$. When *dN/dh* is higher than this value, it corresponds to subrefraction conditions and in the contrary case to superrefraction. When *K* is negative, which corresponds to superrefraction, the rays are curved toward the ground; consequently, the rays from the transmitter reach the receiver either directly while deviating from Earth or after reflection on the ground, as shown in Figure 1.48. On the other hand, when *K* is positive and lower than 1, which corresponds to subrefraction, the rays are deflected upward; it follows that the lower rays issued from the transmitter reach the receiver while approaching the ground.

In the event of subrefraction, the ground can thus become an obstacle to the propagation of the rays, which then are affected by an additional loss by diffraction, while in superrefraction, the direct rays pass largely above the ground, but these conditions also favor the reflected rays, which can interfere with the direct rays, as we will see. Figure 1.49 summarizes the behavior of electromagnetic waves which cross layers of air of different indexes; this phenomenon explains the mirages which occur in the desert when the image of the sky is reflected on the ground (curvature of the rays upward) as well as the vision at very long distance above the sea (curvature of the rays downward). The main cause of the subrefraction corresponds to an unstable arrange-

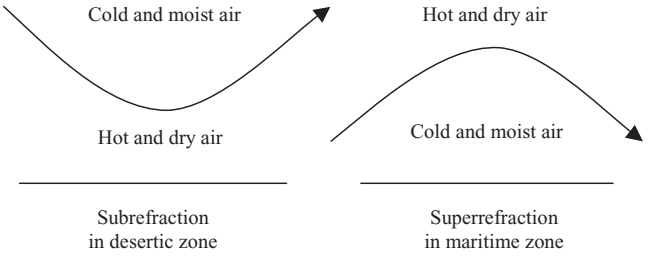

Figure 1.49 Typical examples of ray curvature.

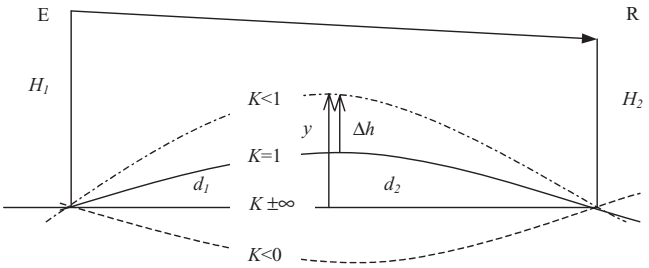

Figure 1.50 Effective Earth radius.

ment of the layers of the atmosphere, contrary to that which is at the origin of the superrefraction, and consequently to a small percentage of time.

The effective Earth radius compared to the infinite apparent Earth radius, as presented in Figure 1.50, is given according to the factor K by the following relation using the same unit for heights and distances (kilometers):

$$y = \frac{d_1 d_2}{2a} = \frac{d_1 d_2}{2KR} \tag{1.84}$$

The Earth curvature y from a flat Earth ($K = \pm\infty$) at midpath is represented in Figure 1.51 as well as the height difference Δh from the actual Earth ($K = 1$), which is given by the relation

$$\Delta h = \frac{d_1 d_2}{2R}\left(\frac{1}{K} - 1\right) \tag{1.85}$$

1.8.5 Variation of Launch and Arrival Angles of Rays

Ray curvature results in variation of the launch and arrival angles of rays, both direct and reflected, at the antennas. The approximate value of this variation can be calculated as follows on the basis of the geometric elements presented in Figure 1.52. For greater convenience, we will consider a ray issued from the source S, located at a height h, and tangent to the Earth at point T, which is

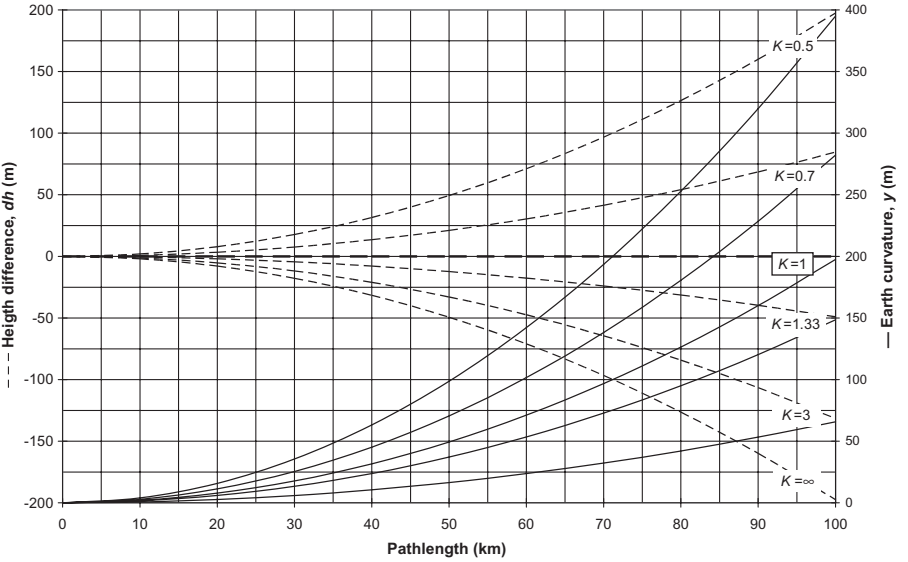

Figure 1.51 Earth curvature and height difference at midpath.

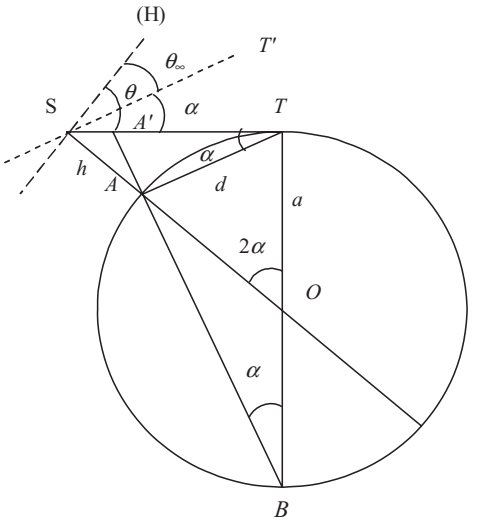

Figure 1.52 Apparent launch/arrival angles.

the same as a path between two points placed at altitudes differing by the height h. The launch angle θ of the ray is related to the horizontal line (H) passing by the source S. Moreover, the distance d and the height h are small with respect to the effective Earth radius a. The similarity of triangles ATA' and ABT makes it possible to write

$$\tan\alpha = \frac{AA'}{AT} = \frac{AT}{AB}$$

from which we get the downward slope from the horizon line, such as $AB \approx 2a$ and $h << d << a$:

$$\alpha \approx \frac{d}{2a}$$

The angle θ is the sum of the angle θ_∞, which corresponds to the elevation angle for $a = \infty$, and the angle α, which is equal to half of the angle at the center of Earth, that is,

$$\theta = \theta_\infty + \alpha \approx \frac{h}{d} + \frac{d}{2a} \tag{1.86}$$

The launch and arrival angles of the direct ray, $\Delta\theta_{DL}$ and $\Delta\theta_{DA}$, thus vary with the factor K according to the expressions[10]

$$\Delta\theta_{DL} = \Delta\theta_{DA} \approx -\frac{d}{2a} = -\frac{d}{2KR}$$

The launch angle $\Delta\theta_{RL}$ and arrival angle $\Delta\theta_{RA}$ of the reflected ray vary at first approximation and using relation (1.84) according to the expressions[11]

$$\Delta\theta_{RL} \approx -\frac{y}{d_1} = -\frac{d_1 d_2}{2ad_1} = -\frac{d_2}{2a} = -\frac{d_2}{2KR} \tag{1.87}$$

$$\Delta\theta_{RA} \approx -\frac{y}{d_2} = -\frac{d_1 d_2}{2ad_2} = -\frac{d_2}{2a} = -\frac{d_1}{2KR} \tag{1.88}$$

1.8.6 Positive Minimal Value of Effective Earth-radius Factor

The factor K varies throughout a given path; therefore, one defines an equivalent factor K_e for this path. The positive minimal value $K_{\min}$ can then be obtained in the following way:

- Determine the distribution of the vertical refractivity gradient at a point of the path $(dN/dh)_0$ and evaluate its median value μ_0 as well as its

[10]The minus sign refers to the fact that the terrestrial curvature varies in the opposite direction to that of the curvature of the rays.

[11]It is seen that the launch and arrival angles of the reflected ray vary less than those of the direct ray, that is, in the ratios d_1/d and d_2/d.

standard deviation σ_0 for the positive gradients by supposing that it is about a normal distribution.

- Assume that the distribution is the same throughout the path and, since the instantaneous value varies from one point to another, utilize an equivalent vertical refractivity gradient $(dN/dh)_e$, which makes it possible to obtain the equivalent factor K_e by the relation

$$K_e = \frac{157}{157 + [dN/dh]_e}$$

- The median value of $(dN/dh)_e$, which is the average vertical refractivity gradient along the path, and its standard deviation are respectively given by the relations

$$\mu_e \approx \mu_0 \qquad \sigma_e \approx \frac{\sigma_0}{\sqrt{1 + d/d_0}}$$

where: $d_0 = 13.5\,\text{km}$.

- Calculate the values of $(dN/dh)_e$, and thus those of K_e, which are exceeded during any percentage of time using the following Gaussian coefficients C_G:

Percentage of Time	$(dN/dh)_e$	Percentage of Time	$(dN/dh)_e$
50	$(dN/dh)_e \approx \mu_e$	99.9	$(dN/dh)_e \approx \mu_e + 3.09\sigma_e$
84.14	$(dN/dh)_e \approx \mu_e + \sigma_e$	99.99	$(dN/dh)_e \approx \mu_e + 3.719\sigma_e$
90	$(dN/dh)_e \approx \mu_e + 1.28\sigma_e$	99.999	$(dN/dh)_e \approx \mu_e + 4.265\sigma_e$
99	$(dN/dh)_e \approx \mu_e + 2.327\sigma_e$	99.9999	$(dN/dh)_e \approx \mu_e + 4.753\sigma_e$

The positive minimal value $K_{\min}$ can thus be defined for any given percentage of time by the expression

$$K_{\min} = \frac{157}{157 + [dN/dh]_{50\%} + C_G\sigma_0/\sqrt{1 + d/d_0}} \tag{1.89}$$

Figure 1.53 presents the positive minimal value $K_{\min}$ in temperate climate for percentages of time of the average year ranging between 99 and 99.9999% using the following parameters[12]:

- Median value of vertical gradient: $[dN/dh]_{50\%} = -40\,\text{N km}^{-1}$
- Standard deviation: $\sigma_0 = 50\,\text{N km}$
- Reference distance: $d_0 = 13.5\,\text{km}$

[12]These values are in agreement with the distribution for Paris in Figure 1.43.

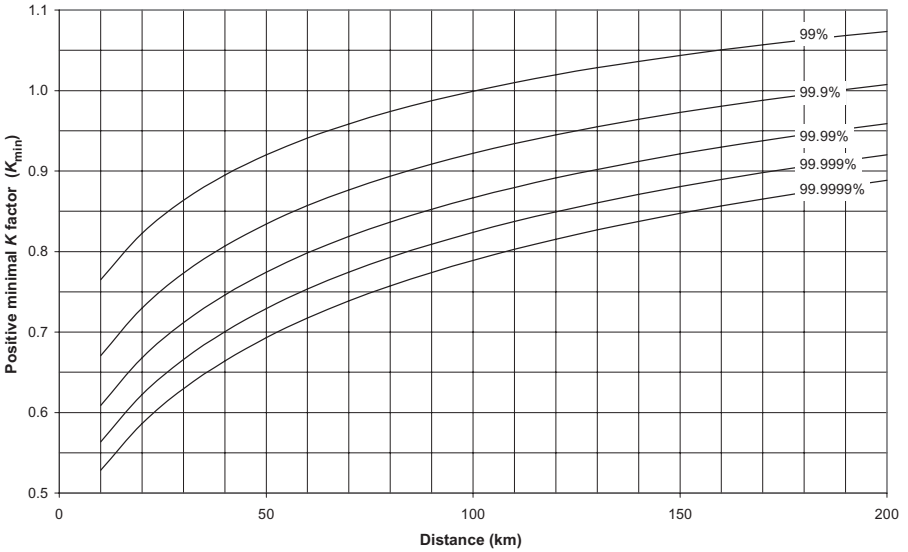

Figure 1.53 Positive minimal value $K_{\min}$ for various percentages of average year.

Figure 1.54 presents the positive minimal value $K_{\min}$ of the equivalent factor K_e versus pathlength that is exceeded during roughly 99.9% for any month in continental temperate climate.

1.8.7 Tropospheric Radio Ducts

1.8.7.1 Conditions of Appearance We saw previously that the atmosphere can be divided into quasi-horizontal layers with different refractive indexes and whose vertical refractivity gradients can take very negative values, resulting in superrefraction conditions of propagation which may trap the waves inside a layer called a radio duct. The meteorological conditions which cause such stratification of the troposphere are the following:

1. Evaporation caused by the sun above a wetland or a broad stretch of water
2. Advection, that is, the horizontal movement of a mass of hot and dry air passing above a mass of cold and wet air
3. Cooling of the ground by radiation at the same time as the air at its contact while the upper layers of the atmosphere cool more slowly
4. Subsidence, which corresponds to downward movement, contrary to thermal ascent, of a mass of air which cools slowly above a mass of colder and wetter air

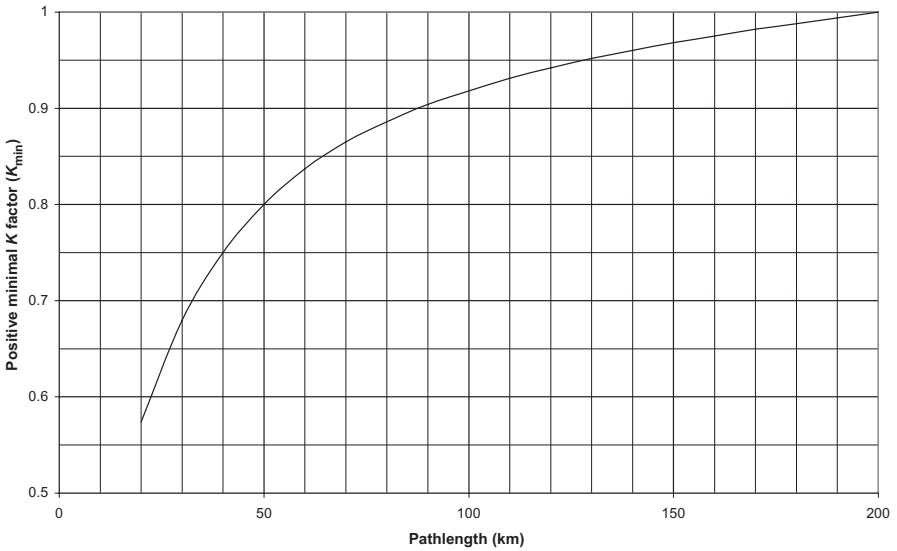

Figure 1.54 Positive minimal value K_{min} for 99.9% of any month (ITU-R P.530).

These weather conditions correspond to a stable arrangement of the air masses since the densest ones occupy the low part of the atmosphere and can consequently last several hours and extend over very vast zones.

Tropospheric radio ducts generate a major and slow fading of the signal which can reach several tens of decibels, called depression or a radioelectric hole, which is accompanied by a very fast and deep fading due to multipath, having a speed of variation of several tens to several hundreds of decibels per second, alternating with periods of important reinforcement of the field strength. Recommendation ITU-R P.453-9 provides world statistics on the frequency of occurrence, average intensity, and average height of the following ducts types:

(a) Surface ducts
(b) Surface elevated ducts
(c) Elevated ducts

For example, Figures 1.55 and 1.56 illustrate duct types (a) and (b), commonly encountered near the ground in microwave radio links, which are characterized by a modified refractive index profile according to the height by considering the refractive modulus M defined by

$$M = \left(n + \frac{h}{a} - 1\right) \times 10^6 \Rightarrow M(h) = N(h) + 157h$$

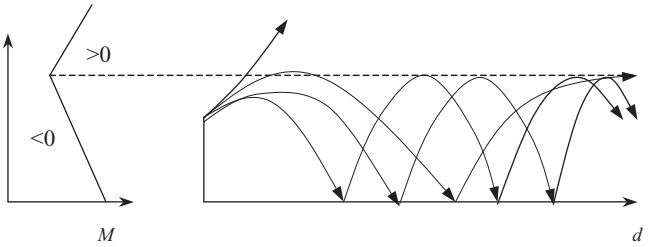

Figure 1.55 Propagation in surface duct.

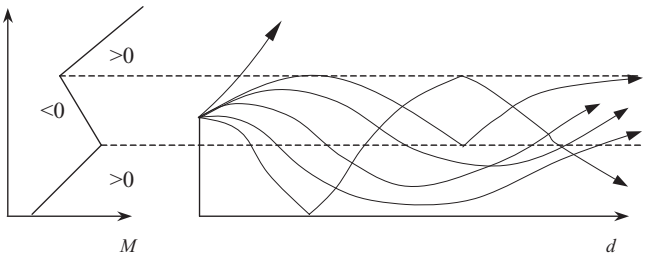

Figure 1.56 Propagation in elevated surface duct.

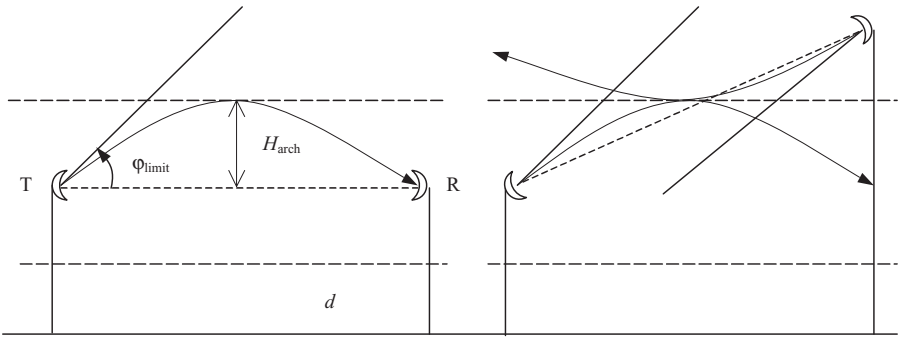

Figure 1.57 Height of direct arch and angle limit of rays in duct with very negative vertical refractivity gradient.

1.8.7.2 Trajectories of Rays in Radio Duct We saw previously that radioelectric rays are curved downward when the vertical refractivity gradient is strongly negative and are curved upward if it is positive; Figures 1.55 and Figure 1.56 illustrate these trajectories in superrefractive conditions, which characterize the guided propagation.

Figure 1.57 presents the parameters of the parabolic trajectory of a direct ray between a transmitter and a receiver that are placed at the same height inside a radio duct with a very negative vertical refractivity gradient. It is shown that the trajectory of waves in a duct with a very negative vertical refractivity gradient is parabolic and one can then define the height of the

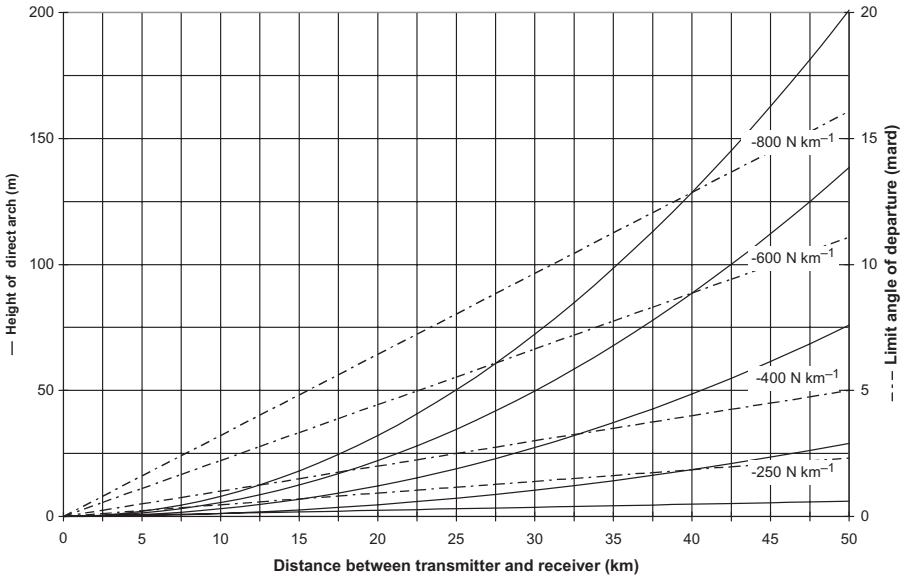

Figure 1.58 Height of direct arch and limit angle.

direct arch, H_{arch}, expressed in meters, as well as the limit angle φ_{limit}, expressed in milliradians, which are necessary to reach a receiver placed at the same height as the transmitter and at a distance d using the following relations:

$$H_{\text{arch}} = -\frac{157 + dN/dh}{8000} d^2 \tag{1.90}$$

$$\varphi_{\text{limit}} = -\frac{157 + dN/dh}{2000} d \tag{1.91}$$

In addition to the curvature of the rays according to the refractivity of the atmosphere, these can thus be reflected by the interface between two layers of different indexes or by the ground, according to the parameters in Figures 1.24 and 1.25, or leave the duct when the incident angle is higher than the limit angle.

Figure 1.58 presents the height of the direct arch and the value of the limit launch angle of the rays versus distance between the transmitter and the receiver for various values of the vertical refractivity gradient.

1.9 PROPAGATION BY DIFFRACTION

Figure 1.59 illustrates an obstruction on a path that divides two zones known as zone of visibility and zone of diffraction. According to geometric optics, the

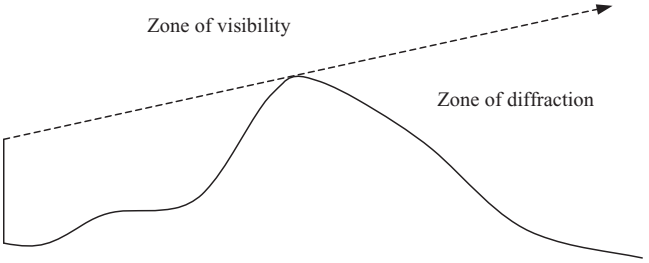

Figure 1.59 Diffraction due to an obstacle.

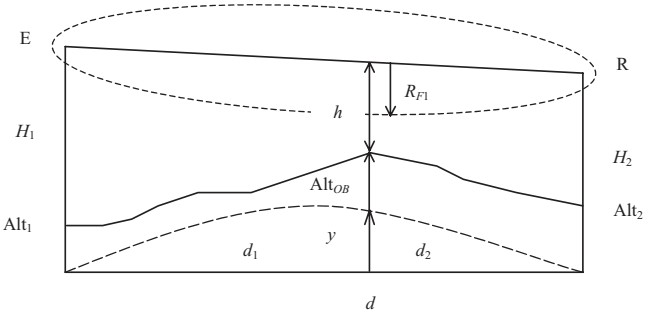

Figure 1.60 Clearance of microwave line-of-sight radio link.

field strength below the ray to the horizon or the tangent ray is null; however, because of propagation by diffraction, the radiated field goes around the obstacle and penetrates into the shadow zone by decreasing rapidly as the receiver moves deeper inside. Thus, when an obstacle interposes between the transmitter and the receiver, there is an additional transmission loss which depends on a great number of parameters related to its nature, the wavelength, the polarization, the height of the antennas, and the geometry of the link. The nature of the ground and the polarization play a great part at low frequencies, but, as microwave links in the majority of the cases are established at frequencies higher than 300 MHz, we will see in what follows that their influence can be neglected; however, although the ITU recommendation does not indicate higher limit of validity in frequency, a certain prudence is essential when this exceeds some gigahertz.

It is advisable to first define the parameter of clearance of the connection, h/R_{F1}, which is the ratio of the clearance h under the line joining the two ends of the path and the first Fresnel's ellipsoid radius R_{F1}, as illustrated in Figure 1.60, which presents a microwave line-of-sight radio link established between a transmitter E and a receiver R, respectively located at heights H_1 and H_2 on a path profile of length d. The relief is reported to the arc of the Earth great circle corresponding to the level of reference whose plane passes by E and R, with respective altitudes Alt_1 and Alt_2, and we consider the prevailing obstacle

of altitude Alt_{OB} placed at distance d_1 from E and at distance d_2 from R. We define the clearance h geometrically as

$$h = \text{Alt}_1 + H_1 + [\text{Alt}_2 + H_2 - (\text{Alt}_1 + H_1)]\frac{d_1}{d} - (y + \text{Alt}_{OB}) \tag{1.92}$$

Then, starting from relation (1.65) and giving the radius of Fresnel's first ellipsoid R_{F1}, we deduce the clearance criterion[13] h/R_{F1}. Generally, there are five obstacle types:

Smooth spherical Earth
Knife edge
Rounded edge
Multiple edges
Irregular terrain

1.9.1 Diffraction over Smooth Spherical Earth

The diffraction field strength E relative to free-space field strength E_0, expressed in decibels, is given by the following relation (ITU-R P.526):

$$20\log\left(\frac{E}{E_0}\right) = F(X) + G(Y_1) + G(Y_2) \tag{1.93}$$

where X = pathlength
Y_1 = height of transmission antenna
Y_2 = height of reception antenna

and

$$X = 2.2\beta f^{1/3} a^{-2/3} d \qquad Y = 9.6\times 10^{-3}\beta f^{2/3} a^{-1/3} H$$

where d = pathlength (km)
a = equivalent terrestrial radius (km)
H = antenna height (m)
f = frequency (MHz)
β = Boithias's parameter depending on nature of ground

with

$$\beta = \frac{1 + 1.6\kappa^2 + 0.75\kappa^4}{1 + 4.5\kappa^2 + 1.35\kappa^4}$$

[13]By convention, we will consider that the clearance h is negative when the chord joining E and R passes over the top of the obstacle and positive in the contrary case.

where the standardized surface admittance factor κ depends on polarization:

$$\kappa_H = 0.36(af)^{-1/3}\left[(\varepsilon_r - 1)^2 + \left(1.8\times 10^4 \frac{\sigma}{f}\right)^2\right]^{-1/4}$$

$$\kappa_V = \kappa_H\left[\varepsilon_r^2 + \left(1.8\times 10^4 \frac{\sigma}{f}\right)^2\right]^{1/2}$$

where ε_r = relative permittivity
σ = conductivity

Then

$$F(X) = 11 + 10\log X - 17.6X$$

$$G(Y) \approx \begin{cases} 17.6\sqrt{Y-1.1} - 5\log(Y-1.1) - 8 & \text{for } Y > 2 \\ 20\log(Y + 0.1Y^3) & \text{for } 10\kappa < Y < 2 \\ 2 + 20\log\kappa + 9\log\left(\dfrac{Y}{\kappa}\right)\left[\log\left(\dfrac{Y}{\kappa}\right) + 1\right] & \text{for } \dfrac{\kappa}{10} < Y < 10\kappa \\ 2 + 20\log\kappa & \text{for } Y < \dfrac{\kappa}{10} \end{cases}$$

When $\kappa < 10^{-3}$, the electric characteristics of the ground and polarization are without influence. For horizontal polarization at all frequencies and for vertical polarization above 20 MHz over land or 300 MHz over sea, β can be taken equal to 1. For frequencies below these values, which are not of interest for usual microwave links, β must be calculated as a function of κ.

Figure 1.61 gives the relative permittivity and conductivity of various ground types versus frequency. The values for obstacle diffraction loss over a smooth spherical Earth obtained thus are close to those given by Bullington's method, according to the clearance criterion h/R_{F1} established above, by using the following relation expressed in decibels:

$$A_{OB} = \left(14 + 22.24\frac{h}{R_{F1}}\right)\frac{2.456}{M^{0.15}} \tag{1.94}$$

where

$$M = \frac{3.28H_1}{4K^{1/3}}\left(1 + \sqrt{\frac{H_2}{H_1}}\right)^2\left(\frac{F}{4000}\right)^{2/3}$$

and F is the frequency (in megahertz), K is the effective Earth radius factor, and h, R_{F1}, H_1, and H_2 are in meters.

Figure 1.62 presents curves of diffraction loss over a smooth spherical Earth that have been established according to Bullington for various values of the coefficient M from $h/R_{F1} \geq -1$ with a coefficient of reflection of –1.

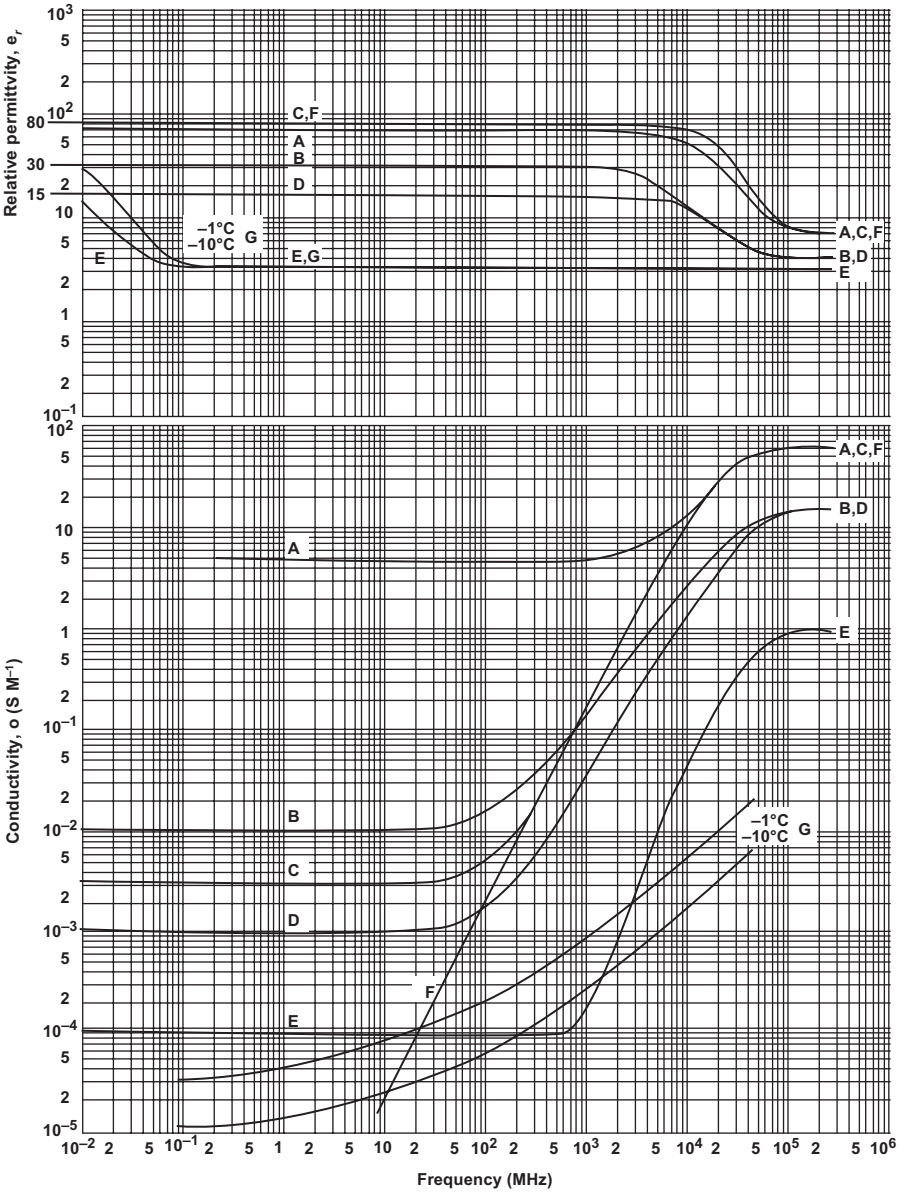

Figure 1.61 Relative permittivity and conductivity versus frequency for various ground types (ITU-R Rec.527): A, sea water of average salinity at 20 °C; B, wet ground; C, fresh water at 20 °C; D, medium dry ground; E, very dry ground; F, pure water at 20 °C; G, ice (fresh water).

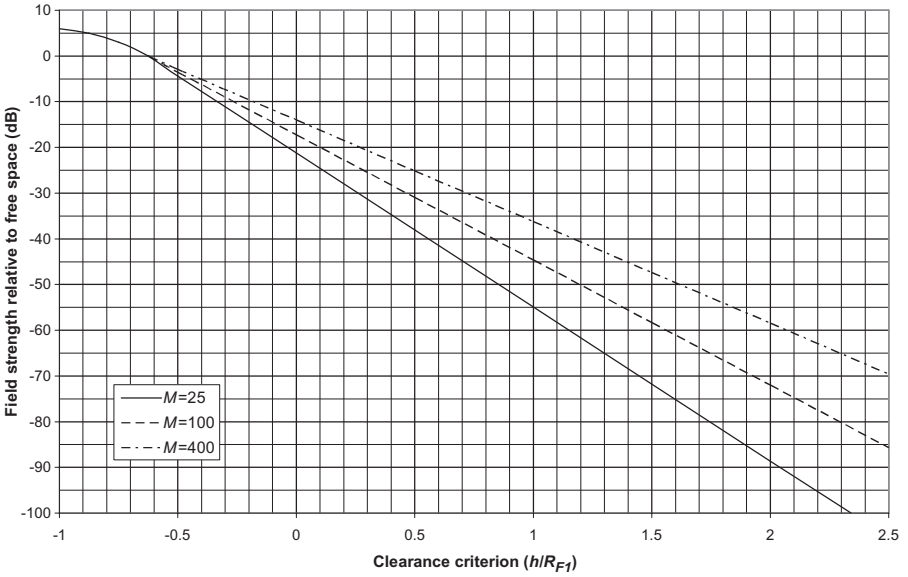

Figure 1.62 Diffraction loss over smooth Earth according to Bullington.

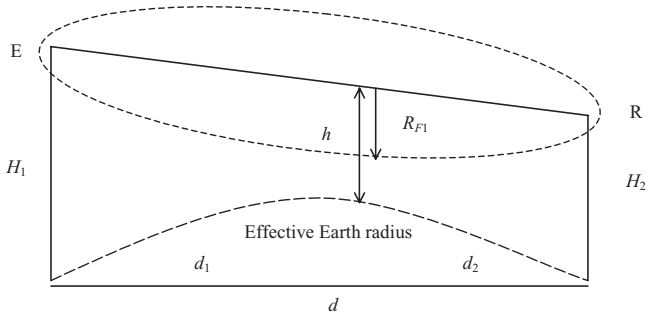

Figure 1.63 Graphic determination of $(h/R_{F1})_{\min}$.

It is however necessary to seek the minimal value of the h/R_{F1} criterion, which cannot be obtained directly from expressions (1.65), (1.84), and (1.92); the value of h is given by the following relation using the same unit for heights and distances (kilometers):

$$h = H_1 + (H_2 - H_1)\frac{d_1}{d} - \frac{d_1 d_2}{2a} \tag{1.95}$$

Using this method, h/R_{F1} is calculated by successive approximations or determined graphically on the real path profile, as shown in Figure 1.63, for the considered effective Earth radius. The attenuation due to the spherical

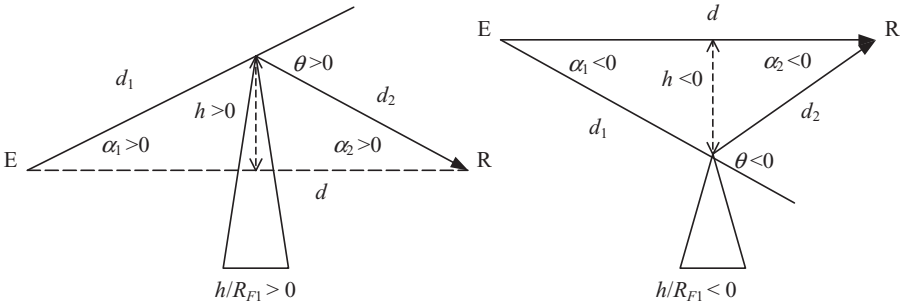

Figure 1.64 Diffraction over knife edge.

diffraction varies considerably according to the vertical refractivity gradient *dN/dh*; one can calculate this loss for various percentages of time while varying the effective Earth radius in expressions (1.83) and (1.95). The minimal value of the clearance criterion $(h/R_{F1})_{\min}$ corresponds to the minimal positive value of the equivalent factor K_e presented in Figures 1.53 and 1.54 or calculated for the considered effective Earth radius.

1.9.2 Diffraction over Single-Knife-Edge Obstacle

Assume that the wavelength is small compared to the size of the obstacle, which is in general the case at frequencies higher than 30 MHz. The Fresnel–Kirchhoff obstacle loss due to midpath single-knife-edge diffraction as presented in Figure 1.64 is given by the following relation expressed in decibels (ITU-R P.526):

$$J(\nu) = 6.9 + 20\log\left[\sqrt{(\nu-0.1)^2+1} + \nu - 0.1\right]$$

$$\nu = h\sqrt{\frac{2(d_1+d_2)}{\lambda d_1 d_2}} = \theta\sqrt{\frac{2d_1d_2}{\lambda(d_1+d_2)}} = \sqrt{\frac{2h\theta}{\lambda}} = \sqrt{\frac{2d\alpha_1\alpha_2}{\lambda}} \qquad (1.96)$$

where h = height of top compared to chord ER (m)
d, d_1, d_2 = distances, $d \approx d_1 + d_2$ (m)
α_1, α_2 = obstruction angles (rad)
θ = diffraction angle of same sign as h (rad) given by $\alpha_1 + \alpha_2$
= arcsin (h/d_1) + arcsin $(h/d_2) \approx h/d_1 + h/d_2$

Figure 1.65 presents the diffraction loss due to knife-edge-type obstacle with a negligible thickness which depends on the clearance parameter h/R_{F1} according to the following expression derived from relation (1.96):

$$A_{OB} = 6.9 + 20\log\left[\sqrt{\left(\frac{h}{R_{F1}}\sqrt{2} - 0.1\right)^2 + 1} + \frac{h}{R_{F1}}\sqrt{2} - 0.1\right]$$

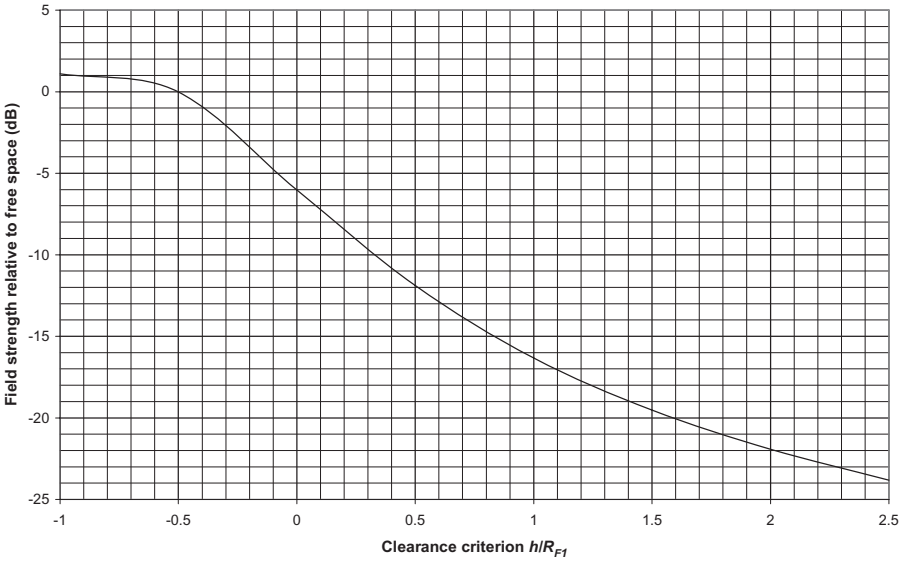

Figure 1.65 Diffraction loss single over knife edge.

where

$$v = \frac{h}{R_{F1}}\sqrt{2}$$

1.9.3 Diffraction over Single Rounded Obstacle

Figure 1.66 gives the geometric elements needed for determination of the obstacle loss that results from a single rounded obstruction. The diffraction loss over a rounded obstacle can be expressed by the relation (ITU-R P.526)

$$A_{OB} = J(v) + T(m, n) \tag{1.97}$$

The attenuation $J(v)$, which corresponds to the equivalent sharp edge of height h, is given by relation (1.96) and the additional loss $T(m,n)$, due to the obstacle curvature, by the expression

$$T(m, n) = km^b$$

with

$$k = 8.2 + 12n \qquad m = \frac{R[(d_1 + d_2)/d_1 d_2]}{(\pi R/\lambda)^{1/3}}$$

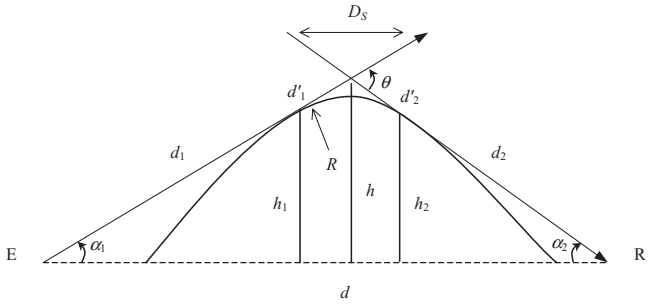

Figure 1.66 Diffraction over a rounded edge.

$$b = 0.73 + 0.27[1 - \exp(-1.43n)] \qquad n = \frac{h}{R}\left(\frac{\pi R}{\lambda}\right)^{2/3}$$

where R = equivalent radius of curvature of obstacle (m)
h = height of vertex (m)
λ = wavelength (m)
d_1, d_2 = distances from ends to vertex (m)

The equivalent radius of curvature of the obstacle can be calculated as

$$R = \frac{D_S}{\theta} \qquad \text{or} \qquad R = K\frac{D_S}{\theta}$$

where Ds = occultation distance along rounded edge (m)
K = effective Earth radius factor according to whether K is considered in calculation of h_1, h_2, and h
θ = angle of diffraction, such as $\theta < 0.2$ (rad)

with

$$\theta = \arcsin\left(\frac{h_1}{d_1}\right) + \arcsin\left(\frac{h_2}{d_2}\right) = \arcsin\left(\frac{h}{d'_1 + D_S/2}\right) + \arcsin\left(\frac{h}{d'_2 + D_S/2}\right)$$

where d'_1 and d'_2 are the distances between the terminals and their horizons to the obstacle in meters. Note that when R tends towards zero, expression (1.97) is reduced to the first term, which corresponds to the knife-edge loss.

1.9.4 Diffraction over Double Isolated Edges

When the two edges have similar altitudes, we use the method of Epstein and Peterson, whose geometric elements are presented in Figure 1.67. The method of Epstein and Peterson consists in successively applying to the two obstacles

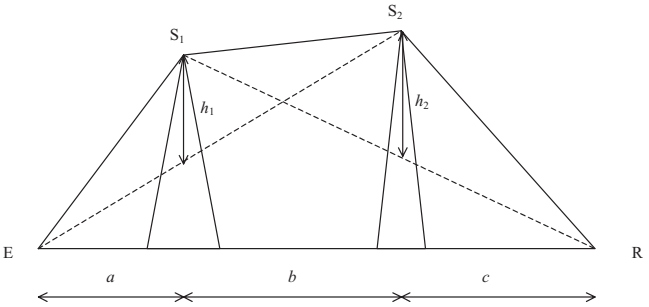

Figure 1.67 Method of Epstein and Peterson.

the theory of diffraction by a single knife edge, the top of the first obstacle being used as the source of diffraction over the second. The first path, defined by the distance $a + b$ and the height h_1, gives the loss A_1 and the second path, defined by the distance $b + c$ and the height h_2, gives the loss A_2, to which one adds a term of correction A_C. The obstacle loss is thus given by the relation

$$A_{OB} = A_1 + A_2 + A_C \tag{1.98}$$

where

$$A_C = 10\log\left(\frac{(a+b)(b+c)}{b(a+b+c)}\right)$$

which is valid when A_1 and A_2 each exceed approximately 15 dB.

When one of the edges is prevalent, Deygout's method is applied using the geometric elements presented in Figure 1.68.

In Deygout's method, the first path of diffraction corresponds to the edge which is prevalent and is defined by the distances a and $b + c$ and by the height h_1; in the same way, the second path is determined by the distances b and c and the height h_2. The obstacle loss is then given by the relation

$$A_{OB} = A_1 + A_2 \tag{1.99}$$

The diffraction loss over a knife edge, expressed in decibels, can be calculated using the following simplified relation when its value is higher than about 15 dB:

$$A = 16 + 20\log\left(\frac{h}{R_{F1}}\right) \tag{1.100}$$

In the case of rounded top obstacles, the same method can be applied by using relation (1.97).

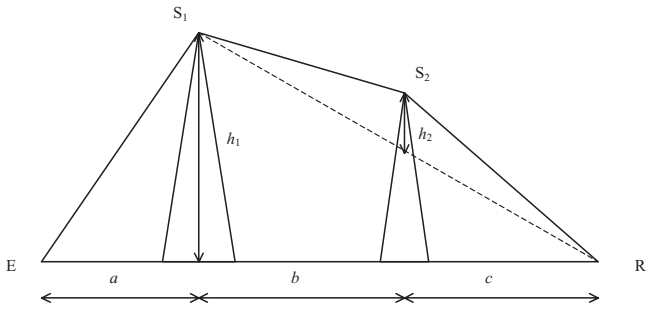

Figure 1.68 Deygout's method.

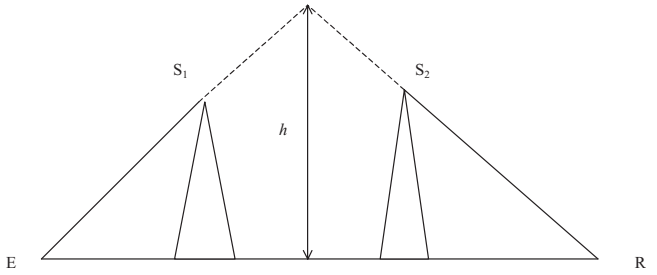

Figure 1.69 Millington's method.

Millington's method consists in replacing the obstacles met on the whole path by a single obstacle at the location of the vertex as shown in Figure 1.69.

1.9.5 Diffraction Loss General Curves

In the case of an irregular terrain, we can employ the following approximate formula, expressed in decibels, which is intermediate between diffraction over a smooth spherical Earth and a knife edge, where h is the height of the most significant obstacle:

$$A = 9 + 20\frac{h}{R_{F1}} \quad \text{for } \frac{h}{R_{F1}} > -0.5 \tag{1.101}$$

In the same way, for diffraction over a smooth spherical Earth, we can use the following approximate formula:

$$A = \begin{cases} 14 + 28\dfrac{h}{R_{F1}} & \text{for } \dfrac{h}{R_{F1}} > 0 \\ 14 + 23\dfrac{h}{R_{F1}} & \text{for } -0.5 < \dfrac{h}{R_{F1}} < 0 \end{cases} \tag{1.102}$$

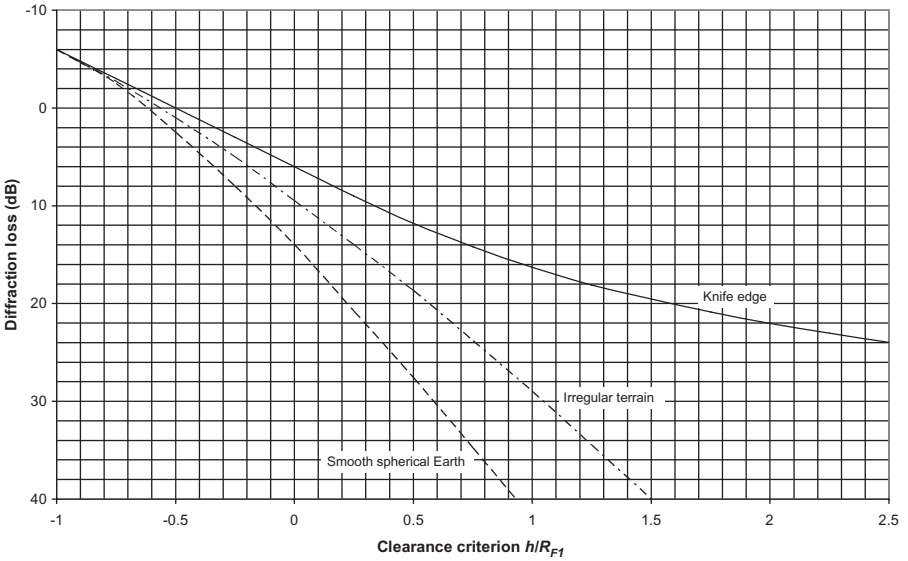

Figure 1.70 Diffraction loss for main obstacle types.

Figure 1.70 presents a synthesis of the diffraction loss for the main obstacle types which can be useful for an approximate calculation in the majority of cases. The curves corresponding to the knife edge and the smooth spherical Earth are very close to the values obtained using the general relation of diffraction loss (1.97).

1.9.6 Attenuation by Vegetation

Figure 1.71 presents specific attenuation through vegetation versus frequency for horizontal and vertical polarizations given by ITU-R Rep.1145 using an empirical method.

1.10 ATTENUATION BY ATMOSPHERIC GASES

Attenuation by atmospheric gases is due primarily to molecular absorption by oxygen and water vapor; oxygen has an absorption line at 118.74 GHz and a series of resonance lines between 50 and 70 GHz while water vapor presents three absorption lines at frequencies of 22.2, 183.3, and 325.4 GHz. Recommendation ITU-R P.676 gives the procedures to be used to accurately calculate gaseous attenuation at frequencies up to 1000 GHz. However, as most radio links are realized at frequencies lower than 50 GHz, for which the influence of dry air and water vapor is predominant, we will restrict interest to this limit in the following analysis which is based on reports such ITU-R Rep.719 and Rep.564 as well as on technical note 101 (NBS, 1966).

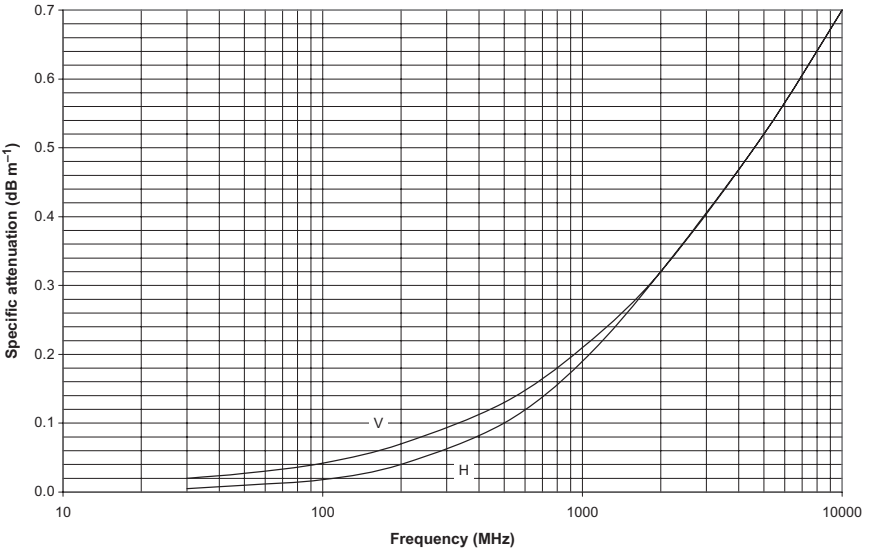

Figure 1.71 Attenuation by vegetation.

1.10.1 Specific Attenuation

Figure 1.72 presents specific attenuation by dry air and water vapor under normal conditions at ground level (1013 hPa; 15 °C; 7.5 g m^{-3}) as well as total specific attenuation versus frequency.

The specific absorption produced by either dry air or water vapor at ground level (1013 hPa, 15 °C), expressed in decibels per kilometer, breaks up into two terms: γ_0, which represents the contribution of dry air, and γ_W, which represents that of water vapor:

$$\gamma_0 = \begin{cases} \left[7.19\times10^{-3} + \dfrac{6.09}{f^2+0.227} + \dfrac{4{,}81}{(f-57)^2+1.5}\right] f^2\times10^{-3} & \text{for } f < 57\,\text{GHz} \\ \left[(3.79\times10^{-7})f + \dfrac{0.265}{(f-63)^2+1.59} + \dfrac{0.028}{(f-118)^2+1.47}\right](f+198)^2\times10^{-3} & \text{for } f > 63\,\text{GHz} \end{cases} \tag{1.103}$$

$$\gamma_W = \left[0.05 + 0.0021\nu + \frac{3.6}{(f-22.2)^2+8.5} + \frac{10.6}{(f-183.3)^2+9} + \frac{8.9}{(f-325.4)^2+26.3}\right] f^2\nu \times 10^{-4} \quad \text{for } f < 350\,\text{GHz}$$

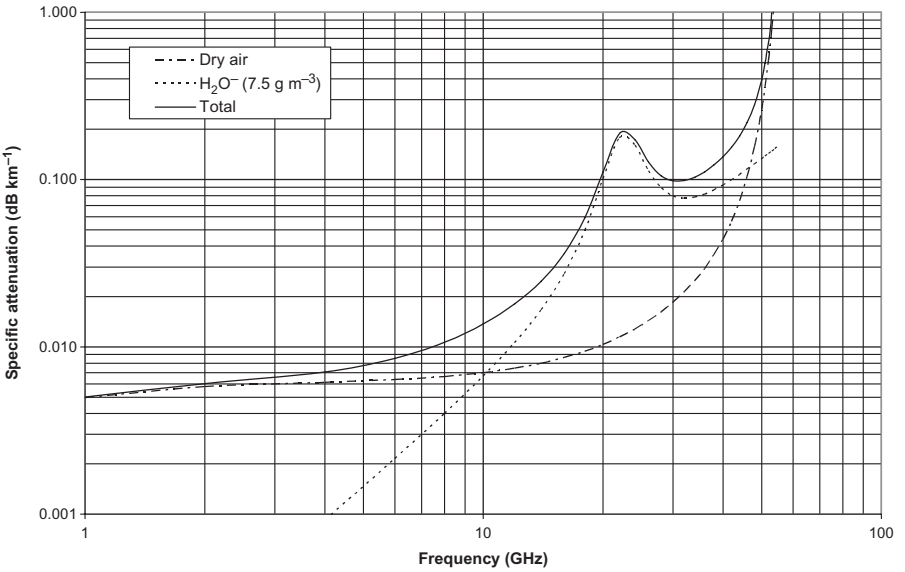

Figure 1.72 Specific attenuation by atmospheric gases.

where v is water vapor concentration in grams per cubic meter. Figures 1.40 and 1.41 give the geographical distribution for various periods of the year of water vapor concentration, and this can also be given from usual weather data using relations (1.78).

1.10.2 Terrestrial Paths

Total absorption by atmospheric gases on a terrestrial radio link of length d becomes

$$A_a = (\gamma_0 + \gamma_W)d \tag{1.104}$$

Figure 1.73 presents another way to evaluate the median absorption according to distance and frequency that is largely used in the calculation of very long microwave radio links budgets such as those which use the troposcatter mode. The median absorption by water vapor and oxygen according to frequency and distance, expressed in decibels, can be calculated using the relation

$$A_a = 0.01485\sqrt{f}\left(0.004075d + 1.45 - \sqrt{0.00001173d^2 - 0.0097875d + 2.1}\right) \tag{1.105}$$

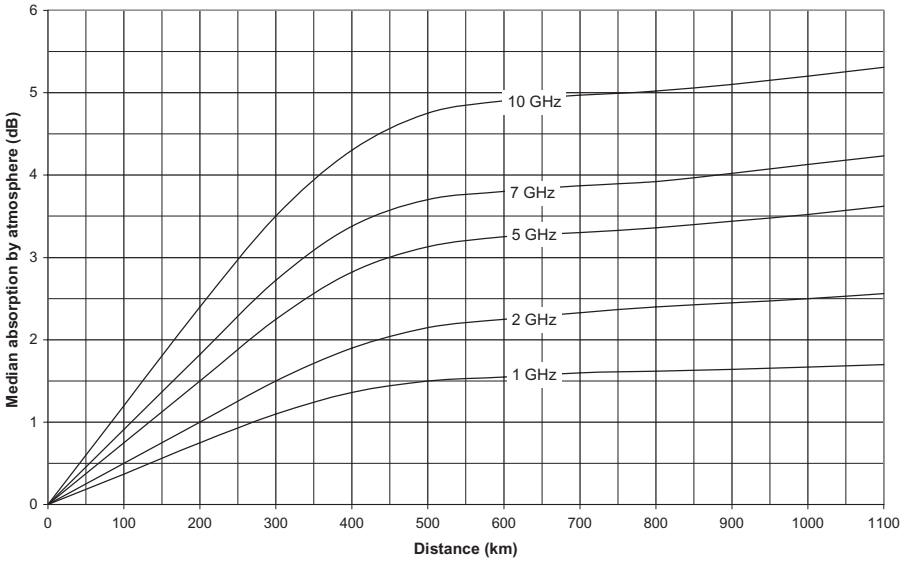

Figure 1.73 Median absorption versus frequency and distance (NBS, 1966).

where f = frequency (MHz)
d = distance (km)

1.10.3 Slant Paths

In the case of oblique paths, we suppose an exponential decrease of air density with altitude and utilize an equivalent height h_0 for dry air and h_W for water vapor, expressed in kilometers, for frequencies outside the range 57–63 GHz, such as

$$h_0 = \begin{cases} 6\,\text{km} & \text{for } f < 57\,\text{GHz} \\ 6 + \dfrac{40}{(f-118.7)^2 + 1} & \text{for } 63\,\text{GHz} < f < 350\,\text{GHz} \end{cases}$$

$$h_W = h_{W0}\left[1 + \frac{3}{(f-22.2)^2+5} + \frac{5}{(f-183.3)^2+6} + \frac{2.5}{(f-325.4)^2+4}\right] \quad \text{for } f < 350\,\text{GHz}$$

where h_{W0} equals 1.6 km in clear weather and 2.1 km in rainy weather. Total attenuation in the direction of the zenith starting from sea level then becomes

$$A_a = h_0\gamma_0 + h_W\gamma_W \tag{1.106}$$

1.10.3.1 Elevation Angle Greater Than 10° Total attenuation in the case of inclined paths between a satellite and an Earth station situated at sea level is given by the relation

$$A_a = \frac{\gamma_0 h_0 + \gamma_W h_W}{\sin\theta} \tag{1.107}$$

Figure 1.74 presents the total attenuation at sea level for water vapor concentrations of respectively 7.5 g m^{-3} (continental climate) and 20 g m^{-3} (oceanic and tropical climates) versus frequency for various values of elevation angle. To determine the attenuation on an oblique path, in which elevation angle θ is generally higher than 10°, from a station located at an altitude h_S, this last expression becomes

$$A_a = \frac{\gamma_0 h_0 \exp(-h_S/h_0) + \gamma_W h_W}{\sin\theta} \qquad \theta > 10°$$

Relation (1.107) is also applicable to terrestrial inclined paths between a station situated at an altitude h_1 and another one at a higher altitude h_2 by replacing the values h_0 and h_W by the following values:

$$h_0' = h_0\left[\exp\left(-\frac{h_1}{h_0}\right) - \exp\left(-\frac{h_2}{h_0}\right)\right] \qquad h_W' = h_W\left[1 - \exp\left(\frac{h_1 - h_2}{h_W}\right)\right]$$

1.10.3.2 Elevation Angle between 0° and 10° In the case of inclined paths between a satellite and an Earth station situated at sea level, the total attenuation becomes

$$A_a = \frac{\sqrt{a}}{\cos\theta}\left[\gamma_0\sqrt{h_0}F\left(\tan\theta\sqrt{\frac{a}{h_0}}\right) + \gamma_W\sqrt{h_W}F\left(\tan\theta\sqrt{\frac{a}{h_W}}\right)\right]$$

where a = effective Earth radius including refraction (km)
θ = elevation angle
F = function defined as $F(x) = 1\Big/\left(0.661x + 0.339\sqrt{x^2 + 5.51}\right)$

1.11 ATTENUATION AND DEPOLARIZATION BY HYDROMETEORS

An attenuation can be experienced on terrestrial paths, either on microwave radio links or between an Earth station and a satellite, as a result of absorption and scattering by rain, snow, hail, or fog. Normally, for the very small percentage of time that is of interest in system design at frequencies above 5 GHz, we need only consider the attenuation due to rain. Attenuation by rain depends

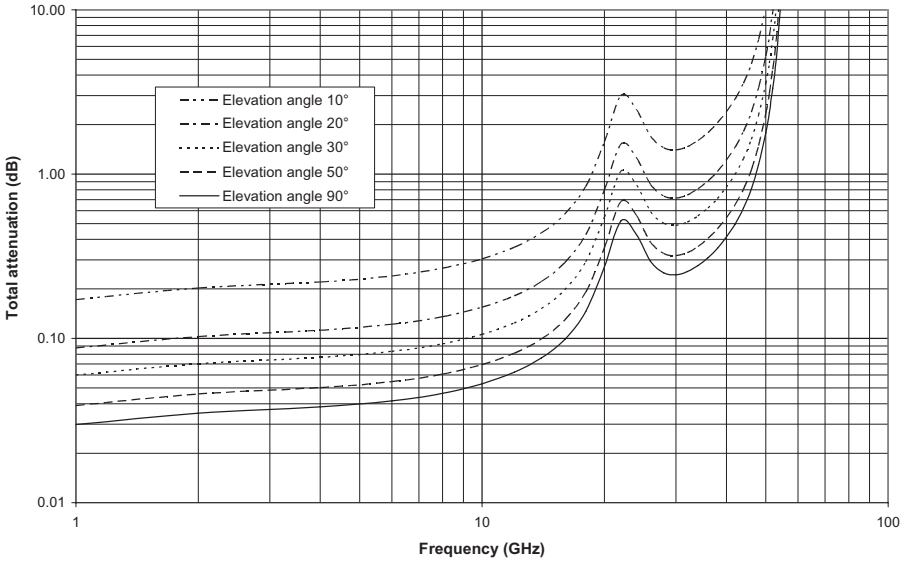

(*a*)

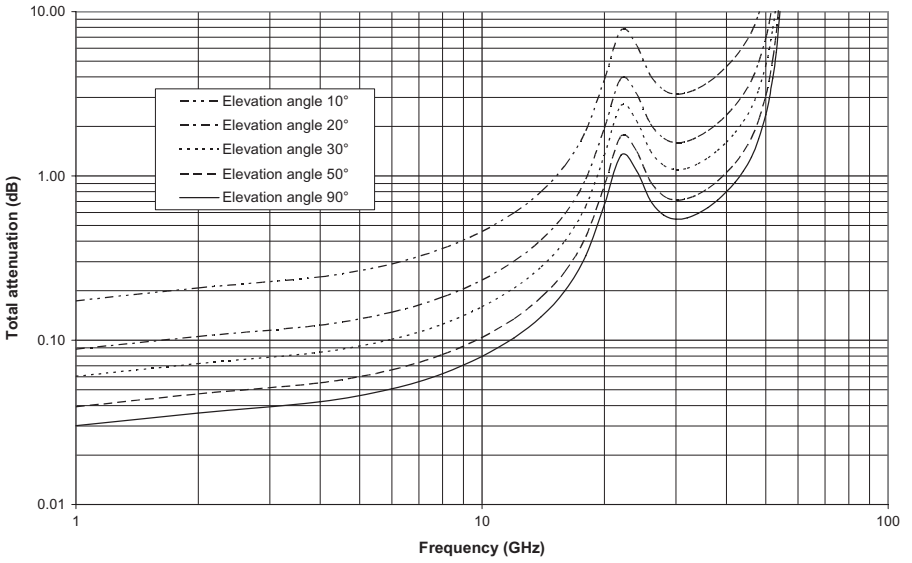

(*b*)

Figure 1.74 Total attenuation at sea level for water vapor concentration of (a) $7.5\,g\,m^{-3}$ and (b) $20\,g\,m^{-3}$ on oblique paths.

on the frequency and intensity of precipitation as well as the distance because of the nonuniformity of the rainfall rate throughout the path. Moreover, as the drops of rain have a lentil form during the fall, their axis of revolution being vertical, the attenuation differs according to whether the wave is horizontally or vertically polarized; it appears, in the course of propagation, as a component whose polarization is orthogonal to the expected polarization due to a phenomenon called cross-polarisation.

1.11.1 Rain Attenuation

Figure 1.75 shows the attenuation coefficient due to the rain, γ_R, versus frequency and rainfall rate. The relation between specific attenuation γ_R (in decibels per kilometer) and rainfall rate R (millimeters per hour) given by ITU-R P.838 is

$$\gamma_R = kR^{\alpha} \tag{1.108}$$

with

$$k = \frac{k_H + k_V + (k_H - k_V)\cos^2(\theta)\cos(2\tau)}{2}$$

$$\alpha = \frac{k_H\alpha_H + k_V\alpha_V + (k_H\alpha_H - k_V\alpha_V)\cos^2(\theta)\cos(2\tau)}{2k}$$

where θ = path elevation (deg)
τ = tilt angle of linearly polarized electric field vector with respect to horizontal or 45° in circular polarization (deg)

The coefficients k and α are given by the relations

$$\log k = \sum_{j=1}^{4} a_j \exp\left[-\left(\frac{\log f - b_j}{c_j}\right)^2\right] + m_k \log f + c_k$$

$$\alpha = \sum_{j=1}^{4} a_j \exp\left[-\left(\frac{\log f - b_j}{c_j}\right)^2\right] + m_\alpha \log f + c_\alpha$$

where the regression coefficients k_H, k_V, α_H, and α_V are given below:

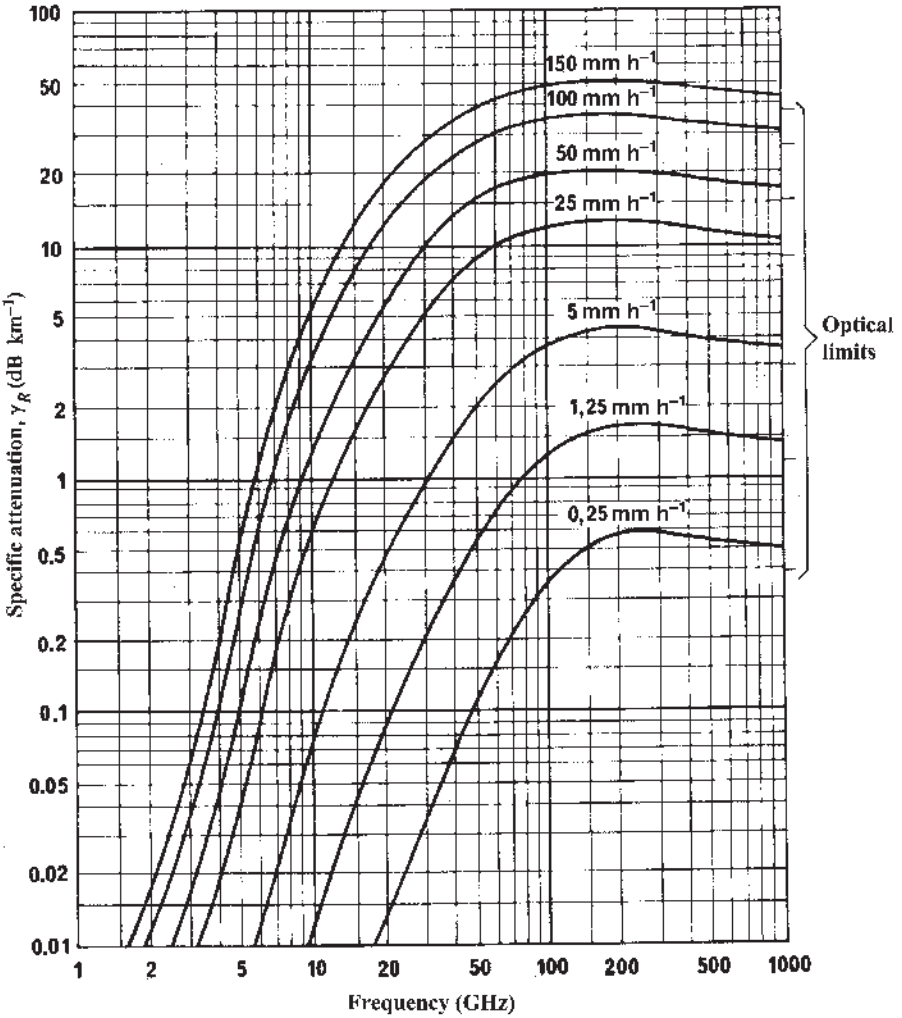

Figure 1.75 Rain attenuation (ITU-R Rep.721).

REGRESSION COEFFICIENTS FOR K_H

j	a_j	b_j	c_j	m_k	c_k
1	–5.33980	–0.10008	1.13098	–0.18961	0.71147
2	–0.35351	1.26970	0.45400	–0.18961	0.71147
3	–0.23789	0.86036	0.15354	–0.18961	0.71147
4	–0.94158	0.64552	0.16817	–0.18961	0.71147

REGRESSION COEFFICIENTS FOR K_V

j	a_j	b_j	c_j	m_k	c_k
1	–3.80595	0.56934	0.81061	–0.16398	0.63297
2	–3.44965	–0.22911	0.51059	–0.16398	0.63297
3	–0.39902	0.73042	0.11899	–0.16398	0.63297
4	0.50167	1.07319	0.27195	–0.16398	0.63297

REGRESSION COEFFICIENTS FOR α_H

j	a_j	b_j	c_j	m_k	c_k
1	–0.14318	1.82442	–0.55187	0.67849	–1.95537
2	0.29591	0.77564	0.19822	0.67849	–1.95537
3	0.32177	0.63773	0.13164	0.67849	–1.95537
4	–5.37610	–0.96230	1.47828	0.67849	–1.95537
5	16.17210	–3.29980	3.43990	0.67849	–1.95537

REGRESSION COEFFICIENTS FOR α_V

j	a_j	b_j	c_j	m_k	c_k
1	–0.07771	2.33840	–0.76284	–0.053739	0.83433
2	0.56727	0.95545	0.54039	–0.053739	0.83433
3	–0.20238	1.14520	0.26809	–0.053739	0.83433
4	–48.2991	0.791669	1.47828	–0.053739	0.83433
5	48.5833	0.791459	3.43990	–0.053739	0.83433

Recommendation ITU-R P.838 is bound to ITU-R P.837, which call for precise data files for all locations on the globe and a wide range of probabilities with an integration time of 1 min. For a quick calculation, the following tables, from ITU-R Rep.563, Rep.721, Rep.564, and Rep.724, provide the cumulative distribution over the average year, by rainfall climatic zones, of the exceeded rate of precipitation in millimeters per hour as well as the regression coefficients that correspond to the main frequency bands.

P (%)	A	B	C	D	E	F	G	H	J	K	L	M	N	P	Q
1	<0.1	0.5	0.7	2.1	0.6	1.7	3	2	8	1.5	2	4	5	12	24
0.3	0.8	2	2.8	4.5	2.4	4.5	7	4	13	4.2	7	11	15	34	49
0.1	2	3	5	8	6	8	12	10	20	12	15	22	35	65	72
0.03	5	6	9	13	12	15	20	18	28	23	33	40	65	105	96
0.01	8	12	15	19	22	28	30	32	35	42	60	63	95	145	115
0.003	14	21	26	29	41	54	45	55	45	70	105	95	140	200	142
0.001	22	32	42	42	70	78	65	83	55	100	150	120	180	250	170

Frequency (GHz)	k_H	k_V	α_H	α_V
1	0.0000387	0.0000352	0.912	0.880
2	0.000154	0.000138	0.963	0.923
4	0.000650	0.000591	1.121	1.075
6	0.00175	0.00155	1.308	1.265
7	0.00301	0.00265	1.332	1.312
8	0.00454	0.00395	1.327	1.310
10	0.0101	0.00887	1.276	1.264
12	0.0188	0.0168	1.217	1.200
15	0.0367	0.0335	1.154	1.128
20	0.0751	0.0691	1.099	1.065
25	0.124	0.113	1.061	1.030
30	0.187	0.167	1.021	1.000
35	0.263	0.233	0.979	0.963
40	0.350	0.310	0.931	0.929
45	0.442	0.393	0.903	0.897
50	0.536	0.479	0.873	0.868
60	0.707	0.642	0.826	0.824
70	0.851	0.784	0.793	0.793
80	0.975	0.906	0.769	0.769
90	1.06	0.999	0.753	0.754
100	1.12	1.06	0.743	0.744
120	1.18	1.13	0.731	0.732
150	1.31	1.27	0.710	0.711
200	1.45	1.42	0.689	0.690
300	1.36	1.35	0.688	0.689
400	1.32	1.31	0.683	0.684

1.11.1.1 Terrestrial Paths The intensity of precipitation varies from one point to another one and over time; as a result, the size of the rain cells is smaller as the intensity increases and the radio wave meets different rain conditions along the path. The estimate of the value of the attenuation A_R due to rain exceeded during a percentage of time p ranging between 0.001 and 1% can be obtained using the following relations (ITU-R P.530):

- For latitudes[14] ≥30°:

$$A_R = 0.12 A_{0.01} p^{-(0.546+0.043\log p)} \tag{1.109}$$

- For latitudes[15] <30°:

$$A_R = 0.07 A_{0.01} p^{-(0.855+0.139\log p)}$$

[14]This formula was established in order to obtain values equal to 0.12, 0.39, 1, and 2.14 for respectively 1, 0.1, 0.01, and 0.001% of time.
[15]This formula was established in order to obtain values equal to 0.07, 0.36, 1, and 1.44 for respectively 1, 0.1, 0.01 and 0.001% of time.

with

$$A_{0.01} = \gamma_{R0.01} d r_{0.01} \qquad \gamma_{R0.01} = k R_{0.01}^{\alpha}$$

$$r_{0.01} = \frac{1}{1 + d/d_0} \qquad d_0 = 35 \exp(-0.015 R_{0.01})$$

where $r_{0.01}$ = pathlength[16] reduction factor
$A_{0.01}$ = exceeded attenuation for 0.01% of time
d = pathlength (km)
$R_{0.01}$ = exceeded rainfall rate for 0.01% of time[17] (integration time 1 min)

Where long-term attenuation statistics exist at one polarization on a given link, the attenuation for the other polarization over the same link may be estimated as

$$A_V = \frac{300 A_H}{335 + A_H} \qquad A_H = \frac{335 A_V}{300 - A_V}$$

Figure 1.76 presents the 15 rainfall zones. Recommendation ITU-RP.841 gives further detailed information and data about the conversion of the statistics over the average year into statistics over any month (called "worst month" in the past); concerning the effects due to the rain, the percentage of annual time, p_A, and the percentage of time for any month, p_M, are generally related by the following formulas, which are illustrated in Figure 1.77:

$$p_A = 0.3 p_M^{1.15} \qquad P_M = 2.85 p_A^{0.87} \tag{1.110}$$

1.11.1.2 Earth–Space Paths The approximate method of calculation of the long-term statistics of attenuation due to the rain on an oblique way (ITU-R Rep.564) rises from the preceding one by considering the following parameters, which are presented in Figure 1.78:

H_S: altitude of Earth station (km)
θ: elevation angle (deg)
φ: latitude of Earth station (deg)

We calculate the effective rain height H_R, in kilometers, starting from the latitude of the Earth station:

$$H_R = \begin{cases} 3 + 0.028\varphi & \text{for } 0 \le \varphi \le 36° \\ 4 - 0.075(\varphi - 36) & \text{for } \varphi \ge 36° \end{cases} \tag{1.111}$$

[16]The attenuation by rain covers the atmospheric attenuation for the $r_{0.01}$ fraction of the path.
[17]If $R_{0.01} > 100$ mm/h, use the value 100 mm/h for the determination of d_0.

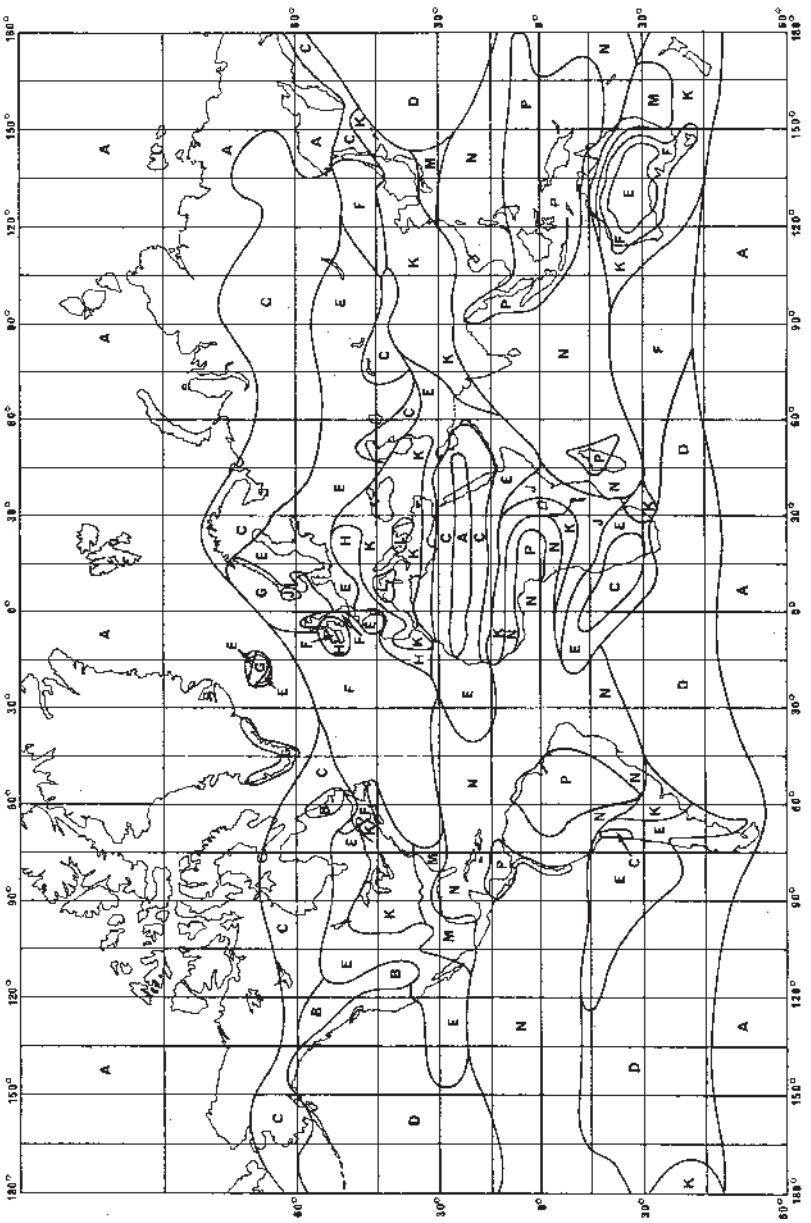

Figure 1.76 Rainfall zones (ITU-R Rep.724).

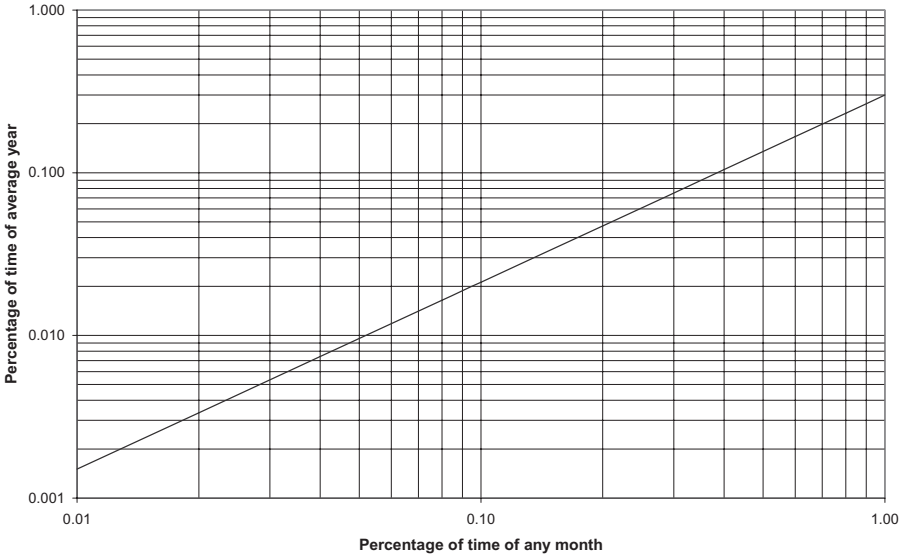

Figure 1.77 Relation between percentage of time for any month and for average year.

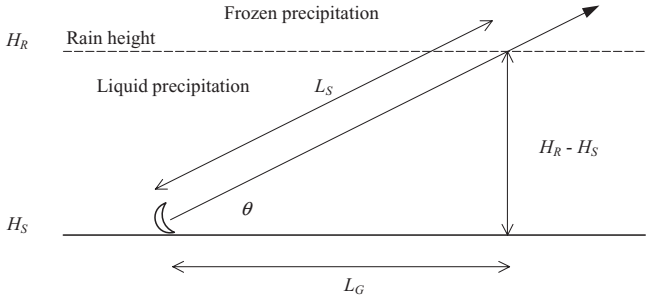

Figure 1.78 Earth–space path.

next, the length of the oblique path, L_S, below the effective rain height:

$$L_S = \frac{H_R - H_S}{\sin\theta} \quad \text{for } \theta \geq 5^\circ \tag{1.112}$$

then, the horizontal projection length L_G of the oblique path:

$$L_G = L_S \cos\theta$$

and, finally, the attenuation A_P given by relation[18] (1.109) with

[18]The Attenuation by rain covers the atmospheric loss for the $r_{0.01}$ fraction of the path defined below.

$$A_{0.01} = \gamma_{R0.01} L_S r_{0.01} \tag{1.113}$$

$$\gamma_{R0.01} = k(R_{0.01})^{\alpha} \qquad r_{0.01} = \frac{1}{1 + L_G / L_0} \qquad L_0 = 35\exp(-0.015 R_{0.01})$$

1.11.1.3 Site Diversity (Rayleigh's Equations for Correlation between Random Variables) As rain cells are of finite size and distributed in a random way, it is possible to improve considerably the availability of communications by satellite that use high frequencies by employing site diversity. We consider two stations located at two distinct sites which are each affected by the same individual probability P_i for a given attenuation A_i and bound by a correlation coefficient K. The combined probability P_c so that both stations simultaneously undergo the same attenuation A_i corresponding to their individual probability P_i is given by Rayleigh's relation:

$$P_c = \frac{P_i^2}{K^2 P_i + 1 - K^2} \tag{1.114}$$

such that for all (K, P_i)

$$P_i^2 \le P_c \le P_i$$

$$P_i = 1 \Rightarrow P_c = 1$$

$$P_i \to 0 \Rightarrow P_c \to P_i^2$$

$$K = 0 \Rightarrow P_c = P_i^2$$

$$K = 1 \Rightarrow P_c = P_i$$

We define the improvement factor by the expression

$$F_a = \begin{cases} \dfrac{P_i}{P_c} \\ \dfrac{K^2 P_i + 1 - K^2}{P_i} \end{cases} \tag{1.115}$$

Figure 1.79 shows the various terms which come into play; we consider there the probabilities P_1, P_2, and P_3 and the individual and combined attenuations which correspond to them in order to determine the diversity gain as well as the equivalent increase of margin. Figure 1.80 illustrates the relation between the combined probability P_c and the individual probability P_i for various values of the correlation coefficient. Figure 1.81 presents the improvement factor F_a according to the individual probability P_i for various values of the correlation coefficient. The diversity gain is given by the relation

$$G_d = A_i(P_2) - A_c(P_2) = A_i(P_2) - A_i(P_1) \tag{1.116}$$

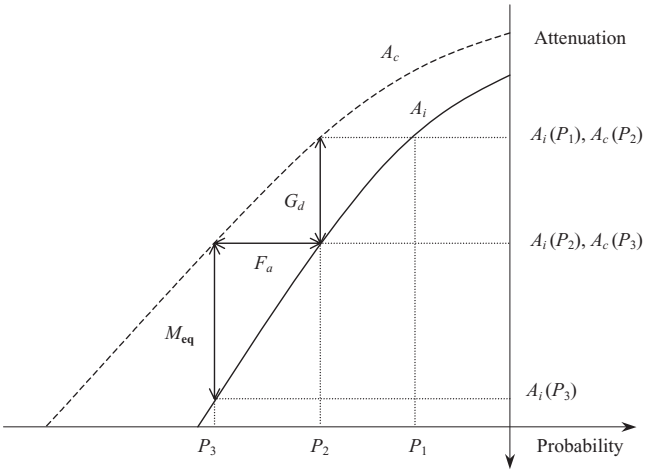

Figure 1.79 Representation of individual and combined distributions.

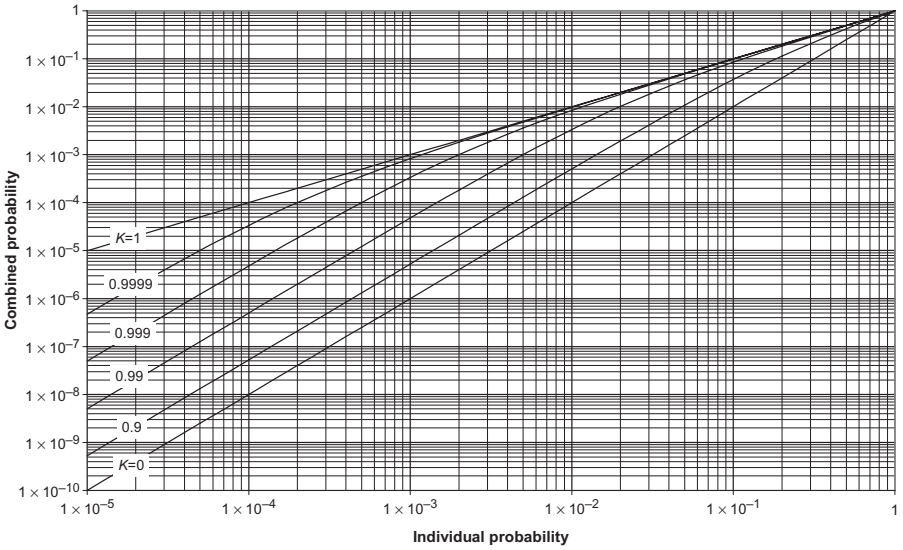

Figure 1.80 Relation between combined probability and individual probability versus correlation coefficient.

where

$$P_2 = \frac{P_1^2}{K^2 P_1 + 1 - K^2}$$

from which we obtain

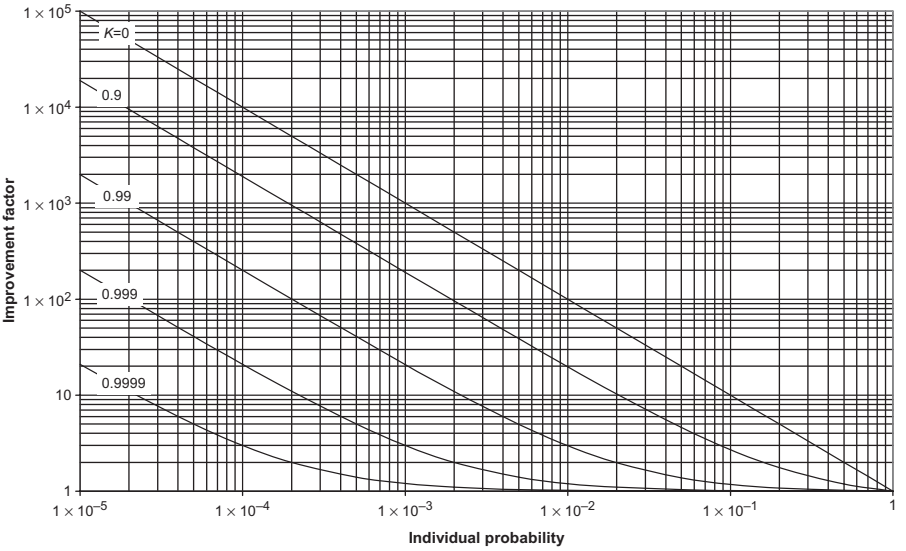

Figure 1.81 Relation between improvement factor and individual probability versus correlation coefficient.

$$P_1 = \frac{1}{2}\left(K^2 P_2 + \sqrt{K^4 P_2^2 + 4P_2(1-K^2)}\right) \tag{1.117}$$

and finally the equivalent increase of margin:

$$M_{\text{eq}} = A_i(P_3) - A_c(P_3) = A_i(P_3) - A_i(P_2) \tag{1.118}$$

where

$$P_3 = \frac{P_2^2}{K^2 P_2 + 1 - K^2}$$

When the two sites are sufficiently distant from one another, the individual probabilities of exceeding a given value can be different. Setting $P_{i1} < P_{i2}$, relation (1.114) becomes

$$P_c = \frac{P_{i1} P_{i2}}{K^2 P_{i2} + 1 - K^2}$$

In practical applications, we consider the probability of exceeding a given value for a single site P_s and the combined probability for the same exceeded value with two sites P_c while posing

$$\frac{1}{K^2} = 1 + \beta^2$$

from which

$$P_c = \frac{P_s^2(1+\beta^2)}{P_s + \beta^2} \tag{1.119}$$

$$F_a = \frac{P_s}{P_c} = \frac{1+\beta^2/P_s}{1+\beta^2} \approx 1 + \frac{\beta^2}{P_s} \tag{1.120}$$

with the following empirical values given by ITU-R P.618:

$$\beta^2 = \begin{cases} 10^{-4} d^{1.33} & \text{in general case} \\ 10^{-4} (\sin\theta)^{0.5} d^{1.5} & \text{considering elevation angle } \theta \end{cases} \tag{1.121}$$

As the rain corresponds to a small percentage of time (~1%), one replaces the probabilities corresponding to the total time by the percentage of time affected by the rain, which yields:

$$p_{c\%} = \frac{p_{s\%}^2(1+\beta^2)}{p_{s\%} + 100\beta^2} \tag{1.122}$$

and

$$F_a = \frac{1+100\beta^2/p_{s\%}}{1+\beta^2} \approx 1 + \frac{100\beta^2}{p_{s\%}} \tag{1.123}$$

Figure 1.82 shows the relation between the percentage of time with and without diversity for the same attenuation.

Introducing the distribution function of the attenuation due to rain (1.109), we obtain

$$A_s = A_{0.01}\, 0.12\, p_{s\%}^{-(0.546+0.043\log p_{s\%})} \tag{1.124}$$

$$A_c = A_{0.01}\, 0.12\, p_{c\%}^{-(0.546+0.043\log p_{c\%})} \tag{1.125}$$

where

$$p_{c\%} = \frac{p_{s\%}}{2}\left[1 + \sqrt{1 + 0.04\frac{d^{1.33}}{p_{s\%}}}\right] \tag{1.126}$$

Figure 1.83 shows, for example, by considering an individual attenuation $A_{0.01}$ of 25 dB, the improvement which would introduce the site diversity versus

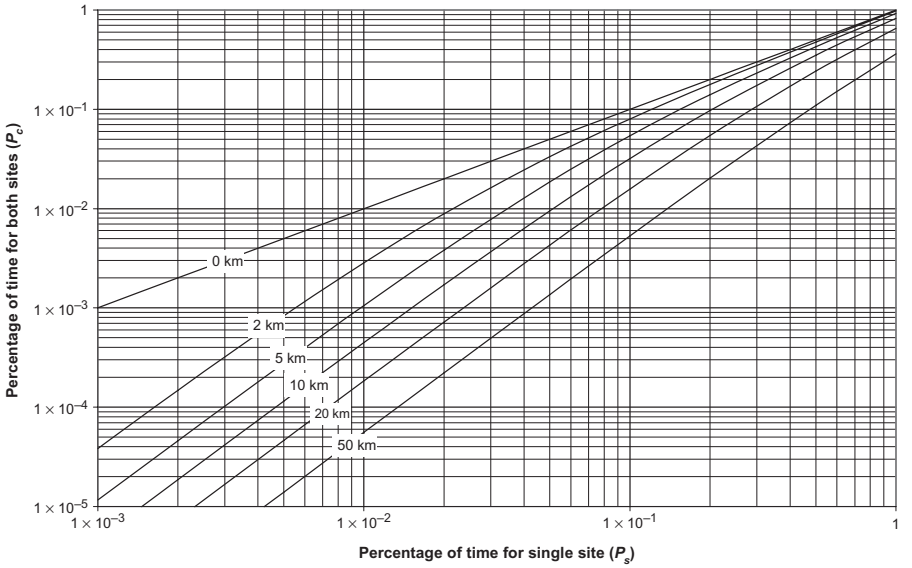

Figure 1.82 Individual and combined probabilities versus spacing.

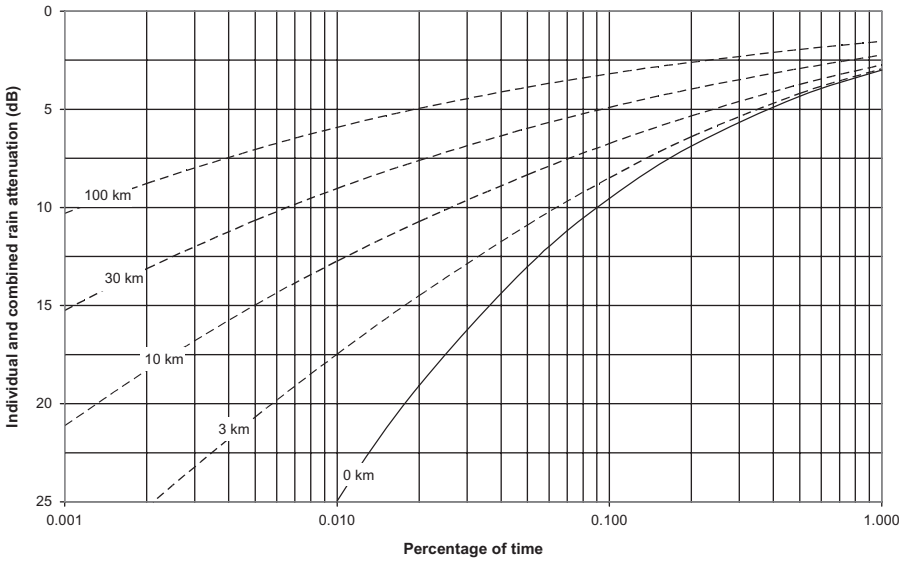

Figure 1.83 Site diversity improvement for $A_{0.01} = 25\,\text{dB}$.

percentage of time and spacing, that is, the distance between both Earth stations. An empirical expression for the diversity gain G is also given by the relation (Hodge, 1982)

$$G = G_d G_f G_\theta G_\psi \tag{1.127}$$

with

$$G_d = a(1 - e^{-bd}) \qquad G_f = e^{-0.025f}$$
$$G_\theta = 1 + 0.006\theta \qquad G_\psi = 1 + 0.002\psi$$

where $a = 0.78A - 1.94(1 - e^{-0.11A})$
$b = 0.59(1 - e^{-0.1A})$
d = distance between two sites (km)
A = attenuation by rain for only one site (dB)
f = frequency (GHz)
θ = elevation angle (deg)
ψ = angle in degrees formed between base connecting two sites and azimuth of satellite chosen so that $\psi \leq 90°$

1.11.1.4 Attenuation Due to Gases, Clouds, and Fog The method of pediction of attenuation due to rain was defined so that the calculated results coincide as much as possible with the experiments; consequently, it includes other losses due to gases, clouds, and fog for frequencies up to 40 GHz.

1.11.2 Depolarization by Hydrometeors

1.11.2.1 Polarization of Electromagnetic Wave As indicated in Section 1.1.5 and 1.3.3, the polarization of an electromagnetic wave is defined by the orientation of the electric field that is perpendicular to the direction of propagation; the projection of the point E of the electric field on a plane (P) perpendicular to the direction of propagation describes an ellipse for one period and this is that one calls the elliptic polarization represented on Figure 1.84. In short, elliptic polarization is characterized by the following parameters:

Direction of rotation
Axial ratio, ellipticity ratio, and angle of inclination ϕ of ellipse

In practice, most of the antennas radiate in linear polarization or in circular polarization which are particular cases of the elliptic polarization:

Polarization is linear when the axial ratio is infinite, that is, when the ellipse is completely flat and the vector E varies only in intensity.
Polarization is circular when the axial ratio is equal to 1.

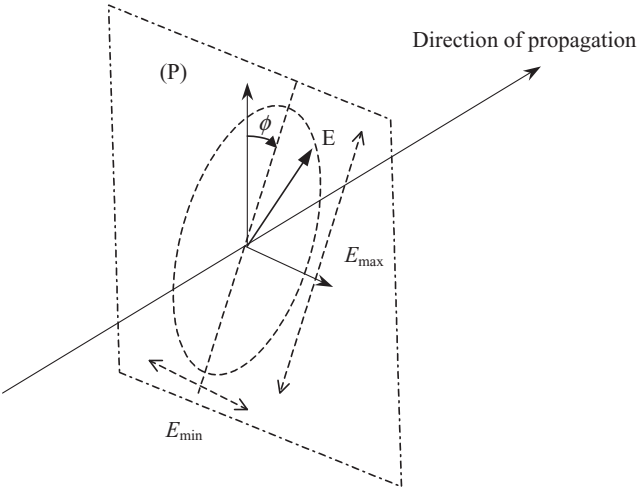

Figure 1.84 Elliptic polarization of radiated wave.

The elliptic polarization can also be regarded as the sum of two orthogonal components whose directions of rotation are opposite; two waves with orthogonal polarizations being in theory insulated, the same antenna can receive and/or emit simultaneously two carriers at the same frequency with polarizations horizontal and vertical or right-circular and left-circular.

1.11.2.2 Cross-Polarization Effects An important characteristic of the radio wave is its purity of polarization, i.e. the ratio between the component known as co-polar, which represents the useful signal, and the component known as cross-polar which constitutes the jamming power.

The cross-polarization results from the mechanism of depolarization by which appears, in the course of propagation, a polarization component which is orthogonal to the one expected; beyond 6 GHz, the principal effects are produced by hydrometeors, that is, the rain and the ice crystals. Figure 1.85 presents, on the one hand, the cross-polarization of two orthogonal waves propagated through a depolarizing medium and, on the other hand, the discrimination of both polarizations at the reception.

For a radio wave transmitted with a given polarization, the ratio of the power received with the expected polarization to the power received with the orthogonal polarization is called cross-polarization discrimination XPD, given by relation (1.47). For two radio waves transmitted with the same power and orthogonal polarization, the ratio of the copolarized power to the cross-polarized power in a given receiver is called cross-polarization isolation[19] (XPI).

[19]The XPI corresponds as well to the isolation between ports, that is, to the ratio of the transmitted power to the power collected on the orthogonal polarization when using the same feed horn for emission and reception.

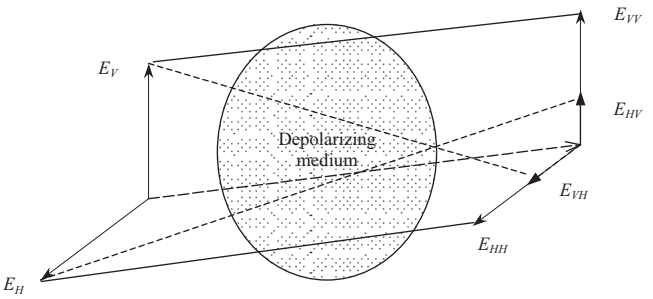

Figure 1.85 Cross-polarization.

Cross-polarization discrimination depends on the depolarization by the propagation medium and on the characteristics of purity of polarization of the emitting and receiving antennas, as it corresponds to the ratio of the copolarized power to the cross-polarised power of the same wave. We see that the wave emitted on vertical polarization E_V is received with level E_{VV} on the vertical polarization, which is the copolarized component constituting the useful signal, and E_{VH} on horizontal polarization, which is the cross-polarized or jamming component—reciprocally, levels E_{HH} and E_{HV} correspond to the wave emitted on horizontal polarization E_H.

Cross-polarization discrimination is given by the relations

$$(\mathrm{XPD})_V = 20\log\left[\frac{E_{VV}}{E_{VH}}\right] \qquad (\mathrm{XPD})_H = 20\log\left[\frac{E_{HH}}{E_{HV}}\right] \tag{1.128}$$

Cross-polarization isolation is given by the relations

$$(\mathrm{XPI})_V = 20\log\left[\frac{E_{VV}}{E_{HV}}\right] \qquad (\mathrm{XPI})_H = 20\log\left[\frac{E_{HH}}{E_{VH}}\right] \tag{1.129}$$

Cross-polarization discrimination due to hydrometeors $(\mathrm{XPD})_{\mathrm{hydro}}$ is strongly correlated with the copolar attenuation by rain, A_R; the method of prediction, given in ITU-R P.618, consists in calculating the terms separately depending on the rain and ice expressed in decibels:

$$(\mathrm{XPD})_{\mathrm{hydro}} = (\mathrm{XPD})_{\mathrm{rain}} - C_{\mathrm{ice}} \tag{1.130}$$

To calculate the long-term statistics of depolarization starting from the statistics of the attenuation due to the rain, we take into account the following parameters:

A_R: attenuation exceeded during percentage of time $p_{\%}$ (dB)
τ: tilt angle of linearly polarized electric field vector with respect to horizontal or 45° in circular polarization (deg)
f: frequency (GHz)
θ: elevation angle (deg)

The cross-polarization discrimination due to rain not exceeded for $p_{\%}$ of the time is given by

$$(\mathrm{XPD})_{\mathrm{rain}} = C_f - C_A + C_\tau + C_\theta + C_\sigma \qquad (\mathrm{dB}) \tag{1.131}$$

with

$$C_f = 30\log(f) \quad \text{for } 8 \le f \le 35\,\mathrm{GHz}$$
$$C_A = \mathrm{V}(f)\log(A_R)$$

where

$$\mathrm{V}(f) = \begin{cases} 12.8 f^{0.19} & \text{for } 8 \le f \le 20\,\mathrm{GHz} \\ 22.6 & \text{for } 20 \le f \le 35\,\mathrm{GHz} \end{cases}$$

and

$$C_\tau = -10\log[1 - 0.484(1 + \cos(4\tau))]$$
$$C_\theta = -40\log[\cos\theta] \quad \text{for } \theta \le 60°$$
$$C_\sigma = 0.0052\sigma^2$$

where σ is the equivalent standard deviation of the distribution of the oblique angle of the rain drops, expressed in degrees, which takes the values of 0°, 5°, 10°, and 15° for 1, 0.1, 0.01, and 0.001% of the time. The term depending on ice crystals is given by the relation

$$C_{\mathrm{ice}} = (\mathrm{XPD})_{\mathrm{rain}}\left[\frac{0.3 + 0.1\log(p_{\%})}{2}\right] \tag{1.132}$$

In the case of terrestrial paths, the depolarization due to ice crystals can be neglected because their presence is above the isotherm 0°, but reduction of the cross-polarization discrimination can occur in clear atmosphere under conditions of multipath propagation or in heterogeneous turbulence along the path.

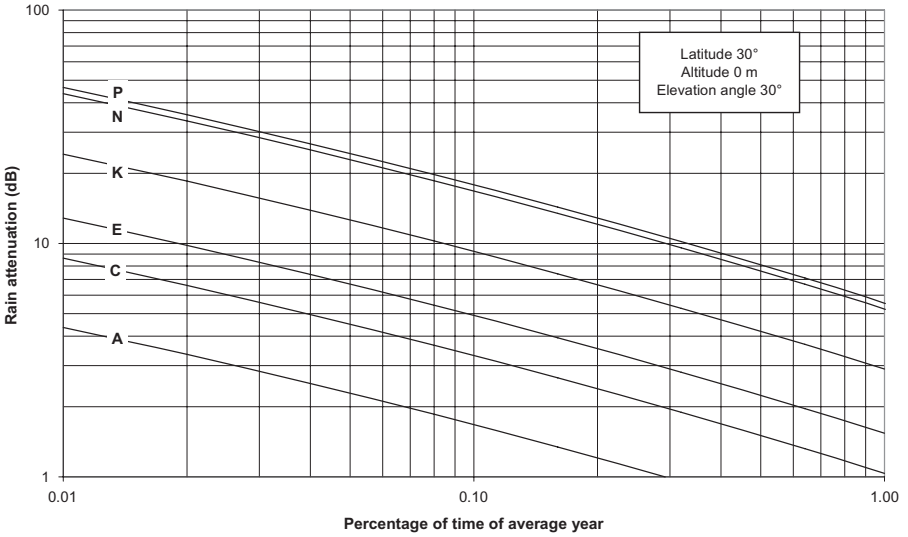

Figure 1.86 Attenuation by rain at 20 GHz.

The cross-polarization due to hydrometeors, $(\mathrm{XPD})_{\mathrm{hydro}}$, is added to the total cross-polarization due to equipment, $(\mathrm{XPD})_E$, which is primarily related to the characteristics of the sources and the antennas concerning their purity of polarization in the following way:

$$(\mathrm{XPD})_{\mathrm{total}} = -10\log(10^{-(\mathrm{XPD})_E/10} + 10^{-(\mathrm{XPD})_{\mathrm{hydro}}/10}) \tag{1.133}$$

Figures 1.86 and 1.87 show, for example, the attenuation and depolarization due to rain according to the percentage of time at frequency 20 GHz for various standard climates on an Earth–space path with:

- Axial ratio and cross-polarization isolation of 30 dB for satellite (ER = 0.5 dB)
- Axial ratio and cross-polarization isolation of 20 dB (ER = 1.7 dB) for Earth station

1.12 INFLUENCE OF IONOSPHERE

The table below, from ITU-R P.618, indicates the estimated maximum values of the ionospheric effects for an elevation angle of approximately 30°; these effects, which occur at the time of the crossing of the ionosphere, vary according to the reverse of the square of the frequency.

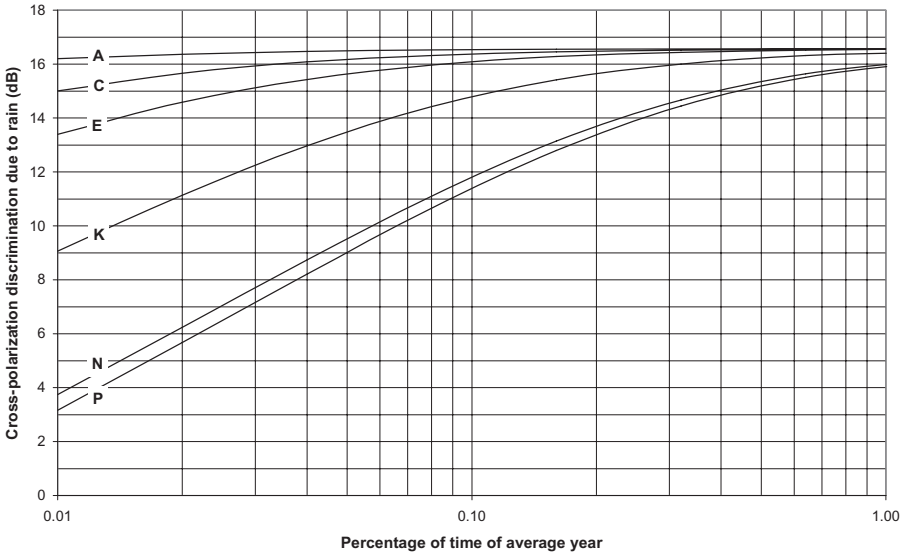

Figure 1.87 Depolarization by rain at 20 GHz.

Effects	Variation	0.1 GHz	0.25 GHz	0.5 GHz	1 GHz	3 GHz	10 GHz
Faraday rotation[a]	$1/f^2$	30 rotations	4.8 rotations	1.2 rotation	108°	12°	1.1°
Propagation delay	$1/f^2$	25 μs	4 μs	1 μs	0.25 μs	0.028 μs	0.0025 μs
Refraction	$1/f^2$	<1°	<0.16°	<2.4′	<0.6′	<4.2″	<0.36″
Variation in direction of arrival (rms)	$1/f^2$	20′	3.2′	48″	12″	1.32″	0.12″
Absorption (midlatitude)	$1/f^2$	<1 dB	<0.16 dB	<0.04 dB	<0.01 dB	<0.001 dB	$<10^{-4}$ dB
Dispersion (ps Hz^{-1})	$1/f^3$	0.4	0.026	0.0032	0.0004	$1.5.10^{-5}$	4.10^{-7}
Scintillation[b]	—	—	—	—	>20 dBcc	≈10 dBcc	≈4 dBcc

[a]Ionospheric effects above 10 GHz are negligible.

[b]Values observed near geomagnetic equator during early nighttime hours at equinox under conditions of high sunspot number.

1.12.1 Scintillation

Scintillation refers to the variations of amplitude, phase, polarization, and arrival angle which appear when radio waves cross zones of turbulent irregularities of the refractive index in the troposphere or the electron density in the ionosphere. Figure 1.88 presents the distribution of the fade depth due to

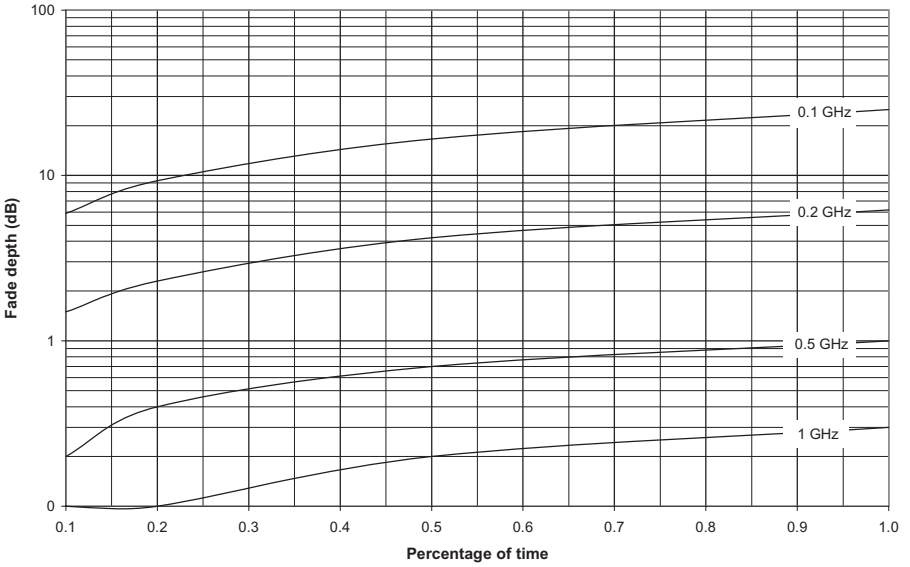

Figure 1.88 Distribution of fade depth due to ionospheric scintillation.

ionospheric scintillation at average latitudes for various frequency bands. In addition, the amplitude of the fast fluctuations of the received signal due to crossing the troposphere is all the more important as the frequency is high, the elevation angle is small, and the moisture is high and decreases when the beamwidth of the antenna decreases; for elevation angles higher than 3°, the standard deviation of the scintillation of amplitude would lie between 0.1 and 1 dB according to the elevation angle at the frequency 7 GHz and between 0.4 and 4 dB at the frequency 100 GHz.

1.12.2 Faraday's Rotation

Recommendation ITU-R P.531 expresses Faraday's rotation of the plane of polarization of a linearly polarized wave due to the Earth magnetic field and the ionosphere by the relation

$$\theta = 2.36\,10^2 B_{av} N_T f^{-2} \tag{1.134}$$

where θ = angle of rotation (rad)
B_{av} = average Earth magnetic field (Wb m^{-2})
f = frequency (GHz) and the electron density N_T of the ionosphere is given as

$$N_T = \int_s n_e(s)\, ds$$

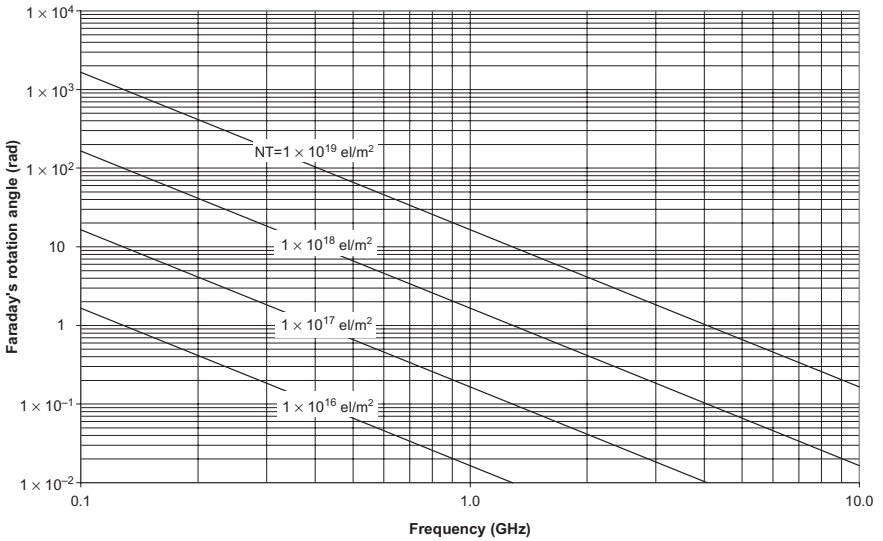

Figure 1.89 Faraday's rotation.

where n_e = electron concentration (el/m^3)
s = traversed path

Figure 1.89 shows the variation of Faraday's rotation angle versus frequency for various values of electron density.

1.12.3 Propagation Time Delay

The presence of charged particles in the ionosphere causes a delay in electromagnetic wave propagation; the propagation time delay is given by the relation

$$t = 1.345 \times 10^{-7} \frac{N_T}{f^2} \tag{1.135}$$

Figure 1.90 presents the propagation delay due to crossing the ionosphere versus frequency for various values of electron density.

1.13 THERMAL RADIATION

1.13.1 Origin of Thermal Radiation

Any hot body emits a thermal radiation whose intensity increases with the temperature; this radiation transports energy that is propagated in the form

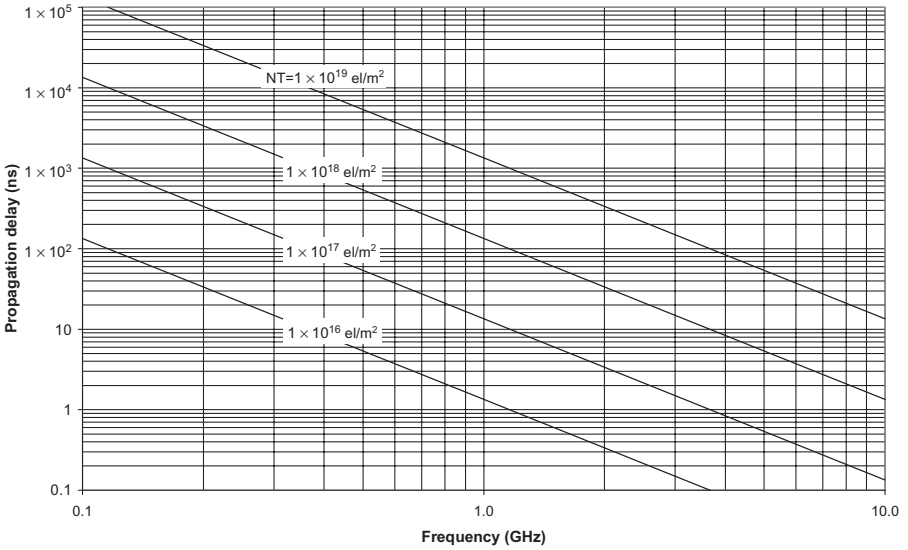

Figure 1.90 Propagation delay due to crossing of ionosphere.

of electromagnetic waves and has a continuous spectrum; that is, that it comprises components at all the frequencies with different intensities. The macroscopic concept of temperature rests on the thermal agitation of the elementary corpuscles which constitute the matter. The first theories, which lead to Rayleigh's law for blackbody, postulated the presence of a great number of elementary oscillators radiating all possible frequencies; these oscillators are the electrons bound to the atoms of the body that emit radiation while oscillating and are excited by absorbing other radiation. Since Rayleigh's law is valid only for radio frequencies, it is by introducing the concept of minimal quantity of energy, or quantum of energy, that Planck could establish the law which bears his name and that represents perfectly the phenomena observed at all frequencies; that is, electrons can radiate or absorb energy only by jump(s) or quanta of value $h\nu$, where h is the Planck's constant and ν is the radiated frequency.

1.13.2 Propagation of Thermal Radiation

Consider a surface S sufficiently small to constitute a point source of radiation in all directions of space, as shown in Figure 1.91. The quantity of energy which crosses in 1 s the surface S' located on a sphere at a certain distance from S is propagated inside the cone C and is called the power flux; bringing back the surface to $1\,m^2$, we obtain the power flux density, which is the quantity of energy which crosses this unit of area per second and is expressed in watts per square meter.

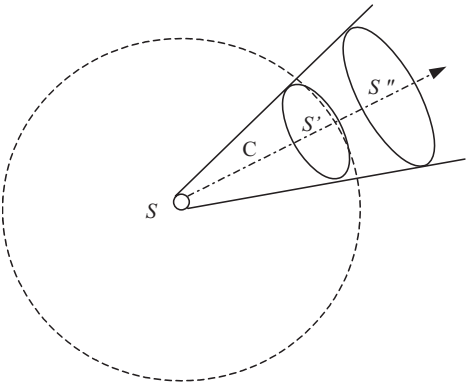

Figure 1.91 Propagation of thermal radiation.

In the same way, another surface S'' located on a more distant sphere would receive a power flux density whose intensity would be in the ratio S'/S''; the power flux density thus varies as the inverse ratio of the square of the distance to the radiating source and depends only on the properties of the surface S and the inner volume of cone C. The inner portion of space of the cone C constitutes a solid angle; the unit of solid angle, the steradian (sr), is that under which one sees a unit of area from the center of the sphere. When the radiating source is sufficiently extended to comprise zones from which the characteristics of radiation are different, we use the unit of brightness, that is, the power flux density that is received from an area of the source which is seen under a given solid angle, expressed as watts per square meter per steradian.

The power flux density and the brightness of a body depend on the spectrum part which has been chosen for the observation; by considering an interval of frequencies dv in the vicinity of the frequency v sufficiently small so that the characteristics of radiation are constant, we report these terms to an interval of 1 cycle/s or 1 Hz and thus obtain:

- Monochromatic power flux density in vicinity of frequency v ($\mathrm{W\,m^{-2}\,Hz^{-1}}$)
- Spectral brightness or monochromatic brightness ($\mathrm{W\,m^{-2}\,Hz^{-1}\,sr^{-1}}$)

The spectral brightness $B(v)$ of a body in the vicinity of the frequency v depends only on its temperature and its capacity to absorb radiations at the frequency v.

1.13.3 Blackbody

A blackbody is a body which absorbs all radiation that it receives; it is shown that, for such a body, the spectral brightness depends only on its temperature

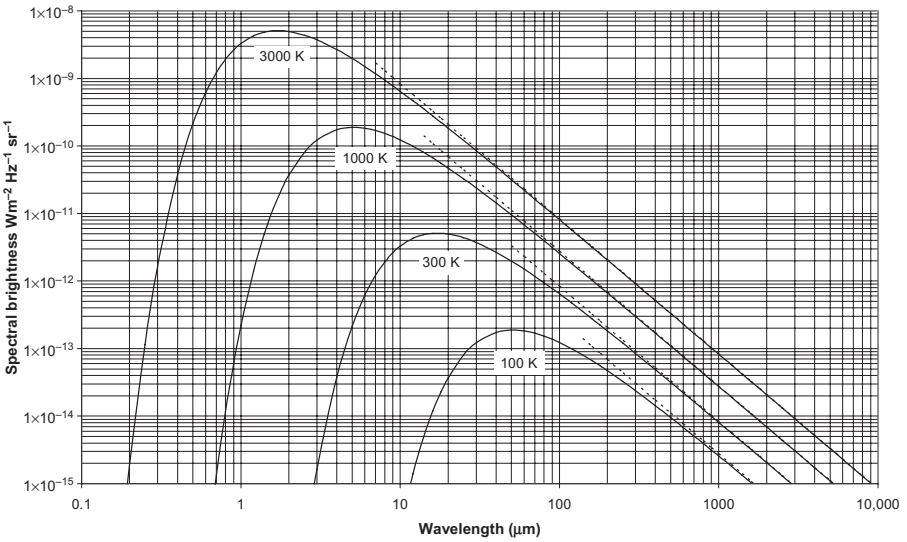

Figure 1.92 Spectral distribution of brightness of blackbody (Planck's law and Rayleigh's law).

and on the frequency considered, and the law of radiation of the blackbody, or Planck's law, is given by the relation

$$B(\nu) = \frac{2h\nu^3 c^{-2}}{\exp(h\nu/kT) - 1} \qquad (\mathrm{W\,m^{-2}\,Hz^{-1}\,sr^{-1}}) \tag{1.136}$$

where Planck's constant $h = 6.62618 \times 10^{-34}\,\mathrm{J\,s}$
Speed of light $c = 299{,}792{,}458\,\mathrm{m\,s^{-1}}$
Frequency ν is in hertz
Boltzmann's constant $k = 1.380664 \times 10^{-23}\,\mathrm{J\,K^{-1}}$
Absolute temperature T is in kelvin ($0\,\mathrm{K} = -273.16\,^{\circ}\mathrm{C}$)

Figure 1.92 presents the spectral brightness of blackbodies brought up to usual temperatures versus wavelength in micrometers. The monochromatic brightness is maximum at a given temperature when

$$\frac{c}{\nu_m} T = 5.0996 \times 10^{-3}\,\mathrm{m\,K} \quad \text{for } \frac{dB_V}{d\nu} = 0$$

$$\lambda_m T = 3.6698 \times 10^{-3}\,\mathrm{m\,K} \quad \text{for } \frac{dB_\lambda}{d\lambda} = 0$$

In the field of radio waves, where the wavelengths are large, $h\nu$ becomes much smaller than kT and one obtains the law by Rayleigh before that of Planck, which is illustrated by the dotted lines in Figure 1.92:

$$B(\nu) = \frac{2kT\nu^2}{c^2} = \frac{2kT}{\lambda^2} \tag{1.137}$$

with

$$\lambda = \frac{c}{\nu} \quad \text{for } h\nu \ll kT$$

The brightness temperature of a body is the temperature of the blackbody which would have the same spectral brightness for the frequency of observation. By integrating Planck's law on the whole spectrum, we obtain the relation of Stefan–Boltzmann, which represents the total power radiated per unit area of a blackbody:

$$B_{\text{total}} = \frac{2h}{c^2}\int_0^\infty \frac{\nu^3}{\exp(h\nu/kT)-1}\,d\nu$$

which becomes

$$B_{\text{total}} = \sigma T^4 \tag{1.138}$$

with Stefan's constant

$$\sigma = \frac{2\pi^5 k^4}{15h^3c^2} = 5.66956\times10^{-8}\ \text{W m}^{-2}\ \text{K}^{-4}$$

Figure 1.93 presents the total power radiated per unit area according to the law of Stefan–Boltzmann.

1.13.4 Gray Body

A gray body is a body which is not perfectly absorbent; when it receives energy, it absorbs a certain fraction $p(\nu)$ in the vicinity of the frequency ν which is the absorption coefficient. According to Kirchhoff's law, the spectral brightness of a gray body is equal to that of the blackbody at the same temperature and the same frequency multiplied by $P(\nu)$. Kirchhoff's law makes it possible to interpret and determine all the phenomena of absorption of radiation.

Let one consider, for example, a body of brightness temperature T_S which is seen by a sensor through an absorbing medium at temperature T_a, as represented on Figure 1.94, and suppose that, in the vicinity of frequency ν, this absorbing medium retains a fraction p of the incidental energy.

The power flux coming from the source is thus proportional to T_S (Rayleigh's law), then a flux proportional to $(1 - p)Ts$ crosses the absorbing medium which radiates in turn a flux proportional to $p\ T_a$; in this manner, the

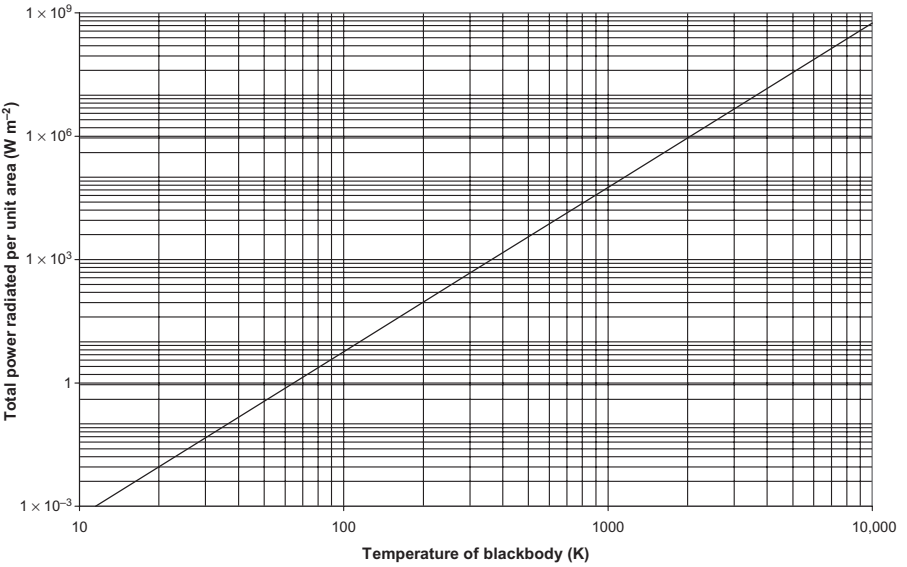

Figure 1.93 Total radiated power by blackbody (Stefan–Boltzmann).

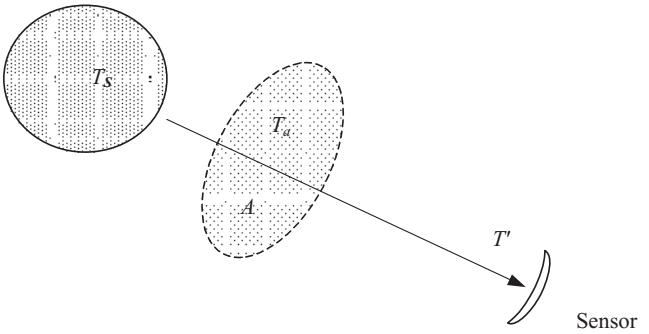

Figure 1.94 Partial absorption by a grey body.

received power flux density is that of a black body which would have the apparent temperature T', such as:

$$T' = (1-p)T_S + pT_a \tag{1.139}$$

By calling A the attenuation caused by the grey body, one obtains:

$$p = 1 - \frac{1}{A}$$

and the relation (1.139) becomes:

$$T' = \frac{T_S}{A} + T_a\left[1 - \frac{1}{A}\right] \tag{1.140}$$

1.14 PROBABILITY DISTRIBUTIONS

1.14.1 Introduction

The electromagnetic wave propagation in the vicinity of the Earth is carried out in a random medium; it is thus necessary to analyze the phenomena of propagation by using the statistical methods in order to lead to a model which would be able to describe satisfactorily the variations of the transmitted signals in the course of the time and across the space.

The statistical distributions are described either by a density of probability or by a function of distribution:

- The probability density function $p(X)$ is such as the probability that a variable X takes a value ranging between x and $x + dx$ is $p(x)dx$,
- The cumulative distribution function $F(x)$ indicates the probability that the variable takes a value lower than x, just as $[1 - F(x)]$ is the probability for a value higher than x.

The relations between these two functions are thus the following:

$$p(x) = \frac{d}{dx}[F(x)] \tag{1.141}$$

$$F(x) = \int_c^x p(t)dt \tag{1.142}$$

where: c is the lower limit that can take the variable X.

There are many laws of distribution among which the Gauss's law, known as the normal law, and the Rayleigh's law, called diffusion law, are used to represent most of the phenomena of propagation of the electromagnetic waves.

1.14.2 Gauss's Law of Distribution

By considering a random variable X, of mean value m and standard deviation σ, the probability density and the distribution function are written:

$$p(x) = \frac{1}{\sigma\sqrt{2\pi}} \exp\left[-\frac{1}{2}\left(\frac{x-m}{\sigma}\right)^2\right] \tag{1.143}$$

$$F(x)=\frac{1}{\sigma\sqrt{2\pi}}\int_{-\infty}^{x}\exp\left[-\frac{1}{2}\left(\frac{x-m}{\sigma}\right)^2\right]dx \tag{1.144}$$

which has as an approximate value:

$$F(x)\approx\frac{\exp\left[-\frac{1}{2}\left(\frac{x-m}{\sigma}\right)^2\right]}{\sqrt{2\pi}\left[0.661\left|\frac{x-m}{\sigma}\right|+0.339\sqrt{\left(\frac{x-m}{\sigma}\right)^2+5.51}\right]}$$

Figure 1.95 and Figure 1.96 represent the probability density function and the cumulative distribution function, expressed in percentage, of a variable reduced to its standard deviation and of null mean value.

The Gaussian distribution meets especially when the considered variable results from the additive effect of many random causes of comparable importance (central limit theorem).

When this distribution intervenes to represent the logarithm of a variable, a log-normal distribution is obtained.

This distribution is characterized by the following Gaussian coefficients:

0.0001%	0.001%	0.01%	0.1%	1%	10%	15.857%	50%
99.9999%	99.999%	99.99%	99.9%	99%	90%	84.143%	
±4.753	±4.265	±3.719	±3.091	±2.327	±1.282	±1	0

and by the following remarkable values:

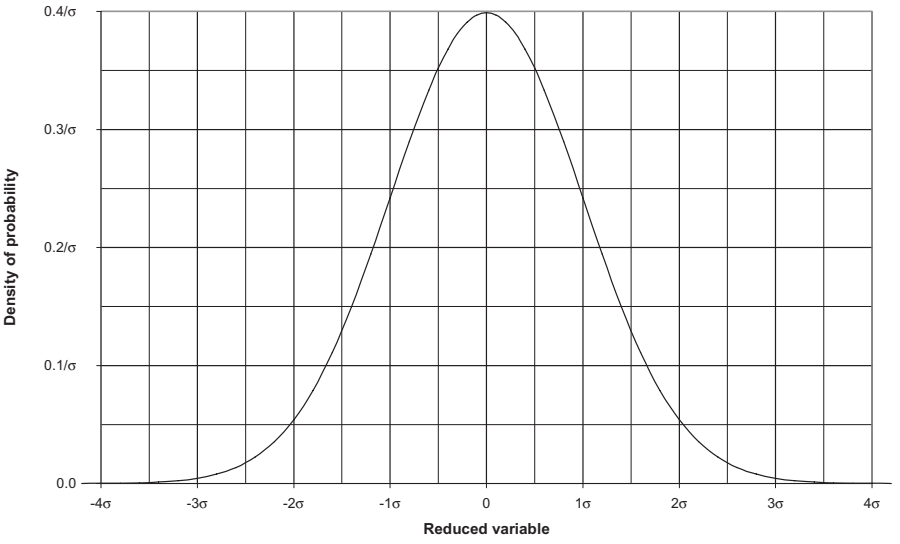

Figure 1.95 Probability density function of Gauss's law.

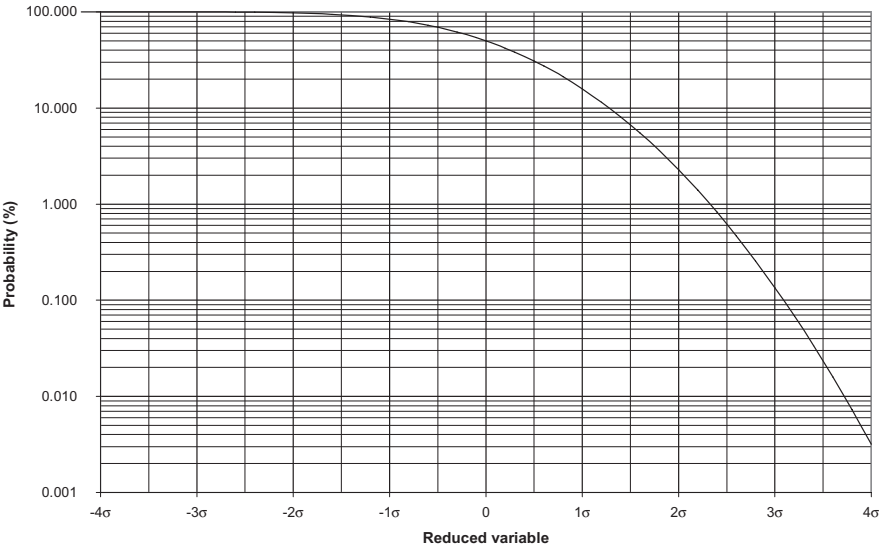

Figure 1.96 Cumulative distribution function of Gauss's law.

— Most probable value $\exp(m - \sigma^2)$
— Median value $\exp(m)$
— Variance σ^2
— Mean value $\exp(m + \sigma^2/2)$
— Mean square value $\exp(m + \sigma^2)$

1.14.3 Rayleigh's Law of Distribution

This distribution applies to a positive continuous variable; the density of probability and the function of distribution are given by the relations:

$$p(x) = \frac{x}{q^2}\exp\left(-\frac{x^2}{2q^2}\right) \tag{1.145}$$

$$F(x) = 1 - \exp\left(-\frac{x^2}{2q^2}\right) \tag{1.146}$$

Figure 1.97 and Figure 1.98 represent the density of probability and the function of distribution, expressed in percentage, of a variable reduced to its most probable value q.

The Rayleigh's law presents the following characteristics:

- the probability that a variable X has a value lower than x is roughly proportional to the square of this value; for example, if the variable

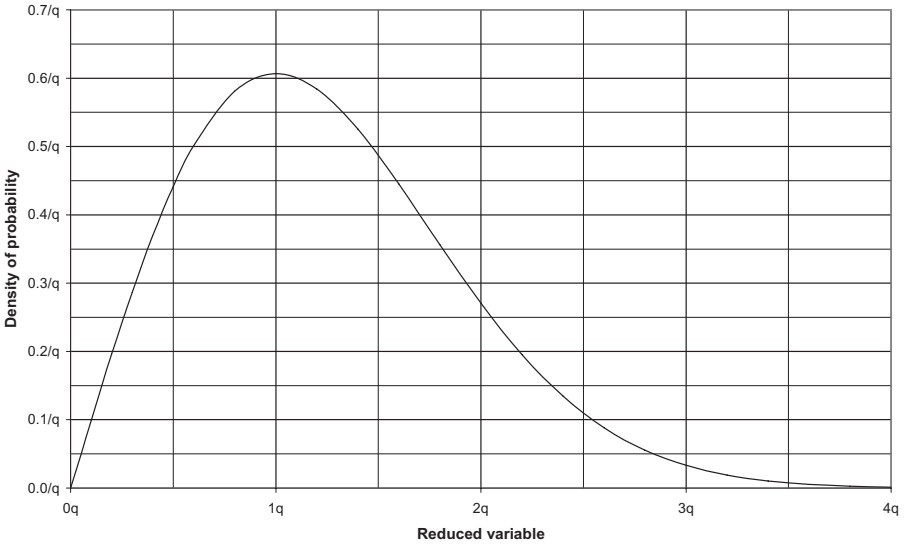

Figure 1.97 Probability density function of Rayleigh's law.

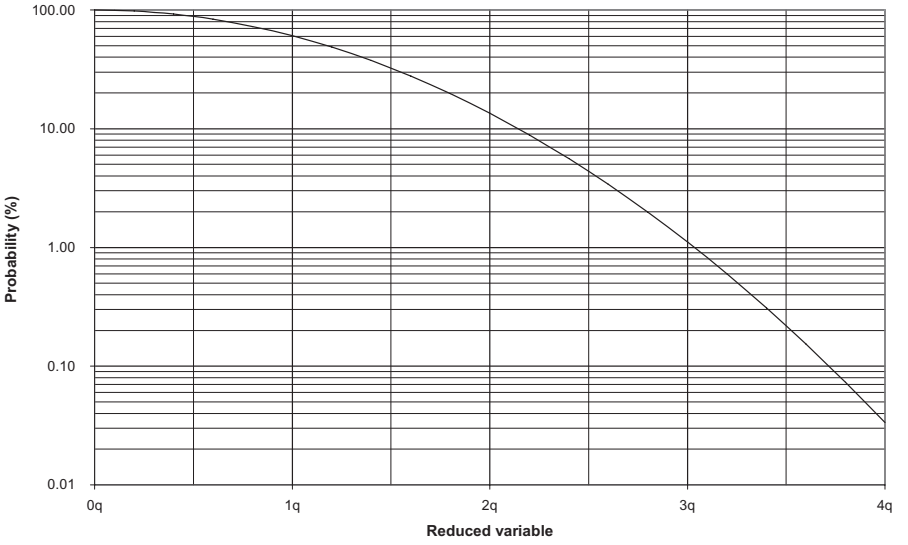

Figure 1.98 Cumulative distribution function of Rayleigh's law.

considered is a tension, the power decrease of 10 dB for each decade of probability,

- if one considers two independent variables x and y of null mean value and of same standard deviation σ, the random variable $r = \sqrt{x^2 + y^2}$ obeys a Rayleigh's distribution and the most probable value of r is equal to σ.

The distribution coefficients of the variable are:

0.001%	0.01%	0.1%	1%	10%	50%	90%	99%	99.9%	99.99%	99.999%
4.7985	4.2919	3.7169	3.0349	2.1460	1.1774	0.4590	0.1418	0.0447	0.0141	0.0045

and its remarkable values are:

— Most probable value q
— Median value $q\sqrt{2\ln 2} = 1.18q$
— Mean value $q\sqrt{\pi/2} = 1.25q$
— Mean square value $q\sqrt{2} = 1.41q$
— Standard deviation $q\sqrt{2-\pi/2} = 0.655q$

The Rayleigh's distribution thus intervenes particularly in the phenomena of diffusion where the variable results from the sum of a great number of vectors equipollent which amplitudes are of the same order of magnitude and which phases would have a uniform distribution.

1.14.4 Other Laws of Distribution

There are some other useful probability distributions such as:

1. Combined Gauss-Rayleigh distribution, where the random variable varies according to the GAUSS's law for the long-term and to the Rayleigh's law for the short-term with the following relations:

$$F_z(x) = 1 - \exp\left(-\frac{x^2}{z^2}\right)$$

$$p(z) = \frac{\exp\left[-\frac{1}{2}\left(\frac{\ln z - m}{\sigma}\right)^2\right]}{\sigma\sqrt{2\pi}z}$$

   where: z is the mean square value of the Rayleigh's variable which is distributed according to a log-normal law
2. Rice's distribution, where the random variable is the sum of two statistically independent Gaussian variables,

3. Nakagami *m* distribution, which fits various types of fade and includes as particular cases the normal distribution and the Rayleigh's distribution,
4. Nakagami-Rice *n* distribution, about the modulus of the vector resulting from the sum of a fixed vector and a vector varying according to the Rayleigh's distribution,
5. CHI-SQUARE distribution, where the random variable is the square of a Gaussian variable,
6. GAMMA distribution, which can be used to represent the rainfall rate distribution for percentages of time up to 10%,
7. Gumbel distribution, called law of extremes, which can be used to represent the high rainfall rate distribution for small percentages of time,
8. Pearson distribution . . .